Aus der Medizinischen Klinik mit Schwerpunkt Rheumatologie und
Klinische Immunologie
der Medizinischen Fakultät Charité – Universitätsmedizin Berlin

In Kooperation mit
The ANZAC Research
Institute
The University of Sydney, Australia

DISSERTATION

The Influence of Interleukin-6 Receptor Antibodies on Breast Cancer Metastases in Bone

zur Erlangung des akademischen Grades
Doctor medicinae (Dr. med.)

vorgelegt der Medizinischen Fakultät
Charité – Universitätsmedizin Berlin
von

Katja Börnert
aus Berlin

Datum der Promotion: 11.12.2015

Abstract

Interleukin-6 (IL-6) is a pleiotropic cytokine which has been associated not only with pro-inflammatory, but also with tumour-progressive characteristics and induction and maintenance of bone resorption in breast cancer osteolytic bone metastases. Previous studies showed that high serum levels of IL-6 in patients suffering from metastatic breast cancer are associated with poor prognosis, disease progression and increased number of metastatic sites. This might be due to the direct effects IL-6 exerts in tumour cells, leading to tumour cell proliferation and inhibition of apoptosis as well IL-6-induced bone resorption at metastatic sites, which results in an enhanced release of growth factors affecting tumour cells in the bone microenvironment.

This work examined whether inhibition of IL-6 signalling in human breast cancer cells with the anti-human IL-6R mAb tocilizumab or inhibition of IL-6 signalling in cells of the bone microenvironment with the anti-murine IL-6R mAb MR16-1 affects tumour progression and tumour-induced osteolysis in a mouse model of breast cancer bone metastases.

Athymic nude mice were injected intratibially with the oestrogen-receptor-negative (ER-) human breast cancer cell line MDA-MB-231 and treated with different antibodies or placebo intraperitoneally. In order to impair IL-6 signalling in human breast cancer cells, groups of mice were injected regularly with either tocilizumab, MR16-1 or a combination of both antibodies. Radiographic images of tibiae were taken throughout the course of the study and, after sacrifice of the animals, endpoint analysis of bone and tumour biology was conducted.

Furthermore, in a set of *in vitro* experiments, the effect of tocilizumab on the expression of IL-6 and IL-6R mRNA as well as human IL-6 protein secretion by MDA-MB-231 cells was analysed in order to define whether an autocrine feed-forward mechanism exists leading to augmented IL-6 or IL-6R expression after IL-6R activation.

We found that both tocilizumab as well as MR16-1 impaired tumour growth of human breast cancer cells in bone. Animals treated with either antibody displayed diminished sizes of osteolytic areas throughout the study. Endpoint analysis revealed that both antibody treatments lead to a smaller number of active osteoclasts at the bone-tumour interface, smaller tumour areas and greater numbers of apoptotic tumour cells and a smaller number of cells undergoing mitosis in the tumours. The combination of both antibodies did have less effect on osteolysis and tumour growth than the single antibody treatment.

In vitro experiments revealed that inhibition of IL-6R activation in MDA-MB-231 cells with tocilizumab led to reduced gene expression leves of IL-6 and IL-6R mRNA.

Kurzdarstellung

Das pleiotrope, für seine proinflammatorischen Eigenschaften bekannte, Zytokin Interleukin-6 (IL-6) weist zudem auch tumorprogressive Eigenschaften auf und übt einen Einfluss auf die Induktion und die Aufrechterhaltung der Knochenresorption in osteolytischen Metastasen des Mammakarzinoms aus. In vorhergehenden Studien konnte gezeigt werden, dass Patientinnen mit metastasiertem Mammakarzinom, welche einen hohen IL-6-Serumspiegel aufweisen, sowohl ein höheres Risiko für weitere Krankheitsprogression, vermehrte Metastasen als auch eine generell schlechtere Prognose haben. Dies könnte einerseits an direkten Effekten von IL-6 auf die Tumorzellen liegen, welche zu einer augmentierten Zellproliferation und einer Hemmung der Apoptose führen, als auch an einer IL-6-induzierten vermehrten Knochenresorption mit nachfolgender Freisetzung von Wachstumsfaktoren aus dem ossären Kompartiment, welche letztlich auf die Tumorzellen im Umfeld wirken. In dieser Studie wurde der anti-humane IL-6 Rezeptor Antikörper (IL-6R mAb) Tocilizumab als auch der anti-murine IL-6R mAb MR16-1 in einem murinen Xenograftmodel getestet. Ziel der Studie war es die Effekte der jeweiligen Antikörperbehandlung auf die Tumorprogression und den Grad der tumorbedingten Osteolyse zu definieren.

Zellen der humanen östrogenrezeptor-negativen Mammakarzinomzelllinie MDA-MB-231 wurden in Tibiae von athymischen Mäusen injiziert und die Tiere daraufhin mit den jeweiligen Antikörpern oder Placebo behandelt. Um die IL-6 Signaltransduktion in den humanen Mammakarzinomzellen zu blockieren, wurde eine Gruppe von Mäusen regelmässig mit Tocilizumab behandelt, wohingegen einer anderen Gruppe MR16-1 injiziert wurden. Weiterhin untersuchten wir den Effekt der Kombination von beiden Antikörperbehandlungen. Um den Verlauf der Entwicklung von osteolytischen Knochenmetastasen zu dokumentieren, wurden regelmässig radiologische Untersuchungen der Tibiae angefertigt. Endpunktanalysen zielten auf die histologische und immunhistochemische Analyse der Knochenmorphologie und der Tumorbiologie ab.

Des Weiteren wurde in einem *in vitro* Experiment der Effekt von Tocilizumab auf die Expression von humaner IL-6 und humaner IL-6-Rezeptor mRNA und die Sekretion von humanem IL-6 durch MDA-Mb 231 Zellen untersucht. Hierbei stellte sich vor allem die Frage, ob ein autokriner feed-forward Mechanismus nach Aktivierung von IL-6 Rezeptoren in MDA-MB 231 Zellen existiert.

Die Behandlung athymischer Mäuse mit Tocilizumab als auch mit MR16-1 führte zu einer Verminderung der Progression von osteolytischen Mammakarzinommetastasen. Hierbei wurde

nicht nur der Grad der Knochenresorption verändert, sondern auch die Tumorbiologie der humanen Mammakarzinomzellen im Hinblick auf eine reduzierte Rate an proliferierenden und eine erhöhte Rate an apoptotischen Tumorzellen. Die Kombination beider Antikörperbehandlungen zeigte geringere Effekte als die Behandlung mit den einzelnen Antikörpern.

Humane Mammakarzinomzellen, welche *in vitro* mit Tocilizumab behandelt wurden, zeigten eine reduzierte Rate an IL-6 und IL-6R mRNA Expression und einen Trend in Richtung einer reduzierten IL-6 Protein Sekretion.

Table of Contents

List of abbreviations

ALP	*alkaline phosphatase*
aa	*amino acid*
AES	*3-Aminopropyl-triethoxysilane*
B cells	*B lymphocytes*
BA	*bone area*
bcl-2	*B-cell lymphoma 2*
bcl-xl	*B-cell lymphoma-extra large*
BMP	*bone morphogenetic protein*
BMU	*basic multicellular unit*
BSA	*Bovine serum albumin*
BTI	*bone-tumour interface*
CA-II	*carboanhydrase II*
CA-IX	*carboanhydrase IX*
CBA	*cortical bone area*
cbfa1	*core-binding factor 1*
CBTI	*cortical bone-tumour interface*
CD	*Castleman's disease*
cDNA	*complementary DNA*
CLC	*cardiotrophin-like cytokine*
CNTF	*ciliary neurotrophic factor*
COX-2	*cyclooxygenase 2*
CRP	*C reactive protein*
CT-1	*cardiotrophin-1*
CTGF	*connective tissue growth factor*
CXCR4	*C-X-C chemokine receptor type 4*
DAB	*diaminobenzidine tetrahydrochloride*
dATP	*Deoxyadenosine-triphosphate*
dCTP	*Deoxycytidine triphosphate*
dGTP	*Deoxyguanosine triphosphate*
DMEM	*Dulbecco's Modified Eagles's medium*
DNA	*Deoxyribonucleic acid*
dNTPs	*Deoxynucleotide Triphosphates*
DPBS	*Dulbecco's phosphate-buffered saline*
dsDNA	*double-stranded DNA*
dTTP	*Deoxythymidine-triphosphate*
dUTP	*Deoxyuridine-Triphosphate*
ECM	*extracellular matrix*
EDTA	*ethylenediaminetetraacetic acid*
ELISA	*Enzyme Linked Immunosorbent Assay*
ER-	*estrogen receptor negative*
ER+	*estrogen receptor positive*
ET-1	*endothelin 1*
F-CFU	*fibroblast colony forming units*
FCS	*fetal calf serum*
FGF	*fibroblast growth factor*
GAPDH	*Glyceraldehyde 3-phosphate dehydrogenase*
GM-CFU	*granulocyte macrophage colony forming unit*
GM-CSF	*granulocyte macrophage colony-stimulating factor*
gp130	*glycoprotein 130*
gp96	*glycoprotein 96*

hGAPDH	*human Glyceraldehyde 3-phosphate dehydrogenase*
HIF-1α	*Hypoxia-inducible factor 1α*
HLA	*human leukocyte antigen*
HRP	*horseradish peroxidase*
i.p.	*Intraperitoneal*
Ig	*Immunoglobulin*
IGF-1	*insulin-like growth factor 1*
IGF-2	*insulin-like growth factor 2*
IgG1	*immunoglobulin G1*
IL-11	*Interleukin 11*
IL-1R	*Interleukin-1 receptor*
IL-1α	*Interleukin 1α*
IL-27	*Interleukin 27*
IL-3	*Interleukin 3*
IL-31	*Interleukin 31*
IL-6	*Interleukin 6*
IL-6R	*Interleukin-6 receptor*
mAb	*Interleukin-6 receptor monoclonal antibody*
IL-8	*Interleukin 8*
JAK 1	*Janus kinase 1*
JAK 2	*Janus kinase 2*
JIA	*juvenile idiopathic arthritis*
JNK	*c-Jun N-terminale Kinasen*
kDa	*kilo Dalton*
LIF	*leukemia inhibitory factor*
LRP5	*low-density lipoprotein receptor-related protein 5*
mAb	*monoclonal antibody*
MAPK	*mitogen-activated protein kinase*
mcl-1	*myeloid cell leukemia sequence 1*
MCP-1	*monocyte chemotactic protein 1*
M-CSF	*macrophage colony-stimulating factor*
MDD	*minimal detectable dose*
mdr1	*multidrug resistance gene 1*
MIB	*mindbomb homolog*
mIL-6	*murine IL-6*
mIL-6R	*membrane-bound Interleukin-6 receptor*
MMP	*matrix metalloproteinase*
mpGN	*mesangioproliferative glomerulonephritis*
m-phase	*mitotic phase*
mRNA	*Messenger ribonucleic acid*
NF-IL6	*nuclear factor IL-6*
NF-κB	*nuclear factor kappa-light-chain-enhancer of activated B cells*
NK cells	*natural killer cells*
Notch3	*Neurogenic locus notch homolog protein 3*
NPN	*Neuropoetin*
OPG	*Osteoprotegerin*
Opn	*Osteopontin*
OSM	*Oncostatin M*
P1NP	*procollagen type 1 amino-terminal propeptide*
p53	*Preotein*
PBMC	*peripheral blood mononuclear cell*
PBS	*phosphate-buffered saline*
PCR	*polymerase chain reaction*
PDGF	*platelet-derived growth factor*

PGE2	*prostaglandin E2*
P-gp	*P-glycoprotein*
PTH	*parathyroid hormone*
PTHrP	*parathyroid hormone-related protein*
qPCR	*Real-time polymerase chain reaction*
RA	*rheumatoid arthritis*
RANK	*receptor activator of NF-κB*
RANKL	*receptor activator of nuclear factor kappa-B ligand*
Rasprotein	*rat sarcoma protein*
Rb	*Retinoblastoma*
RES	*reticuloendothelial system*
RNA	*Ribonucleic acid*
rpm	*rounds per minute*
RT-PCR	*reverse transcription polymerase chain reaction*
Runx2	*runt-related transcription factor 2*
SAA	*serum amyloid A*
SDF-1	*stromal cell-derived factor 1*
sIL-6R	*soluble Interelukin-6 receptor*
s-phase	*synthesis phase*
SRE	*skeletal related event*
STAT	*signal transducer and activator of transcription*
T cells	*T lymphocytes*
TBTI	*trabecular bone tumour interface*
TdT	*terminal deoxynucleotidyl transferase*
TGF-β	*transforming growth factor β*
TMB	*Tetramethylbenzidine*
TNF	*tumour necrosis factor*
TNF-αR	*tumour necrosis factor α receptor*
TRAcP	*Tartrate-resistant acid phosphatase*
TRAcP5b	*tartrate-resistant acid phosphatase 5b*
TuA	*tumour area*
TUNEL	*terminal deoxynucleotidyl Transferase-mediated Biotin-dUTP Nick End Labelling*
TYK 2	*tyrosine kinase 2*
VEGF	*vascular endothelial growth factor*
VNR	*vitronectin-receptor*
µCT	*Micro-computerised tomography*

List of figures and tables

List of figures

List of tables

Introduction

Physiological functions of Interleukin-6 and its signalling pathways

IL-6 is a pleiotropic cytokine produced by a variety of cells including blood monocytes [1], granulocytes [2], blood vessel endothelial cells [3], smooth muscle cells [4], connective tissue fibroblasts [5], chondrocytes [6-7], osteoblasts [8], keratinocytes of the skin [9], mesangial cells of the kidney [10], brain astrocytes, microglial cells [11], anterior pituitary cells and stromal endometrium cells [12]. In healthy individuals, levels of IL-6 are detectable in the circulation only after injury and infection [13]. In these cases, this cytokine exhibits a pleiotropic spectrum of physiological activities as it is involved in initiation of fever, induction of immunoglobulin synthesis in activated B cells (plasma cells), activation of T cells and natural killer (NK) cells, stimulation of megakaryopoiesis, inception of acute-phase protein synthesis in the liver, corticotropin-release by the pituitary gland as well as regulation of bone resorption [14-21]. However, as a mainly pro-inflammatory cytokine, studies also indicate that endogenous IL-6 may limit both the local and the systemic inflammatory response by down-regulating pro-inflammatory cytokine expression while simultaneously inducing the expression of Interleukin-1 receptor (IL-1R) antagonist and soluble p55 tumour necrosis factor α receptor (TNF-αR), as it was shown in tissue macrophages of cancer patients. [22-24].

IL-6 exerts actions on its target cells via a specific dimeric receptor. An 80kDa membrane-bound protein devoid of transducing activities serves as IL-6 binding site – the IL-6 receptor (IL-6R). Complexes of IL-6 and IL-6Rs then induce homodimerization of signal-transducing trans-membrane components - glycoprotein 130 (gp130) [21]. Gp130 is expressed on cells of almost all organs [25], including bone marrow stromal cells, osteoblasts [26] and osteoclasts [27]. In contrast to the abundant presence of gp130, cellular distribution of cognate IL-6Rs is predominantly confined to hepatocytes and leukocyte subpopulations like monocytes, neutrophils, T and B cells [28]. In addition to the membrane-bound IL-6Rs (mIL-6Rs), a naturally occurring soluble form of the IL-6R (sIL-6R) is generated by either limited proteolysis of membrane-integrated proteins or by translation of alternatively spliced IL-6 mRNA [29-30]. sIL-6Rs are found in various body fluids where they also form complexes with circulating IL-6, exhibiting affinity comparable to that of IL-6/mIL-6Rs [31-32]. Subsequently, aggregates of IL-6/sIL-6R activate membrane-bound gp130 and consequently render cells lacking mIL-6Rs sensitive to the cytokine IL-6: this process is called trans-signalling [33-34]. Hence, sIL-6Rs widen the repertoire of cell types responsive to IL-6. Following gp130 homodimerization, Janus

kinase 1 and 2 (JAK1 and JAK2), and tyrosine kinase 2 (TYK2) are activated [35] causing tyrosine phosphorylation of latent cytoplasmatic transcription factors called signal transducers and activators of transcription (STATs) [36]. The main STAT activated through IL-6 signalling is STAT3 [37]. In addition to STAT3, Ras proteins are also activated resulting in hyperphosphorylation of mitogen-activated-protein-kinases (MAPK) and consecutive increase of its serine/threonine kinase activity. MAPK then is capable of phosphorylating the nuclear factor for IL-6 (NF-IL6) rendering it competent of DNA binding [38]. Thus, activation of cells through IL-6/IL-6R/gp130 complexes initiates a series of events culminating in activation of STATs and NF-IL6 and transcriptional regulation of target genes responsible for phenotypical effects (Figure 1).

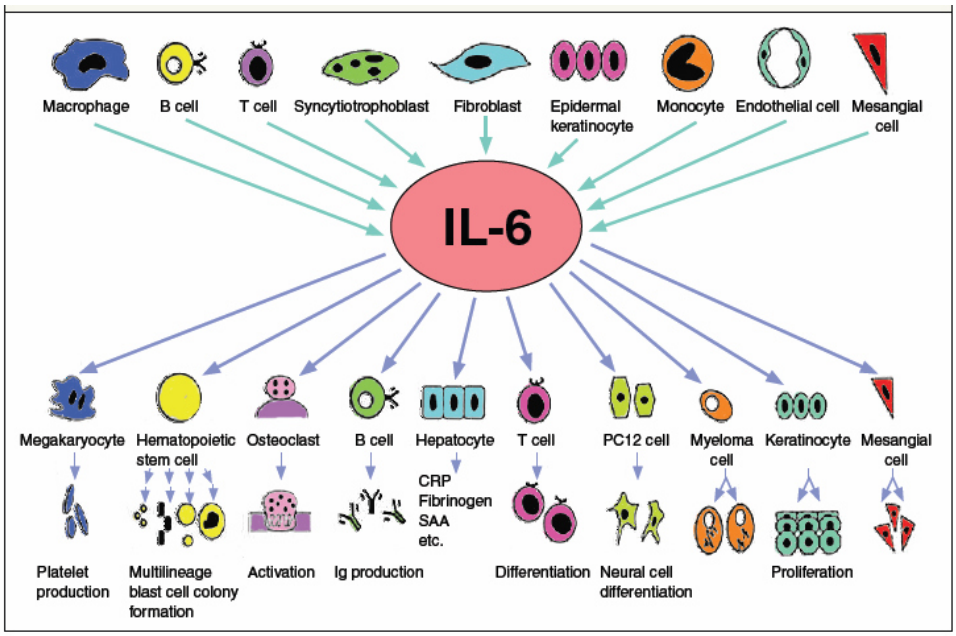

Figure 1: Cells producing IL-6 and the actions of IL-6 in the body. Ig=immunoglobulin, CRP=C reactive protein, SAA=serum amyloid A. Adapted from [39]

Moreover, a soluble form of gp130 is present in human serum which functions as antagonist of membrane gp130 by binding complexes of IL-6/sIL-6R and thus preventing further signalling [40].

The family of Interleukin-6-type cytokines compromises IL-6, Interleukin-11 (IL-11), Oncostatin M (OSM), Leukemia Inhibitory Factor (LIF), Ciliary Neurotrophic Factor (CNTF), Cardiotrophin-1 (CT-1) and Cardiotrophin-Like Cytokine (CLC), Neuropoetin (NPN), Interleukin-27 (IL-27) and Interleukin-31 (IL-31) [28, 33]. They all bind to specific membrane receptor complexes containing the common signal transducer gp130 through which target genes

involved in differentiation, survival, apoptosis and proliferation are regulated. By sharing this signal-transducing component of the receptor complex, functional redundancy of cytokines of the IL-6 type family can be explained.

Pathological functions of Interleukin-6

Contrasting elevation of IL-6 levels following all kinds of severe traumatic or infectious events, increased production of IL-6 may also play a pathophysiological role in many chronic or malignant disorders. Rheumatoid arthritis (RA) is a chronic inflammatory disease characterised by persistent synovitis and progressive joint damage often associated with positive anti-immunoglobuline auto-antibodies - rheumatoid factors [41]. In patients suffering from RA, constitutive overproduction of IL-6 is likely to contribute to onset and maintenance of RA, since levels of this cytokine are elevated consistently in both serum and synovial fluids of afflicted joints [42]. Moreover, serum IL-6 levels correlate with disease activity as well as radiographic joint damage [43-44]. In clinical studies, treatment with IL-6R monoclonal antibodies (mAbs) was well tolerated by patients and revealed significant reduction of disease activity [45]. Consequently, anti-IL-6R mAbs are nowadays approved for treatment of patients suffering from RA. Another chronic inflammatory disease associated with increased IL-6 production is Crohn's disease [46]. Administering IL-6R mAbs to patients during a clinical study also had beneficial effects [47].

IL-6 also plays an important role in pathogenesis of mesangioproliferative glomerulonephritis (mpGN) [48]. It possibly acts as autocrine growth factor, released by mesangial cells, inducing proliferation of same. Urine IL-6 levels in these patients are usually elevated, corresponding positively with disease activity. Similar processes are likely to contribute to pathophysiology of psoriasis since keratinocytes both produce and respond strongly to IL-6 [49]. Psoriatic patients exhibit increased IL-6 levels during active phases of disease which decrease after successful treatment [50].

Castleman's disease (CD) is an atypical lymphoproliferative disorder characterised by benign giant lymph nodes containing follicular and endothelial hyperplasia with capillary proliferation [51]. Again, serum IL-6 concentrations and clinical features, such as fever, anaemia, hypergammaglobulinemia and elevated levels of acute phase proteins, correlate [13, 52] suggesting that dysregulated IL-6 production in affected lymph nodes may be responsible for

systemic manifestations of the disease. Inhibiting IL-6 signalling with IL-6 mAbs or IL-6R mAbs ameliorated disease activity, thus providing evidence for a pivotal role of IL-6 in CD [51, 53].

Patients with solid tumours may exhibit elevated IL-6 serum levels due to constitutive IL-6 production by numerous tumour cell lines. Increased IL-6 levels are associated with adverse prognosis in patients suffering from multiple myeloma [54], lymphoma [55], ovarian cancer [56-57], prostate cancer [58], metastatic renal cell carcinoma [59] and various other neoplastic diseases. IL-6 functions as a growth factor for a variety of cancer cells including myeloma, renal cell carcinoma, cervical carcinoma, AIDS Kaposi's sarcoma derived cells as well as certain T and B cell lymphomas. In addition, over-expression of IL-6 in B cells contributes to the development of myeloma in transgenic mice [60].
Due to its implications in acute-phase responses, high serum IL-6 levels might contribute to weight loss in cancer cachexia, night sweats, fever and other paraneoplastic syndromes [61-62].

The role of IL-6 in breast cancer and its metastasis will be discussed later in this literature.

Bone biology and the role of Interleukin-6

Function and structure of bone

The adult human skeleton, made up of 213 bones, provides structural support for the rest of the body, permits movements and locomotion by serving as scaffold for muscles, shields vital internal organs and structures, ensures maintenance of mineral homeostasis of calcium, magnesium, bicarbonate, phosphate and other minerals and the acid-base balance, serves as reservoir for cytokines and growth factors and supplies an environment crucial for hematopoiesis within the bone marrow [63]. Bone encloses mineralized and organic extracellular matrix, specialized bone cells and bone marrow [64]. Within the mineralized bone, two different architectural designs exist: cortical bone and trabecular bone are present in a ratio of approximately 80% to 20% [64]. The dense and solid cortical bone surrounds the marrow space whereas trabecular bone is composed of a three-dimensional network of honeycomb-like trabeculae interspersed in the bone marrow compartment maintaining a close relationship to the hematopoietic compartment [64]. Both cortical and trabecular bone are usually formed in a lamellar pattern in which collagen type I fibrils are arranged in alternating orientations, ensuring great strength of bone despite minimal mass. In contrast to lamellar bone, collagen fibrils in

woven bone are laid down in a disorganized manner rendering it less resistant. Woven bone is usually produced during formation of primary bones or in states of increased bone turnover [64]. Besides the structural protein collagen I, there are various other proteins stored within bone exerting different functions locally or systemically [65-68].

Long bones such as tibiae are composed of a shaft, the diaphysis, a cone-shaped metaphysis below the growth plate and a rounded epiphysis located above the growth plate. The diaphysis contains mainly dense cortical bone whereas metaphysis and epiphysis are primarily made up of trabecular bone, which is surrounded by a thin layer of cortical bone [64]. Three specialized cell types are present in bone: osteoblasts and osteoclasts as major effectors of bone turnover, while osteocytes represent the most common cells in bone [69].

Osteoblasts and bone formation

Osteoblasts originate from pluripotent mesenchymal stem cells of the bone marrow [64, 70] that exhibit the potential to differentiate into osteoblasts, fibroblasts, chondrocytes, adipocytes or muscle cells from common progenitor cells called fibroblast-colony forming units (F-CFU) [71]. Commitment of mesenchymal stem cells to the osteoblast lineage requires the canonical Wnt/ β-catenin signalling pathway [72-73] and Runx2/Cbfa1 (core-binding factor 1) [74-75]. Further growth factors like TGF-β, IGF-1 and IGF-2, FGF, PDGF, BMP and LRP5 regulate osteoblast proliferation and differentiation in an auto- or paracrine manner [76-77]. Phenotypic markers of osteoblasts are alkaline phosphatase (ALP) and collagen I [71]. Active mature osteoblasts synthesize organic bone matrix containing collagen I and other non-collagen proteins. This unmineralized bone matrix is called osteoid. Osteoblastic cell activity is controlled systemically by hormones and locally by cytokines and mechanical stress. Once activated, osteoblasts also regulate mineralization of the matrix and activity of other bone cells, particularly osteoclasts [78], by secreting colony-stimulating factors GM-CSF and M-CSF and cytokines like RANKL, IL-6 and IL-11 [79-81].

Osteocytes

Osteocytes are terminally differentiated osteoblasts assembling syntactical networks to support bone structure and metabolism. They are located within lacunae in the mineralized tissue [82] interlinked metabolically and electrically [64] by extensive filipodial processes containing gap junctions composed of connexin 43 [83]. The primary function of osteocytes is mechanosensation - transduction of stress signals received into adaptive bone remodelling by

means of PGE_2, COX-2, various kinases, Runx2 and nitrous oxide [64, 84]. The presence of empty lacunae in ageing bone suggests that osteocytes undergo apoptosis due to disruption of their intercellular gap junctions or cell-matrix interactions [85]. Moreover, osteocytes are involved in the bone resorption process by phagocytising unmineralized osteoid [64].

Osteoclasts and bone resorption

Multinucleated osteoclasts are derived from hematopoietic granulocyte-macrophage colony forming units (GM-CFU) [86-87]. Mononuclear monocyte-macrophage precursor cells, though present in various tissues, differentiate into mature osteoclasts when in contact with bone matrix. Activated mature osteoclasts are the only cells capable of resorbing mineralized bone. RANKL and M-CSF, produced by bone marrow stromal cells and osteoblasts in membrane-bound and soluble forms, are necessary and sufficient for osteoclastogenesis [88-90]. Mature osteoclasts express TRAcP (Tartrate-resistant acid phosphatase), cathepsin K, calcitonin receptor and $\alpha\beta_3$ integrin [90]. M-CSF is crucial for proliferation, survival and differentiation of osteoclast precursors as well as for mature osteoclast survival and the cytoskeletal rearrangement preceding bone resorption [64]. RANKL, a member of the TNF family, is critical for osteoclastogenesis [64]. Activated osteoclasts bind to the bone matrix via integrin receptors and hence convert to polarized cells, forming a ruffled border at the bone-facing membrane. Here, H^+ ions are produced by carboanhydrase II (CAII) [91] and H^+ and Cl^- are secreted via H^+- ATPase and chloride channels into the resorption compartment, called Howship's lacunae, in order to dissolve the mineral component of bone [92]. Furthermore, vesicles containing lysosomal cathepsin B, K and L [69], matrix metalloproteinases (MMPs) [93] and other enzymes [94] are released via exocytosis to digest the proteinaceous matrix [64, 95]. Factors such as TGF-β can induce osteoclast apoptosis while others like IL-6, PTH, 1,25 dihydroxyvitamin D can inhibit apoptosis, thus influencing the life-span of osteoclasts and their activity.

Bone remodelling

Adult bone represents a dynamic tissue undergoing continuous cellular and matrix remodelling which occurs in discrete pockets spread throughout the skeleton [69, 96]. Local resorption of old bone by osteoclasts and following osteoblastic bone formation are coupled processes responsible for renewing the skeleton and consequently preventing accumulation of micro-damages while maintaining structural and anatomical integrity of bone [71] as well as adapting the skeleton to changes of mechanical stress [69]. Bone remodelling is controlled by hormonal, mechanical,

nutritional and genetic influences. Furthermore, a number of growth factors and cytokines, such as IL-6, are able to alter this process [71]. Normally, bone formation and bone resorption are balanced [97] with 20% of trabecular bone being remodelled at any time [98]. Abnormalities in bone remodelling occur in some common human diseases like osteoporosis [71], arthritis [41, 99] and tumour-related osteolysis [100-101], all of these are characterised by disruption of this subtle balance. Remodelling sites may develop randomly but also are targeted to areas that require repair [102] or are subject to mechanical stress. They consist of small groups of cells (osteoblasts and osteoclasts) called basic multicellular unit (BMU). Hence, initiation of bone remodelling is most likely controlled locally, either by factors produced by cells of the bone microenvironment acting auto- or paracrinally or by mechanical loading [69].

Bone remodelling itself is a multi-step process commencing with activation of osteoclast precursors and their consecutive differentiation into mature osteoclasts. Osteoblastic lining cells prepare bone for osteoclastic bone resorption by dissolving the first layer of unmineralized osteoid by means of proteolytic enzymes such as MMPs, collagenases and gelatinases [103]. After osteoclasts have digested old bone, osteoprogenitor cells proliferate and differentiate locally into mature osteoblasts and migrate into the Howship's lacunae where they disclose osteoclast activity. This so-called reversal phase is dependent on coupling mechanisms [104]. Various growth factors such as TGF-β, IGF-1 and IGF-2 are deposited in abundance within the mineralized bone. They are released and activated upon resorption [71] to inactivate osteoclasts and attract osteoblasts [105-106]. Furthermore, osteoclasts undergo apoptosis after excessive periods of bone resorption and accumulation of ionized calcium [69], which also ceases osteoclast activity. Subsequently, osteoblasts deposit new, unmineralized bone matrix, osteoid, in the lacuna. Once embedded in osteoid, osteoblasts transform into osteocytes, whereas osteoblasts resting on the surface of the newly formed bone restrain quiet lining cells until activation (Figure 2) [69].

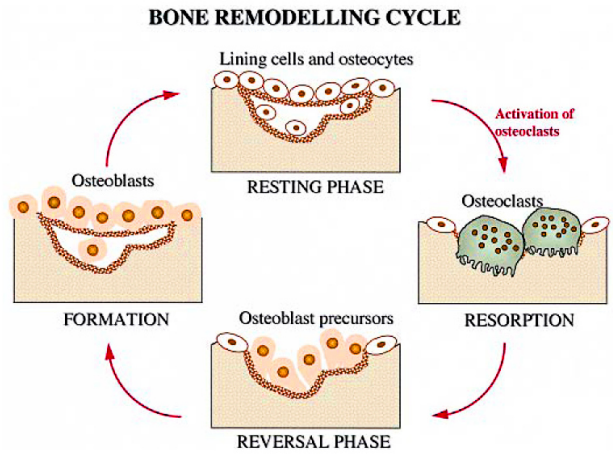

Figure 2: Stages of bone remodelling. In the resorptive phase, activated multinucleated osteoclasts resorb a small area of mineralized bone matrix. Subsequently, in the so-called reversal phase, osteoprogenitor cells differentiate into mature osteoblasts, migrate to the area of bone resorption and form new bone matrix in the formation phase. In the following resting phase, embedded osteoblasts become osteocytes whereas osteoblasts lying on the surface of the newly formed bone stay lining cells, which can be activated at later stages of bone remodelling. Adapted from [69]

The RANKL/RANK/OPG system regulates bone formation and resorption

Osteoblasts and bone marrow stromal cells play a major role in mediating the hormonal control of osteoclastogenesis and bone resorption and therefore in maintaining the balance necessary in the bone remodeling process [107]. Furthermore, osteoblasts and stromal cells are essential for *in vitro* osteoclastogenesis since they regulate osteoclast differentiation by producing soluble factors and by direct signalling to osteoclast progenitors [108-109]. The RANKL/RANK/OPG system can be attributed to most of these interactions, marking the final pathway of many pro-resorptive agents that exert actions on osteoclastic bone resorption via osteoblastic cells.

RANKL occurs either as 40-45kDa protein in membranes of osteoblasts, bone marrow cells or cells of the lymphoid tissues or as soluble 41kDa protein generated by proteolytic cleavage [110]. Soluble or membrane-bound RANKL binds to RANK receptors expressed on osteoclast precursor cells and mature osteoclasts [110]. RANKL activates c-jun terminal kinases and sends signals to NF-κB, promoting differentiation, activation and inhibition of apoptosis in osteoclastic cells and their precursors [111-112].

OPG is a member of the TNF-receptor superfamily produced by numerous tissues including lung, heart, kidney, liver, stomach, intestine, brain, spinal cord, thyroid gland and cells of the bone microenvironment [113-114]. It does not contain a transmembrane or cytoplasmatic

domain and thus functions as a soluble decoy receptor for RANKL, inhibiting RANKL activities in a dose-dependent manner [113, 115].

Consequently, ratios of RANKL and OPG modulate osteoclastic performance by controlling osteoclastogenesis, degree of bone resorption and skeletal remodelling (Figure 3). Deregulation of this equilibrium shifts the subtly regulated balance of bone remodelling. This appears in numerous diseases such as osteoporosis.

Furthermore, many pro-resorptive agents supporting osteoclast formation, such as 1,25 dihydroxyvitamin D, IL-6, IL-11, PGE_2, glucocorticoids and PTH/PTHrP, act indirectly by signalling to marrow stromal cells or osteoblasts and inducing upregulation of RANKL and down-regulation of OPG [89, 110].

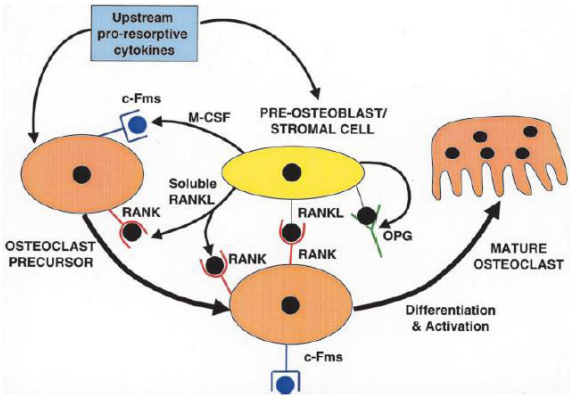

Figure 3: Scheme of osteoblastic/stromal cell control of osteoclast differentiation and activation. Up-stream pro-resorptive factors as 1,25 dihydroxyvitamin D, PTH/PTHrP, IL-6, IL-11, PGE_2 and glucocorticoids act indirectly on osteoclast by binding to their cognate receptors expressed on osteoblasts or bone marrow stromal cells and inducing an alteration of expression of osteoclast-regulating proteins, namely RANKL/OPG and M-CSF. Subsequently, these molecules bind the appropriate receptors on osteoclasts and osteoclast precursor cells resulting in differentiation and activation and, thus, bone resorption. Adapted from [110].

The role of interleukin-6 in bone turnover

Production of IL-6

IL-6 within the bone microenvironment is derived both from systemic and local sources. Locally, IL-6 is produced and secreted at very low levels by unstimulated osteoblastic cells, which increase immensely after stimulation with bone-resorbing agents such as PTH/PTHrP, 1,25 dihydroxyvitamin D or IL-1α [8]. On the other hand, oestrogens and androgens inhibit IL-6 transcription in these cells [116-117]. Thus, loss of gonadal function results in increased production of IL-6 with consecutively enhanced osteoclastogenesis and bone loss. Therefore, IL-

6 is involved in pathogenesis of postmenopausal osteoporosis. Onset of these effects was avoided by administering IL-6 neutralizing antibodies or 17-β estradiol [118].

IL-6 in cells of osteoblasts and the osteoclast lineages

Generally, mIL-6Rs are very scarce or absent on osteoblastic cell lines, making it crucial to add sIL-6Rs to *in vitro* experiments in order to mediate actions of IL-6 [119-122]. *In vivo*, bone marrow stromal cells express mIL-6Rs constitutively, thus being a source of sIL-6Rs [122]. Some studies suggest mIL-6Rs are expressed on osteoblastic cells in late stages of osteoblast differentiation [123]. Activation of gp130 on osteoblastic cells initiates a cascade of events enforcing the effects of IL-6 on osteoblasts: proliferation of pre-osteoblastic cells *in vitro* is inhibited while differentiation occurs, determined by enhanced expression of Runx2 and osteocalcin mRNA, which mark late stages of osteoblastic differentiation [124] as well as production of ALP [121]. Furthermore, IL-6 signalling increases the rate of mature osteoblastic cells undergoing apoptosis positive for caspase 3 expression [123]. So briefly, IL-6 appears to control both function and lifespan of osteoblasts by initially pushing, but in the long term inhibiting osteoblastic bone formation [123]. IL-6, in concert with sIL-6Rs, also enhances expression of collagenase 3 and gelatinase [125]. As mentioned above, these enzymes are pivotal for initiation of bone remodelling through degradation of osteoid by lining cells. Moreover, IL-6 augments PTHrP mRNA transcription in human osteoblastic cell lines and osteosarcoma cell lines [121, 126]. IL-6 and PTHrP act synergistically to increase bone resorption.

RANKL is induced in osteoblast-like cell lines after IL-6 stimulation and therefore functions as mediator of resorptive effects of IL-6 [127-128]. On the other hand, IL-6 signalling resulted in diminished RANK expression on mature osteoclasts [129], associated with suppressed IκB degradation and less activation of JNK labelling active RANK signalling [128]. IL-6 stimulates early stages of hematopoiesis and osteoclastogenesis; it synergizes with IL-3 to enforce formation and maturation of GM-CFUs and later promotes determination towards osteoclast precursors within these colonies [130]. Addition of M-CSF, IL-6 and sIL-6R to peripheral blood mononuclear cells induces formation of $TRAcP^{+}$, vitronectin-receptor positive ($VNR^{+)}$ multinucleated cells capable of forming resorption pits on dentine slices which proved to be independent of RANKL [81]. However, the cells' bone resorbing capacity was extremely low when compared to peripheral blood mononuclear cells (PBMCs) stimulated with M-CSF and RANKL. In concert with IL-1, IL-6 stimulates bone resorption *in vivo* [131]. Still, it is unclear whether IL-6 exerts effects on mature osteoclasts by itself, or if pro-resorptive actions are solely

caused by promoting earlier stages of differentiation or are mediated by neighbouring cells of the bone environment [132]. The latter hypotheses were underlined by showing that IL-6 induces formation of osteoclasts and stimulates bone resorption in cocultures with osteoblasts and bone marrow cells [32].

To sum up, IL-6 signalling alone likely fuels proliferation of osteoclast precursors but hinders final differentiation. Hence, a greater pool of osteoclastic precursors is provided but osteoclastic bone resorption itself is not enhanced by IL-6 alone. However, together with other pro-resorptive factors that affect committed osteoclast precursors, as PTHrP [133], IL-6 potentiates effects exerted by these molecules by supplying more osteoclast precursors.

Regulation of RANKL and OPG expression in osteoblastic cells in response to IL-6 is probably controlled by PGE_2. PGE_2, major eicosanoid product of the COX-2 catalyzed reaction, has been attributed to osteoclast formation [134] as well as osteoblast differentiation and consequent bone formation and repair [135]. Liu et al. showed that IL-6 induces PGE_2 synthesis in osteoblastic cells, which in turn upregulates RANKL and downregulates OPG expression, thus influencing osteoclast formation and activation. These effects are blocked by addition of COX-2 inhibitors, indicating that PGE_2 is crucial in this process [136]. Hence, interactions between the COX-2/PGE_2 and the IL-6 system tip the balance of OPG/RANKL towards osteoclastogenesis and bone resorption.

IL-6 and pathological bone resorption

In physiological circumstances, IL-6 is either redundant or below a critical threshold of sensitivity for osteoclastogenesis. IL-6 deficient mice are healthy and exhibit no specific bone phenotype [137]. However, the cytokine is important for osteoblast generation and osteoclastogenesis in pathologic conditions [121], as levels of IL-6 and sIL-6Rs appear elevated [32, 138]. This excess production may subsequently contribute to excessive osteoclastic bone resorption found in numerous metabolic diseases like multiple myeloma [139-140], Paget's disease [141] and rheumatoid arthritis [142] - diseases characterized by enlarged osteoclast activation and focal osteolytic lesions. Similarly, nude mice treated with exogenous IL-6 display augmented osteoclastogenesis and accelerated bone resorption with increased numbers of $TRAcP^+$ multinucleated cells as well as a marked decrease of trabecular bone volume when compared to placebo-treated mice [127].

Breast cancer

Breast cancer is the most common cancer (29%) and the leading cause of cancer-related death among women (17%) followed by cancer of the colon and rectum and lung cancer (Figure 4) [143-147]. If detected in localized stages confined to the primary site, prognosis is quite favourable, enclosing a mean five-year survival rate of 98%, which declines to only 26% when breast cancer is diagnosed initially in metastatic states [148].

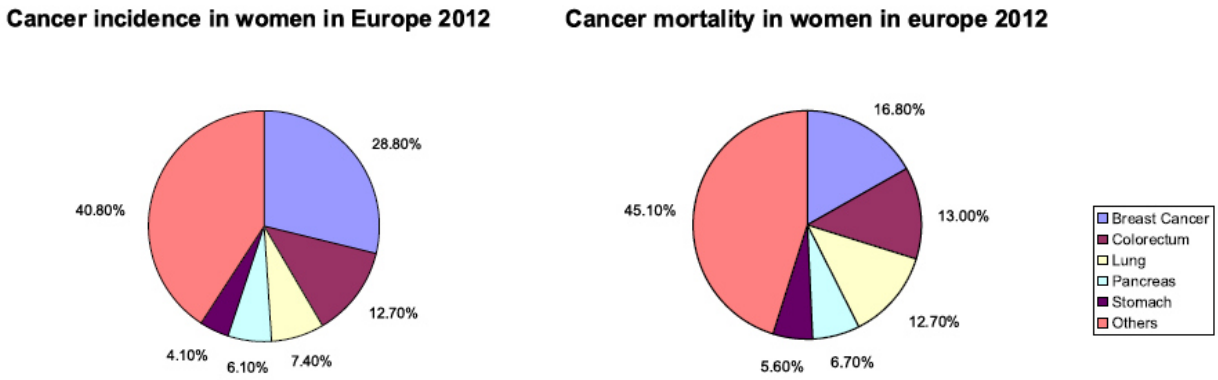

Figure 4: Incidence and mortality in % of common cancers in women in Europe 2012. Adapted from [147]

Breast cancer bone metastases

Most cancer-related deaths are not attributed to primary tumours, but to their spread to secondary sites [78, 149]. Micro-metastases persisting in various tissues after removing the primarius represent the pathophysiological basis for cancer relapse as overt metastases [150]. Patients with advanced breast or prostate cancer almost always develop bone metastases, and chances are high that, in patients originally diagnosed with breast or prostate cancer, the majority of the tumour mass at the time of death will appear in bone [78]. The skeleton is the preferred metastatic site for breast and prostate cancer, tumours of the lung, renal cell carcinoma, melanoma and multiple myeloma [143]. Not every type of cancer can prosper in all secondary sites. The concept that there is a relationship between the seed - the tumour cell - and the soil – the metastatic site - that determines the cancer's capacity to grow and thrive was first proposed by Paget in 1889: "One remote organ is more prone to be the seat of secondary cancer growth than others. […] In cancer of the breast, the bones suffer in a special way, which cannot be explained by any theory of embolism alone." [151] He also stated that the bone microenvironment provides a fertile soil for prosperity and aggressive behaviour of breast cancer cells, thus rendering the seed dependent on the soil [151-152]. Molecular interactions between tumour cells and host cells of the bone

microenvironment are crucial for providing a fertile soil for secondary growth of cancer cells [78, 152]. Bone metastases are infrequently silent since they are usually associated with intractable pain. Furthermore, patients suffer from so-called skeletal-related events (SREs) which comprise increased bone fragility, causing pathological fractures in 60%; bone deformation resulting in nerve and spinal cord compression syndromes among 10% of all patients; and hypercalcemia and leukoerythroblastic anaemia due to bone marrow suppression [78, 143, 153-154]. Subsequently, SREs increase morbidity and mortality and diminish quality of life significantly [143].

Traditionally, two phenotypes of bone metastases are distinguished: osteolytic ones characterized by increased bone resorption due to osteoclast-activating factors such as PTHrP, IL-11, IL-8 and IL-6 [76], and osteoblastic ones in which ET-1 and PDGF stimulate osteoblast proliferation and differentiation, leading to extensive disorganized bone formation [78, 143-144]. The preferred type of metastases seems to be dependent on the cancer cells invading bone: multiple myeloma almost always causes osteolytic metastases, whereas prostate cancer bone metastases are mainly osteoblastic [78]. Secondary tumour growth of breast cancer in bone causes, in most cases, osteolytic metastases. 80% of patients suffering from advanced breast cancer exhibit osteolytic lesions [143-144]. Nevertheless, up to 15% of patients with bone metastases from breast cancer develop osteoblastic or mixed metastases [143]. However, it is not possible to determine bone metastases by these characteristics alone, since most lesions incorporate components of both phenotypes. Rather, there is a spectrum ranging from osteolytic to osteoblastic with heterogeneity within and in between lesions [155].

Whereas the predominant effect of the breast cancer cells in bone is osteolysis, usually, there is also a local bone formation response, which can be regarded as an attempt at bone repair. Bone resorption and formation are still coupled, even though the equilibrium is often distorted [76, 78]. Hence, serum markers of osteoblast activity as ALP or P1NP increase in parallel with elevated indicators of bone resorption like TRACP [78].

Establishing bone metastases is an inefficient multi-step process occurring in late stages of tumour progression [78, 143]. To begin with, cancer cells detach from primary tumours and invade surrounding tissues. This crucial step is facilitated by tumour-produced factors that increase motility of cancer cells and enhance production of proteolytic enzymes such as MMP1, a collagenase essential for degrading ECM [153]. Later on, tumour cells traverse walls of small blood vessels and enter the circulation – a process called intravasation. Once in the blood stream, tumour cells are attracted by chemotactic agents to distant sites like bone marrow, where they arrest in bone sinusoids and extravasate across sinusoidal walls. Here, cancer cells adhere to the

endosteal surface via integrin αVβ3, invade the marrow stroma and finally colonize bone as micro-metastases or dormant cells [78, 143, 156]. An important molecule that mediates migration of cancer cells to bone is osteoblast-secreted SDF-1, which binds to CXCR4 on cancer cells [153].

After colonizing bone, tumour cells have to survive and evade immune surveillance, grow in, and often alter the new environment and, later, generate their own blood supply as soon as cell complexes are larger than 1mm^3 [78, 150].

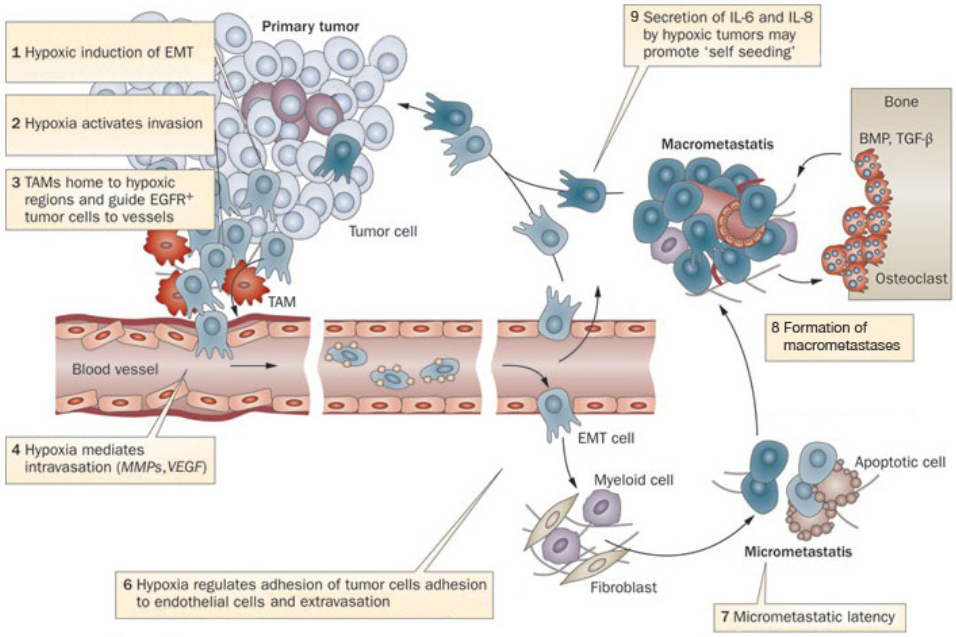

Figure 5: Scheme for establishing bone metastases. TAM = tumour associated macrophage, EGFR+ = epidermal growth factor receptor positive, MMP = matrix-metallo proteinase, VEGF = vascular endothelial growth factor, BMP = bone morphogenetic protein, TGF-β = transforming growth factor β, Adapted from [157]

It is well known that tumour cells, residing in different metastatic sites, show subtle phenotypic differences affecting their behaviour and their response to therapy [78]. Moreover, the ability of cancer cells to metastasize only occurs after gradual accumulation of a necessary set of pro-metastatic mutations and therefore can be regarded as state of advanced disease [149, 158]. The so-called poor prognosis signature of breast cancer cells determines expression patterns of 70 genes in primary tumours in order to predict metastatic potential and survival. This specific signature is associated with ER- and is also found in MDA-MB-231 cells [158].

Kang et al. identified the bone-metastatic signature of breast cancer cells: mRNA expression patterns that strongly correlate with increased metastasis to bone that may already be expressed by some cells within the primary tumour [159]. However, this gene expression profile does not correlate with the poor-prognosis signature. Five of these bone-metastatic mRNAs encode CXCR4, CTGF, MMP-1, IL-11 and Osteopontin (Opn). The receptor CXCR4 conveys chemoattraction of circulating tumour cells to bone. Subsequently, invasion of bone ECM is enabled by MMP-1, making the bone surface palatable for osteoclasts. IL-11 efficaciously stimulates osteoclastic bone resorption, whereas CTGF enhances tumour growth and angiogenesis. Both CTGF and Opn further amplify effects of other growth factors, thus accelerating bone resorption [159]. Although none of these factors promotes bone metastatic ability by itself, the concerted effect of some or all of them is fatal. It is also worth noting, that TGF-β further increases secretion of these proteins, leading to even greater concentrations once cells colonize bone [159]. Hence, growth at certain metastatic sites is dependent on proteins conferring tumour-stroma interactions, which explains why metastatic cells may prosper at one site but not at another [158].

Tumour-induced bone destruction removes a physiological barrier to tumour expansion, while growth factors stored in the bone matrix are released and enhance tumour growth [156]. Extensive cancer-related osteolysis is not primarily caused by direct effects of cancer cells on bone, but mainly attributed to actions of osteoclasts whose number and activity are increased near metastatic foci due to factors secreted by breast cancer cells like PTHrP, IL-1, IL-6, PGE_2 and M-CSF [78, 160-161].

Breast cancer cells produce and secrete PTHrP constitutively at low levels, and increased expression is found in cells exposed to bone [162-163]. Despite the fact that PTHrP expression in primary tumours of the breast is associated with a more favourable outcome [164], the effect on bone metastatic potential is not clear [163-164]. Showing 70% homology with PTH and binding to the common PTH/PTHrP receptor [153], PTHrP is the main mediator of humoral hypercalcemia of malignancy and tumour-induced bone resorption, based on its very strong potential to induce RANKL production in osteoblastic and bone stromal cells [78, 153]. Osteolysis caused by human breast cancer cells was blocked with neutralizing antibodies against PTHrP [165].
Additionally, elevated levels of extracellular calcium at sites of bone resorption, activate calcium-sensing receptors on breast cancer cells, increasing secretion of PTHrP too [100].

Therefore, PTHrP plays an important role in local establishment and progression of breast cancer bone metastases [153].

Other molecules such as IL-6, PGE_2 and 1,25 dihydroxyvitamin D increase RANKL concentrations to a smaller extent than PTHrP [78, 153]. Moreover, IL-6 potentiates effects of PTHrP on osteoclast activation, since it provides additional precursors responsive to PTHrP-induced osteoclast activation.
Furthermore, hypoxia stimulates osteoclast differentiation and thus development of osteolytic metastases [143].

MMPs are produced by both tumour cells and stromal cells, contributing to invasion, migration and colonization of cancer cells in the bone microenvironment. MMP-1, an interstitial collagenase for collagen I, is constitutively expressed in MDA-MB-231 cells and advances osteolysis [143].

The bone matrix is enriched with numerous osteoblast-derived growth factors that are released in the bone microenvironment upon osteoclastic bone resorption. TGF-β is embedded in a latent form, which has to be activated by proteases secreted by osteoblasts or cancer cells such as MMPs [143]. Its role in cancer metastases is well established: this protein enhances motility and invasive potential of MDA-MB-231 breast cancer cells; its signalling reduces HLA expression on tumour cells and therefore facilitates escape from immune surveillance. Moreover, TGF-β increases angiogenesis by enhancing VEGF expression in cancer cells [143]; stimulates further expression of PTHrP, CTGF and IL-11 in breast cancer cells and COX-2 activity in osteoblasts, bone marrow stromal cells and breast cancer cells; augments levels of osteoclast-activating factors RANKL and IL-8 and promotes osteoblast maturation [143, 153].
IGF-1 and IGF-2 are the most abundant growth factors found in the bone matrix. They cause proliferation of metastatic cancer cells while at the same time being anti-apoptotic, and enhance production of pro-resorptive, angiogenic and invasive factors [78, 143].

To summarize all these observations, interactions between tumour cells and the bone microenvironment can be described as the vicious cycle of bone metastases (Figure 6). In this concept, breast cancer cells in bone produce pro-resorptive factors such as IL-6 and PTHrP that induce osteoclast maturation and osteoclastic bone resorption and, following osteolysis, high concentrations of growth factors and elevated levels of extracellular calcium, enhance

proliferation of metastatic cancer cells, serve as chemoattracting factors for circulating cancer cells and increase secretion of pro-resorptive factors that support further osteolysis [78, 100, 143, 153]. The idea of the vicious cycle of bone metastases also alters the approach to treating bone metastases, since inhibitors of osteolysis might also decrease tumour burden. Numerous studies have already demonstrated that inhibition of bone resorption by administering anti-resorptive agents, such as bisphosphonates or OPG, to murine models of bone metastases not only protect skeletal integrity but also decrease breast cancer cell proliferation in bone and induce apoptosis of metastatic cells [78, 150, 166-168]. Conversely, accelerated bone resorption by calcium or vitamin-D deficiency as well as osteoclast-activation by GM-CSF [169] enhances breast cancer metastatic growth in bone [170-172]. Despite exerting direct apoptotic effects on breast cancer cells *in vitro* [173], bisphosphonates inhibit tumour progression only within bone. Once in extraosseous space, tumour behaviour does not differ between treated and untreated animals [150, 156]. Thus, delayed proliferation should be regarded as a secondary effect of suppressed bone resorption rather than a direct effect of the agents on breast cancer cells. In particular, the initial growth phase of breast cancer cells in bone is dependent on interactions with the bone microenvironment – once macro-metastases are grown to a certain size they tend to progress autonomously [150].

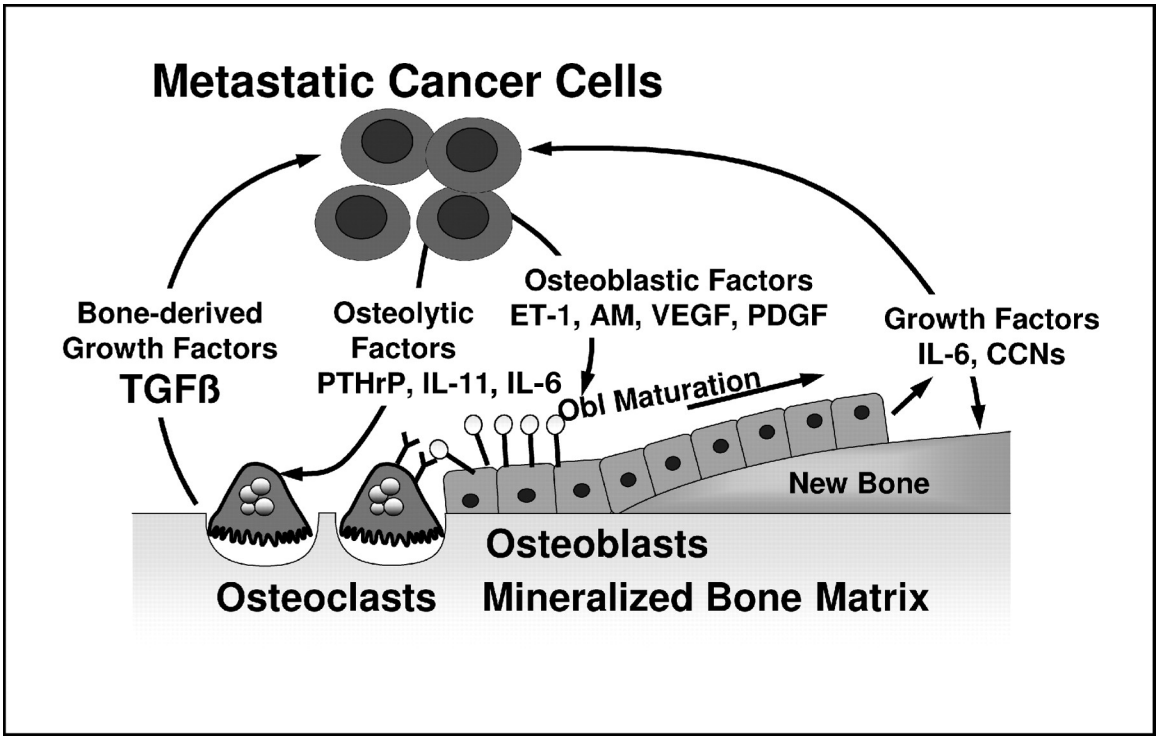

Figure 6: Vicious cycle of bone metastases. Adapted from [76]

Interleukin-6 and breast cancer patients

IL-6 and its major effector STAT3 have been implicated as pro-tumourigenic agents in many cancers, including breast cancer. Serum levels of this cytokine are elevated significantly in breast cancer patients expecting poor prognosis and have been associated with disease progression, augmented number of metastatic sites and poor prognosis in stages of metastatic disease [174-176]. The sources of IL-6 were found to be tumour cells as well as immune cells, especially T cells involved in tumour immunogenic response [175, 177].

Effects of Interleukin-6 on breast cancer cells and their metastases

Breast cancer cells express mIL-6Rs, gp130 and supply sIL-6Rs [160, 178]. As described above, IL-6/IL-6R complexes activate both the MAPK as well the STAT1/STAT3 signalling pathways in target cells [179]. Recently, it has been shown that a cross-talk between these two exists [60]. Berishaj et al. showed that the principal mechanism of STAT3 activation in breast cancer cells is through the IL-6/gp130/JAK pathway, even though other molecules are theoretically capable of STAT3 phosphorylation. Furthermore, they demonstrated that STAT3 phosphorylation is blocked by JAK inhibition, gp130 or IL-6 blockage, thus indicating that high levels of phosphorylated STAT3 correlate with high IL-6 levels [180].

Normal mammary epithelial cells produce IL-6 and IL-8 [181]. Several breast cancer cells within primary tumours as well as certain breast cancer cell lines like MDA-MB-231 [178] express IL-6 constitutively. Production of IL-6 is up-regulated by cytokines like IL-1 and TNF, as well as by specific oncogenes as mutated Rb and p53 [182]. Thus, over-expression of this cytokine in malignancies is probably due to loss of function of these genes [38]. Rates of IL-6 expression in human primary tumours do not correlate with any clinical prognosticator, but a trend towards advancing bone metastases is described [160]. Moreover, STAT3 cooperates with NFκB in IL-6 induction [179, 183]. In oestrogen-receptor negative (ER-) breast cancer cell lines like MDA-MB-231, IL-6 is constitutively produced and secreted and consequently STAT3 is constitutively active in these mIL-6R expressing cells.

On the contrary, oestrogen receptor positive (ER+) breast cancer cells like MCF-7 show activation of STAT3 after stimulation with IL-6 [184]. Thus, auto- or paracrine IL-6 stimulation of cancer cells might lead to augmented IL-6 production, which again enforces effects of IL-6 on tumour cells and the bone microenvironment in a feed-forward mechanism.

Concerning the vitality of *in vitro* breast cancer cells, IL-6 seems to be a double-edged sword: there are several reports indicating IL-6 to be both a tumour-promoting and a tumour-counteracting cytokine [174, 176]. The role of IL-6 concerning breast cancer cell growth is controversial. It is worth noting, that effects of IL-6 on breast cancer cells concerning proliferation are dependent on the oestrogen-receptor status and the environment the cells are exposed to. Whereas increased DNA synthesis is observed in normal mammary epithelial cells after IL-6 stimulation, neoplastic breast tissue does not proliferate in response to IL-6 [181]. Indeed, growth rates of ER+ breast cancer cell lines are usually reduced by IL-6, whereas more aggressive ER- cell lines are frequently resistant to IL-6 induced growth inhibition [160]. Nevertheless, the signalling cascade in these cells after IL-6 stimulation is active, suggesting a selective loss of IL-6 response in ER- breast cancer cell lines [178].

However, there is a consensus that IL-6 promotes metastasis of breast cancer cells by up-regulating gene expression of VEGF, supporting migration and multi-drug resistance [38].

Furthermore, growth-inhibitory effects of TGF-β on ductual carcinomas are diminished compared to normal tissue [181]. MDA-MB-231 cells display selective loss of TGF-β anti-proliferative gene response without loss of receptors or downstream Smad signalling capacities. TGF-β even promotes invasion in metastases rendering it a tumour progression factor. Primary cancer cells experience growth inhibition in response to TGF-β signalling. By contrast, advanced cancer cells frequently escape this effect selectively, while other regulatory functions of TGF-β are retained. In these circumstances, TGF-β induces an epithelial-to-mesenchymal transition of breast cancer cells and stimulates further invasion [143, 153]. Epithelial-to-mesenchymal transition encloses reactivation and loss of regulation of cellular programmes associated with wound healing and embryogenesis, thus loss of differentiation [149].

IL-6 signalling also confers resistance towards apoptosis in ER- breast cancer cell lines by inducing anti-apoptotic, pro-survival proteins. Again, the ER+ breast cancer cell line MCF-7 responds opposingly to IL-6 stimulation by increasing the ratio of apoptotic cells [174]. It was demonstrated that IL-6 protects cells from undergoing apoptosis but does not directly augment proliferation: Cancer cells stimulated with IL-6 display high proportions of cells entering the S-phase mediated via STAT3 induced expression of c-myc, cyclin D1, Pim-1 and Pim-2 which mark cells with high proliferative potential [179, 185-186]. However, IL-6 stimulation does not alter the cell cycle profile itself, since transition from S- into M-phase is an action exerted via

MAPK [179]. There is no evidence that MAPK activities are also increasingly activated in breast cancer cell lines. Thus, IL-6 primarily acts as a survival factor rather than a proliferative factor [187].
Anti-apoptotic effects of IL-6 are mainly mediated via STAT3 activation and include enhanced expression of bcl-xL, bcl-2 and mcl-1 [179, 185, 187]. Furthermore, elevated levels of phosphorylated STAT3 increase survivin gene transcription, a member of the inhibitor of apoptosis protein family. High serum levels of survivin correlate with invasiveness of tumours and survival from chemotherapy [188].

As tumours usually induce a certain degree of inflammatory response, inflammatory cytokines also play a role in cancer progression. It was shown that IL-6 induces DNA-damage and inhibits its repair, therefore promoting accumulation of mutations [149]. Anti-inflammatory properties of IL-6 inhibit local production of IL-1, TNF and MCP-1 and enhance expression of IL-1R antagonists, thus causing local immunosuppression to help the tumour escape from the immune system [189].

Besides its role in apoptosis, IL-6 promotes breast cancer cell motility, indicating a role in metastasis. This effect is possibly mediated by decreased E-cadherin expression and thus diminished cell-cell adhesion after IL-6R activation. Since oestrogen receptors repress IL-6 expression in breast cancer cell lines, up-regulation of this cytokine in ER- cells may be involved in mediating high invasiveness and metastatic capability of these cells [174].

In addition to influencing cancer cell biology, IL-6 induced STAT3 signalling in cancer cells increases production of VEGF in MDA-MB-231 cells, thus promoting metastases [188]. VEGF is an important pro-angiogenic protein, stimulating proliferation of epithelial cells and enabling tumours to exhibit a more malignant phenotype [175]. At some point, tumours face hypoxic conditions due to limited diffusion of nutrients and oxygen. Under physiologic conditions, cells produce HIF-1α, which initiates angiogenesis. MDA-MB-231 cells however, overexpress HIF-1α [143] and hence, pro-invasive, pro-metastatic and angiogenic factors regulated by HIF-1α are also produced extensively. Furthermore, IL-6 induces Notch3 dependent up-regulation of CA-IX, rendering cells more resistant to hypoxia and promoting invasion of tumour cells [176].

In addition, auto- or paracrine IL-6R activation promotes multi-drug resistance in breast cancer cells by enhancing mdr1 transcription. This gene encodes the transmembrane P-glycoprotein (P-

gp), an ATP-dependent pump, reducing intracellular concentrations of anti-cancer drugs [60]. Similarly, exogenous IL-6 induces gp96 transcription in MDA-MB-231 cells – a glucose related stress protein associated with drug resistance in tumour cells [174].

Not only tumour-derived IL-6 exerts actions on breast cancer cells. Within the microenvironment, other cells, such as adipose stromal cells, produce IL-6 that enables phosphorylation and thus activation of STAT3 associated with survival, evasion from the immune system, invasion and migration of MDA-MB-231 cells, too [190] [184, 189]. Knock-down of STAT3 or inhibition of its phosphorylation was shown to delay tumour growth in a xenograft model [183], decrease angiogenesis and up-regulate TIMP-3 expression, an inhibitor of VEGF and MMP-9 [191].

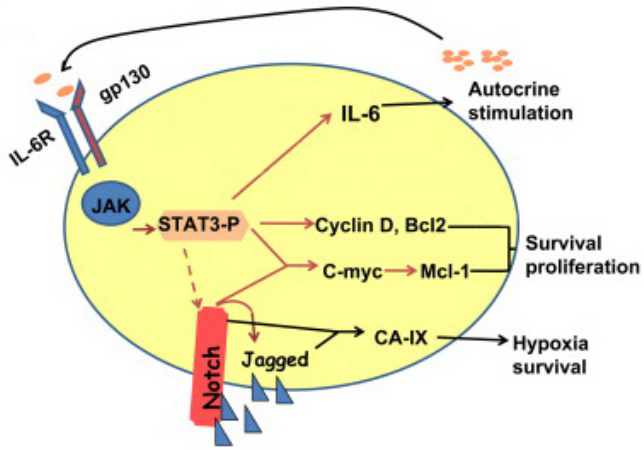

Figure 7: The role of IL-6 signalling in cancer cells. IL-6 dependent STAT3 activation results in numerous downstream events required for tumour growth. The IL-6/Notch/Jagged pathway activates the expression of the hypoxia resistance gene CA-IX. Other IL-6/STAT3 dependent pathways include production of IL-6, activation of genes required for cell survival and proliferation (c-myc, Cyclin D, Bcl2) and initiation of tumour suppressor genes. Adapted from [183]

Tocilizumab

Tocilizumab is a humanized anti-human IL-6R mAb, which prevents IL-6 binding to its receptor in a competitive manner. It is fused from the antigen-binding region of a murine anti-IL-6R antibody and a human IgG1 framework in order to minimize potential immunogenic responses and prolong the half-life time of the antibody [192]. Tocilizumab displays a non-linear pharmacokinetic profile: with increasing dosages maximum concentrations increase, whereas clearance and apparent elimination rate constantly decrease and terminal half-life time and mean

residence time are prolonged. Half-life reaches about 240 hours after the third dose of 8mg/kg tocilizumab in humans. Tocilizumab binds both sIL-6Rs and mIL-6Rs in a dose-dependent manner, saturating receptors at approximately 0.1μg/ml; complete inhibition of IL-6 binding is achieved at 4μg/ml [39, 193]. No cross-reactivity with other IL-6 family cytokine receptors exits and no agonistic effects on the IL-6 receptor are known [193]. Thus tocilizumab is specific for human IL-6Rs.

Initially developed for treatment of inflammatory autoimmune diseases in which IL-6 seems to play a pathogenetic role, clinical trials proved the efficacy of tocilizumab for alleviating symptoms caused by RA, systemic onset of juvenile idiopathic arthritis, Castleman's disease and Crohn's disease [39, 193]. In general, treatment was tolerated well. Adverse events included mild and transient liver function changes and neutropenia, increased risk of infections, especially upper-respiratory tract infections, and nasopharyngitis. The most common side effects reported were mild gastrointestinal events like diarrhoea [192]. Being a humanized antibody, infusion-related events are possible and were observed in a small number of patients. In some cases, anti-tocilizumab antibodies were detected, indicating a certain degree of immunogenicity [39]. Uchiyma et al. revealed that increased blood levels of IL-6 and sIL-6Rs are due to impaired clearance form the serum instead of increased production during tocilizumab treatment. As a result, half-life time of IL-6 is prolonged, with subsequent accumulation of the cytokine which might override effects of antibody efficacy since it competes with IL-6 for the receptor binding [194].

MR16-1

MR16-1 is a rat anti-mouse IL-6R mAb of the IgG1 type [195-196] binding dose-dependently to murine mIL-6Rs and sIL-6Rs and blocking IL-6 induced signalling in a competitive manner. Thus, inhibition can be reversed by high concentrations of IL-6 [197]. Concerning bone biology, treatment of mice with MR16-1 prevented inflammatory osteoclast precursor formation from spleen cells after stimulation with M-CSF and RANKL and thus inhibited bone resorption in states of systemic inflammation [195]. IL-6R blockage in mice proved efficient in suppressing SAA production and consequent amyloid deposition in various organs. It prevented onset of Castleman's disease-like symptoms in IL-6 transgenic mice, as well as C-protein induced myositis in a dose-dependent manner [198-200]. Furthermore, MR16-1 prevented cancer-related anaemia and muscular atrophy in mice inoculated with human IL-6 producing tumour cells [201]. As seen in humans treated with tocilizumab, MR16-1 increases serum levels of IL-6 based

on impaired clearance [202]. Mihara et al. revealed that IL-6 does not always influence specific antibody production, but is crucial for induction of Th_1 cells and differentiation of cytotoxic T cells [199, 202].

MDA-MB-231 human breast cancer cell line

The bone-seeking clone MDA-Tx-SA was derived from the human oestrogen-receptor negative MDA-MB-231 breast cancer cell line. It exhibits a highly dedifferentiated phenotype and elevated potential for invasion [160]. These cell lines do not express RANKL, but various pro-resorptive factors enhancing RANKL production in bone cells and hence mediating osteoclast activation and bone resorption [100]. Previous studies have demonstrated that conditioned medium from the parental cells increases osteoclastogenesis in bone marrow cultures and bone resorbing activity of human osteoclasts. Hence, MDA-MB-231 cells secrete soluble factors influencing osteoclasts' resorptive capability even though the specific factors responsible are not yet determined. However, conditioned medium increases production and secretion of the cytokine IL-6 in human osteoclasts and osteoclast-like cells [203]. Yoneda et al. characterized the bone-seeking clone concerning tumourigenicity, metastatic capacity and biological properties compared to the parental cell line. Tumourigenicity at the orthotopic site does not differ, but in contrast to parental cells, the bone-seeking clone MDA-Tx-SA spreads exclusively to bone where it forms larger osteolytic lesions. Moreover, a greater amount of PTHrP is produced by cells of the bone-seeking clone, which further increases after addition of TGF-β. Whereas TGF-β impairs colony formation in parental cells, it does not inhibit colony formation in bone-seeking clones, even though signalling pathways are activated in both cell types to a similar extent [204]. IGF-1 profoundly induces colony formation in the bone-seeking clone but had no effect on the parental cell line [204].

The murine xenograft model

Murine IL-6 (mIL-6) is specific to the mouse IL-6R, whereas human IL-6 (hIL-6) activates both mouse and human IL-6Rs [184, 197, 205]. The anti-IL-6R mAbs administered are species specific, meaning tocilizumab only blocks human IL-6Rs whereas MR16-1 specifically inhibits IL-6 signalling of murine IL-6Rs [197]. However, in this constellation it becomes clear that MR16-1 does not only prevent activation of murine IL-6Rs by murine IL-6 but also by hIL-6, since the latter induces the receptors of both species [201]. This is once again illustrated in Figure 8.

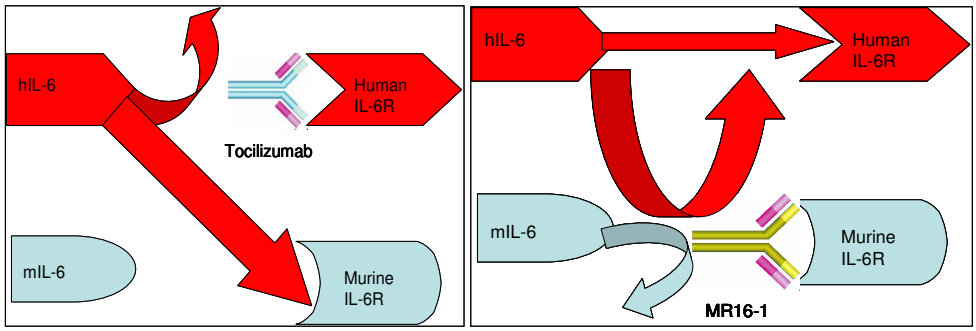

Figure 8: Tocilizumab and MR16-1 in the murine xenograft model. hIL-6 = human IL-6, mIL-6 = murine IL-6, human IL-6R = human IL-6 receptor, murine IL-6R = murine IL-6 receptor.

Hypothesis and Aims

Breast cancer is the most common malignancy and one of the leading causes of cancer death amongst women worldwide. Bone appears to be the most frequent site of breast cancer metastases. These bone metastases are not only associated with increased mortality, but also with significant morbidity, including immobility and the incidence of so-called SREs such as pathological fractures, spinal cord compression and hypercalcemia.

The cytokine IL-6 has been associated with pro-tumourigenic effects in many types of cancer including breast cancer. Significantly elevated serum levels of IL-6 in patients suffering from breast cancer have been related to poor prognosis in stages with metastatic disease, disease progression and an augmented number of metastatic sites.

Based on the literature above, IL-6 seems to have a strong pro-tumourigenic effect in breast cancer bone metastases activity, due to its multiple effects on bone metabolism, survival of tumour cells in bone and angiogenesis.

Tocilizumab is a humanized anti-human IL-6R mAb, which prevents binding of human IL-6 to the human IL-6R. MR 16-1, a rat anti-mouse IL-6R mAb, blocks murine IL-6Rs from being activated by either human IL-6 or murine IL-6.

The main hypothesis in this study was that blocking IL-6 signalling in metastatic human breast cancer cells in murine bone with tocilizumab and/or in cells of the bone microenvironment with MR16-1 reduces growth and vitality of breast cancer metastases in bone.

In order to investigate the effect of blocking IL-6R signalling in either tumour cells and/or bone cells, a murine xenograft model injected intratibially with human MDA MB-231 breast cancer cells was employed.

A minor hypothesis was that IL-6 signalling in human MDA-Tx-SA cells initiates a feed-forward mechanism, which augments IL-6 transcription and secretion by these cells and that this feed-forward mechanism is disrupted by blocking IL-6 signalling with IL-6R antibodies.

To demonstrate this, MDA-Tx-SA cells were cultured *in vitro* and treated with human IL-6 and the anti-human IL-6R mAb tocilizumab.

Materials and Methods

Antibodies

The humanized monoclonal antibody tocilizumab is composed of two heterodimers, each consisting of one heavy and one light chain. The four polypeptide chains are linked intra- and inter-molecularly by disulfide bonds. Heavy chains contain 448 amino acids (aa), while light chains have 214 aa. Tocilizumab has a molecular weight of approximately 148kDa.

MR16-1 is a rat anti-mouse IL-6R monoclonal antibody. The N-terminal region of MR16-1 contains the fibronectin domain II of mouse IL-6Rs (amino acids 214-285), which is required for binding of the antibody [197].

Breast cancer cell line

The ER- human breast cancer cell line MDA-MB-231 was established from a single pleural effusion obtained from a 51-year-old white woman with poorly differentiated adenocarcinoma [206]. A bone-seeking clone of this human breast cancer cell line, MDA-Tx-SA, was derived from the parental cell line and generously provided by Dr. T. Yoneda, Anderson Cancer Center, San Antonio, TX, U.S.A. This particular clone mainly causes metastases to bone when injected intracardially into nude mice, whereas parental cells also spread to brain and adrenal glands.

Tissue culture

Equipment, instruments and materials

EQUIPMENT, INSTRUMENTS	**MANUFACTURER, CITY, STATE, COUNTRY**
Incubator “Heracell 150”	Thermo Fischer Scientific GmbH, Dreiech, Germany
Scale “Mettler AE 240”	METTLER-Toledo GmbH, Gießen, Germany
Neubauer counting chamber, 0.1 mm depth	BRAND GmbH & Co KG, Wertheim, Germany
Tissue culture microscope “Axiovert 25”	Carl Zeiss Jena GmbH, Jena, Germany
Pipettes “Nichipet Ex” (0.5-10µl; 5-20µl; 20-200µl; 100- 1000µl)	Nichiryo Co., Ltd.,Tokyo, Japan
Sterile tissue culture hood “Herasafe”	Thermo Fischer Scientific GmbH, Dreiech, Germany
Liquid nitrogen storage tank (-196°C)	Taylor-Wharton Cryogenics, Theodore, AL, U.S.A.
Liquid nitrogen freezer “LS 3000”	Taylor-Wharton Cryogenics, Theodore, AL, U.S.A.
Freezer (-20°C) “Premium No-Frost”	Liebherr GmbH, Ochsenhausen, Germany

Freezer (-80°C) "Glacier -86"	NuAire, Plymouth, MN, U.S.A.
Vortexer "Vortex Genie 2"	Scientific Industries, Inc., Bohemia, NY, U.S.A.
Water bath (heatable)	Memmert GmbH & Co KG, Schwabach, Germany
Centrifuge "Allegra X15"	Beckman Coulter, Inc., Brea, CA, U.S.A.
Pipetting Aid	Eppendorf AG, Hamburg, Germany

Table 1: Equipment and instruments used in tissue culture experiments

MATERIALS	**MANUFACTURER, CITY, STATE, COUNTRY**
Tissue culture flasks (T75; T175)	BD Biosciences, Bedford, MA, U.S.A.
Falcon tubes (15ml; 50ml)	BD Labware, Franklin Lakes, NJ, U.S.A.
Multi-well plates (6; 96)	BD Labware, Franklin Lakes, NJ, U.S.A.
Pipette tips (0.5-10µl, 5-20µl, 20-200µl, 100-1000µl)	Labcon, Petaluma, CA, U.S.A
Latex gloves	Mediflex Industries, Arncliffe, NSW, Australia
Single-use syringes (10ml; 30ml)	Terumo Medical Corporation, Sommerset, NJ, U.S.A.
21 gauge needles	BD Labware, Franklin Lakes, NJ, U.S.A.
Standard micro test tubes (1.5ml; 2ml)	Eppendorf AG, Hamburg, Germany
Cryo-tubes 1,8ml	NuncBrand, Roskilde, Denmark
Sterile filters 0.22µm	Millipore, Cork, Ireland
RNAse-free pipette tips (0.5-10µl, 5-20µl, 20-200µl, 100-1000µl)	Axygen, Inc., Union City, CA, U.S.A.
Serological pipettes (5ml; 10ml; 25ml)	BD Labware, Franklin Lakes, NJ, U.S.A.
Laboratory parafilm	Pechiney Plastic Packaging, Chicago, IL, U.S.A.
Sterilisation bags "sterilope"	Dräger Medical AG & Co. KG, Lübeck, Germany

Table 2: Materials used in tissue culture

Media, buffer, reagents and supplements

MEDIA, BUFFER, REAGENTS AND SUPPLEMENTS	**MANUFACTURER, CITY, STATE, COUNTRY**
Dulbecco's Modified Eagle Medium - GlutaMAX™-I	Invitrogen, Carlsbad, CA, U.S.A
Dulbecco's Phosphate Buffered Saline (DPBS)	Invitrogen, CA, U.S.A
Fetal calf serum (FCS)	JRH Biosciences, KS, U.S.A
Penicillin (10000U/ml)/Streptomycin (10000µg/ml)	Invitrogen, Carlsbad, U.S.A
Trypan Blue Stain 0.4%	Invitrogen, Carlsbad, U.S.A
Trypsin 0.05%	Invitrogen, CA, U.S.A
Versene	Invitrogen, Carlsbad, CA, U.S.A
Albumin from bovine serum, Cohn V fraction	Sigma-Aldrich, St. Louis, MO, U.S.A.

Table 3: Media, buffer, reagents and supplements used for tissue culture experiments

Cancer cell line propagation

Conditions in tissue culture experiments were standardised at 37°C, 5% CO_2 and 100% humidity at all times. MDA-Tx-SA cells were cultured in Dulbecco's Modified Eagles' medium (DMEM) supplemented with 10% fetal calf serum (FCS) and 1% penicillin-streptomycin solution. Unless otherwise stated, supplemented DMEM refers to this specific supplementation of DMEM. According to necessity, 75cm^3 or 175cm^3 culture flasks were used. When cells reached approximately 80% confluence, they were routinely sub-cultured: medium and phosphate-buffered saline (PBS) were heated to 37°C and 0.05% trypsin was warmed to room temperature. Then, medium was removed from flasks using Pasteur pipettes and afterwards, cell layers were washed gently with PBS to remove any excess medium that might inactivate trypsin. Cells were further washed with 1ml trypsin, prior to detachment of cells from the bottom of the flasks by means of 2ml/4ml of trypsin for 75cm^3/175cm^3 flasks. An incubation period of 5 minutes at 37°C followed to ensure complete uplifting of cells. After having confirmed proper detachment of cells by microscopy, trypsin activity was terminated by adding 8ml/16ml of supplemented DMEM in 75cm^3/175cm^3. Cell suspensions were then transferred into 50ml Falcon tubes and cells were separated using a 10ml or 30ml syringe fitted with a 21-gauge needle in order to obtain single cell suspensions. Cell viability was determined by Trypan Blue exclusion. This routine method is based on the principle that only vital cells possess intact cell membranes that do not allow trypan blue dyes to penetrate, thus only inert cells are stained blue. After counting cells in a Neubauer counting chamber and calculating the cell concentrations, an appropriate dilution was selected for propagation of new subcultures. 75cm^3 flasks were usually filled with 20ml of supplemented DMEM while 175cm^3 flasks contained 50ml supplemented DMEM.

After sub-culturing, cells were incubated in standard conditions. If 80% confluence was not reached after 2-3 days, media were changed to ensure adequate provision of nutrients at all times.

Cell preparation for in vivo injection

For *in vivo* injections, MDA-Tx-SA cells were revived from frozen stock kept at -196°C in liquid nitrogen. Cells were thawed at room temperature and added into 9ml supplemented DMEM in 15ml Falcon tubes and spun for 5 minutes at 1000rpm. Excess medium was removed carefully with Pasteur pipettes and cell pellets were re-suspended before cells were transferred into 175cm^3 flasks containing 50ml supplemented DMEM and cultured in standard conditions. Cell

lines were routinely passaged 1-2 times before preparation for intratibial injections into mice: all medium and PBS were pre-warmed; Versene (0.02% EDTA;) was warmed to room temperature. Following rinsing with PBS, cell layers were rinsed with Versene prior to detachment with 2ml/4ml ($75cm^3$/$175cm^3$ flasks) Versene at 37°C for 30 minutes. Versene, rather than trypsin, was applied to detach cells for *in vivo* injections, since trypsin contains proteases that might harm cells and, therefore, impair growth *in vivo*. Subsequent to detachment, 8ml/16ml ($75cm^3$/$175cm^3$ flasks) PBS was added and cell suspensions were transferred into 50ml Falcon tubes. Cells were then washed twice by centrifugation at 1000rpm for 5 minutes in 10ml PBS, before an aliquot was removed for assessing viability via Trypan Blue exclusion. Only suspensions with > 95% viability were used for intratibial injections.

After final PBS wash and centrifugation, cells were re-suspended in PBS in order to obtain concentrations of $5*10^6$ Tx-SA cells/ml. Cells were left on ice until injection.

EQUIPMENT, INSTRUMENTS	**MANUFACTURER, CITY, STATE, COUNTRY**
Millipore water filter "MilliQ academic"	Milipore, Cork, Ireland
Water filter "Milli RX44"	Millipore, Cork, Ireland
Glassware	Schott Duran AG, Mainz, Germany
Scale "Mettler AE 240"	Mettler-Toledo GmbH, Gießen, Germany
Scale "sartorius portable"	Sartorius Stedim Biotech S.A, Aubagne Cedex, France
Centrifuge "Allegra X15"	Beckman Coulter, Inc., Brea, CA, U.S.A.
Centrifuge "5415D"	Eppendorf AG, Hamburg, Germany
Sterilizer "110A series"	Atherton sterilizers, Melbourne, VIC, Australia
Autoclave	Labec Pharma, Madrid, Spain
Ice machine "AF80"	Scotsman Ice Systems, Vernon Hills, IL, U.S.A.
Transluminator "BioDoc Analyze"	Biometra GmbH, Göttingen, Germany
Spectrometer "Bio Photometer"	Eppendorf AG, Hamburg, Germany
Cuvettes 220-1600nm	Eppendorf AG, Hamburg, Germany
Stirrer and hot plate "Rci basis"	IKA Works, Wilmington, USA
PH Meter "Microprocessor pH 210"	HANNA instruments Inc., Woonsocket, RI, U.S.A.
Vortexer "Vortex Genie 2"	Scientific Industries, Inc., Bohemia, NY, U.S.A.
Pipetting Aid "Easypet"	Eppendorf AG, Hamburg, Germany
Pipettes (0.5-10µl; 5-20µl; 10-100µl; 20-200µl; 100-1000µl)	Eppendorf AG, Hamburg, Germany
Heatblock " Thermomixer comfort"	Eppendorf AG, Hamburg, Germany

Table 4: Equipment and instruments used for general laboratory work

MATERIALS	MANUFACTURER, CITY, STATE, COUNTRY
PBS tablets	AMRESCO Inc., Solon, OH, U.S.A.
100% ethanol	FRONINE Laboratory Supplies, Riverstone, NSW, Australia
100% ethanol, molecular biology grade	FRONINE Laboratory Supplies, Riverstone, NSW, Australia
Pipette tips (0.5-10µl, 5-20µl, 20-200µl, 100-1000µl)	Labcon, Petaluma, CA, U.S.A
Pipette tips RNAse-free (0.5-10µl, 5-20µl, 20-200µl, 100-1000µl)	Axygen, Inc., Union City, CA, U.S.A.
Falcon tubes (15ml; 50ml)	BD Labware, Franklin Lakes, NJ, U.S.A.

Table 5: Materials used for general laboratory work

MATERIALS	MANUFACTURER, CITY, STATE, COUNTRY
innuPREP RNA Mini Kit	Analytic Jena AG, bio solutions, Jena, Germany
Agarose	Invitrogen, Carlsbad, CA, U.S.A
TE Buffer "TBE 10x"	AMRESCO Inc., Solon, OH, U.S.A.
SYBR Green "SYBR Safe"	Invitrogen, Carlsbad, CA, U.S.A
RNA/DNA dye	Invitrogen, Carlsbad, CA, U.S.A

Table 6: Materials used for *in vitro* experiments

Molecular biology and hIL-6 ELISA

RNA extraction and quantification

Ribonucleic acid (RNA) extraction was performed using the innuPREP RNA Mini Kit (Analytic Jena AG, Germany), following the manufacturer's protocol. All materials used were RNAse free. In brief, media were removed from the wells and cell-pellets were washed with chilled PBS twice, before being lysed with 400µl lysis solution for 2 minutes at room temperature. Lysis solution contains large amounts of chaotropic ions and inactivates RNAse immediately. Then, samples were transferred onto spin filters fitted into receiver tubes and centrifuged. Filtrates were then diluted with 70% ethanol (molecular biology grade), solutions were transferred onto another spin filter and spun again before two washing steps with different washing solutions were carried out. The spin filter, fitted into new receiver tubes, was then centrifuged again to remove all traces of ethanol and, finally, placed onto elution tubes. 60µl RNAse-free water was added onto spin filters containing the RNA, incubated for 1 minute at room temperature and then centrifuged again to collect diluted RNA in the elution tubes. RNA was kept on ice until routinely freezing at -80°C for long-term storage to ensure RNA stability.

After subsequent RNA extraction, its quality was assessed in 1% agarose gel supplemented with 6% SYBR GREEN. 2µl RNA sample was diluted in 10µl RNase-free water and 1.5µl RNA-dye and pipetted into pockets of the gel. It was run for 30 minutes at 120V and then assessed under UV light. Additionally, RNA quality and quantity was analysed by spectrometry. Here, isolated RNA was diluted 2:98 in RNAse free water and the amount of RNA in this solution was measured at 260nm (ratio 260/280 >1.8).

Reverse transcription (RT)

In the reverse transcription process, single-stranded DNA molecules are produced from RNA templates. Basically, single-stranded messenger RNA (mRNA) is reverse transcribed into complementary DNA (cDNA) by incubating total cellular RNA with reverse transcriptase enzymes, primers (Oligo-dT), Deoxynucleotide Triphosphates, dNTPs, and RNAse inhibitors. The cDNA obtained is utilized in reverse transcription polymerase chain reactions (RT-PCR). In this work, RT reactions were performed with 1µg RNA incubated with 1µl primer (Oligo-dT), 1µl dNTP Mix (10mM each) and sterile distilled water at 65°C for 5 minutes. This step ensures denaturation of RNA secondary structures, followed by a quick chill on ice to prevent re-naturation. Subsequently, reverse transcription reactions are started by adding RNAse inhibitor, reverse transcriptase, 5x First Strand Buffer and 0.1M Dithiothreitol for 1 hour at 50°C. The enzymes are then inactivated by heating the mixture to 70°C for 15 minutes and, therefore, stopping the reactions.

MATERIALS	**MANUFACTURER, CITY, STATE, COUNTRY**
Oligo (dT) Primer	Promega, Fitchburg, WI, U.S.A.
dNTP Mix (10 mM)	Invitrogen, Carlsbad, CA, U.S.A
Recombinant Ribonuclease Inhibitor "RNaseOUT™"	Invitrogen, Carlsbad, CA, U.S.A
Reverse Transcriptase "SuperScript.III"	Invitrogen, Carlsbad, CA, U.S.A
5x First Strand Buffer	Invitrogen, Carlsbad, CA, U.S.A
0.1M Dithiothreitol (DTT)	Invitrogen, Carlsbad, CA, U.S.A

Table 7: Materials used in reverse transcription reactions

Real-time polymerase chain reaction (qPCR)

Cells regulate expression and turnover of gene transcripts, so-called messenger RNAs (mRNA). As a matter of fact, the number of mRNA transcripts of a certain gene in cells or tissues is

determined by expression and degradation of the former, which correlates in most cases with expression rates of encoded proteins.

The real-time polymerase chain reaction, also called quantitative real time polymerase chain reaction (qPCR), is a technique in molecular biology based on PCR. Standard PCR amplifies DNA or complimentary DNA (cDNA). In brief, thermostable DNA polymerase as well as 5' and 3' (forward and reverse) specific DNA primers are added to cDNA. At the beginning, the reaction mixture is heated to 95°C in order to denature DNA templates. Then, reactions are repeated as denaturation - primer annealing - extending cycles. Usually, denaturation is performed at 95°C for 0.5-2 minutes, annealing for 0.5 minutes at optimal annealing temperatures and extension steps are performed for 0.5-2 minutes at 72°C depending on the length of amplified DNA products. The number of PCR cycles necessary is dependent both on the amount cDNA template at the beginning and on the expected yield of the PCR product. Generally, after approximately 30 cycles the copies of interest are sufficient. After completing the last cycle, samples are usually incubated at 72°C for 5-15 minutes as a final extension step to fill in protruding ends of newly synthesized PCR products.

In contrast to standard PCR, real time PCR not only amplifies genes of interest but also facilitates detection and simultaneous quantification of specific sequences in DNA samples. The procedure follows the general principle of polymerase chain reaction: its key feature being quantification of amplified DNA after each cycle as the reaction progresses. Two common methods for detection of products in real-time PCR are: (1) non-specific fluorescent dyes that intercalate with any double-stranded DNA (dsDNA), and (2) sequence-specific DNA probes consisting of oligonucleotides labelled with fluorescent reporters, permitting detection only after hybridization of probes with complementary DNA targets. In this thesis, the SYBR Green method was applied, in which DNA-binding dye adheres to all dsDNA, causing fluorescence of the dye. Increasing amount of dsDNA during PCR consequently results in augmented fluorescence intensity, thus allowing quantification of DNA concentrations. However, dsDNA dyes such as SYBR Green bind to all dsDNA, including non-specific PCR products such as primers. This can potentially interfere with or prevent accurate quantification of the intended target sequence.

The reactions are prepared by adding 10µl iQ SYBR Green Supermix containing 100 mM KCl, 40 mM Tris-HCI, pH 8.4, 0.4 mM of each dNTP (dATP, dCTP, dGTP, and dTTP), iTaq DNA polymerase, 50 units/ml, 6 mM MgCl2, SYBR Green I, 20 nM fluorecein, and stabilizers, 1µl

forward and 1µl reverse primer for genes of interest and 4µl sterile, distilled water into each well of flat capped PCR tubes. Afterwards, 4µl of cDNA for the respective cDNA sample was added, the solutions were mixed and real-time PCR was run using the iQ5 cycler (BioRad, Munich, Germany). The primers used in this thesis were designed by Associate Professor Hong Zhou.

All samples were prepared in duplicates, as negative control, 4µl sterile, distilled water was added instead of cDNA. The protocol included DNA denaturation at 95°C for 3 minutes, followed by 40 cycles composed of DNA denaturation at 95°C for 10 seconds, primer annealing at 60°C for 15 seconds and extension at 72°C for 30 seconds. All data were analysed using BioRad iQ5 software and normalised against human GAPDH mRNA expression. Relative concentrations of cDNA, present during the exponential phase of the reaction, were determined by plotting fluorescence against cycle number logarithmically. A threshold for detection of fluorescence above background was determined. Cycle threshold C_t determines the cycle at which fluorescence from samples crosses the threshold. The amount of DNA theoretically doubles every cycle during the exponential phase and relative quantities of cDNA can be calculated. Since all sets of primers do not work equally well, reaction efficiency needs to be considered. Thus, by using this as base and the cycle difference as exponent, precise difference in starting templates can be calculated.

Amounts of cDNA were then determined by comparing results to standard curves produced by real-time PCR of serial dilutions of specified amounts of DNA. In order to accurately quantify gene expression, measured amounts of DNA from genes of interest were divided by the amount of DNA from the housekeeping gene hGAPDH measured in the sample to normalize for possible variations in amount and quality of DNA between different samples. This normalization permits accurate comparison of expression of genes of interest between different samples, provided that the expression rate of the reference housekeeping gene is similar across all samples. Choosing a reference gene fulfilling these criteria is therefore of high importance and often challenging, since only very few genes show equal levels of expression across a range of different conditions and tissues.

REAGENT	MANUFACTURER, CITY, STATE, COUNTRY
iQ5 cycler	BioRad, Munich, Germany
flat capped PCR tubes	BIO-Rad flat-capped optical tubes, Bio-Rad, Hercules, CA, U.S.A.
iQ SYBR Green Supermix	Bio-Rad Laboratories, Hercules, CA, U.S.A.

Table 8: Instruments, materials and reagents for qPCR

GENE	FORWARD PRIMERS (5' – 3')	REVERSE PRIMERS (3' – 5')	FRAGMENT SIZE (BP)	TM/R (°C)
hGAPDH	TATGACAACGAATTTGGCTACAG	TGATGGTACATGACAAGGTGC	247	59.2/ 59.4
hIL-6	CCACACAGACAGCCACTCA	GCTTGTTCCTCACTACTCTCAAAT	296	59.4/ 59.8
hIL-6R	GCCATTGTTCTGAGGTTCAA	TCTGTATTGCTGATGTCATAAGG	242	59.6/59.4

Table 9: Primers used for amplification of the genes of interest

Detection of human Interleukin-6 concentrations in supernatants employing a hIL-6 ELISA

Concentrations of hIL-6 in supernatants were measured with Quantikine® Human IL-6 ELISA Kit according to the protocol. This assay is based on the quantitative sandwich enzyme immunoassay technique, in which monoclonal antibodies specific for hIL-6 have been pre-coated onto microtiter plates. In brief, supernatants collected as described above were spun for 5 minutes at 13200rpm in order to reduce possible influence of debris in supernatants. Beforehand, a serial dilution assay was carried out and dilution of 1:50 with supplied Calibrator Diluent RD5T was determined appropriate to obtain extinction values within the standard curve of the assay. Then, standards and samples were pipetted into the wells and during incubation existing hIL-6 bound to immobilized antibodies attached to the plate. After washing away unbound substances, an enzyme-linked polyclonal antibody specific for hIL-6 was added to the wells. Following removal of any unbound antibody-enzyme reagent, substrate solution was added to the wells and colour developed proportionally to the amount of hIL-6 bound in the initial step. Colour development was stopped and absorption was measured at 450nm with correction at 600nm. Results were then analyzed using the software "Wallace Workstation 1420" and "Wiacalc", and concentrations obtained for samples were multiplied with dilution factor 50.

Moreover, DMEM with the corresponding antibody concentrations but without MDA cell incubation was tested for interference of either antibody with the ELISA kit.

The minimal detectable dose (MDD) of hIL-6 by this assay is typically less than 0.70pg/ml. No significant cross-reactivity or interference was observed or reported by the manufacturer. The ELISA kit used measures the total amount of hIL-6 present, the values obtained are insensitive to addition of the recombinant form of a soluble IL-6R.

MATERIALS	MANUFACTURER, CITY, STATE, COUNTRY
Quantikine® Human IL-6 ELISA Kit	R&D Systems, Inc., Minneapolis, MN, U.S.A.
Plate reader "Victor III"	Perkin Elmer, Waltham, MA, U.S.A.
Software "Wallace Workstation 1420"	Perkin Elmer, Waltham, MA, U.S.A.
Software "Wiacalc"	Wallace and Ose

Table 10: Materials for detection of hIL-6 in supernatants

Mouse models of breast cancer metastases to bone

Experimental design of in vivo studies

Five-week-old female BALB/c nude mice were injected intratibially with $5*10^4$ MDA-Tx-SA cells under general anaesthesia, as described below, after being assigned randomly to different treatment groups. One day prior to tumour cell inoculation, a pre-dose of the allocated antibody was administered via i.p. injection into mice using 29 gauge needles. Further doses of antibodies were given on the day of tumour cell implantation and consecutively every three days until day 18 post tumour cell inoculation. Animals were monitored for changes in body weight and behaviour at least every three days. Furthermore, radiographic images of tibiae were taken on days 10, 17 and 21 post-implantation in order to detect osteolytic lesions. A general outline of the time-course of all *in vivo* experiments is illustrated in Figure 9. Mice were sacrificed on day 21 by neck dislocation after applying an overdose of anaesthesia i.p. and blood was collected via cardiac puncture with 25 gauge needles. Endpoint analysis was conducted by micro-CT imaging, histological evaluations including basic histomorphometry, immunohistochemistry for proliferation and apoptosis and TRAcP staining. Moreover, serum biochemistry determined values of N-terminal pro-peptide of collagen I (P1NP) and serum tartrate-resistant acid phosphatase 5b (TRAcP5b), mirroring levels of bone formation and osteoclast activity respectively.

To begin with, a pilot study was designed to define optimal doses for each of the two antibodies and to test efficacy. Following treatment regimens were assessed: control treatment with i.p. injections of PBS (n=3), 20mg/kg/3 days MR16-1 (n=3), 50mg/kg/3 days MR16-1 (n=3),

100mg/kg/3 days MR16-1 (n=3), 50mg/kg/3 days tocilizumab (n=3) and 100mg/kg/3 days tocilizumab (n=2). Application of 20mg/kg/3 days tocilizumab was not included, since previous experiments conducted in our laboratory revealed no effects when mice were treated with 15mg/kg/3 days. The most efficient dose of each antibody was determined by evaluating both the degree of inhibition of bone resorption and tumour growth properties in the bone environment, despite the strong pro-resorptive effects of Tx-SA cells *in vivo* [204].

After this, larger cohorts including a control group (n=8), mice treated with 100mg/kg/3 days MR16-1 (n=8), a group of animals administered with 50mg/kg/3 days tocilizumab (n=8) and a group of mice receiving combined antibody treatment of 100mg/kg/3 days MR16-1 + 50mg/kg/3 days tocilizumab (n=8) were included in further experiments.

Finally, one more *in vivo* experiment was undertaken in which only this combination treatment (n=6), compared to a control group (n=5) was investigated once more.
For clarification, treatment group assignments are shown in table 11.
The set-up of these experiments complies exactly with the outline below (Figure 9):

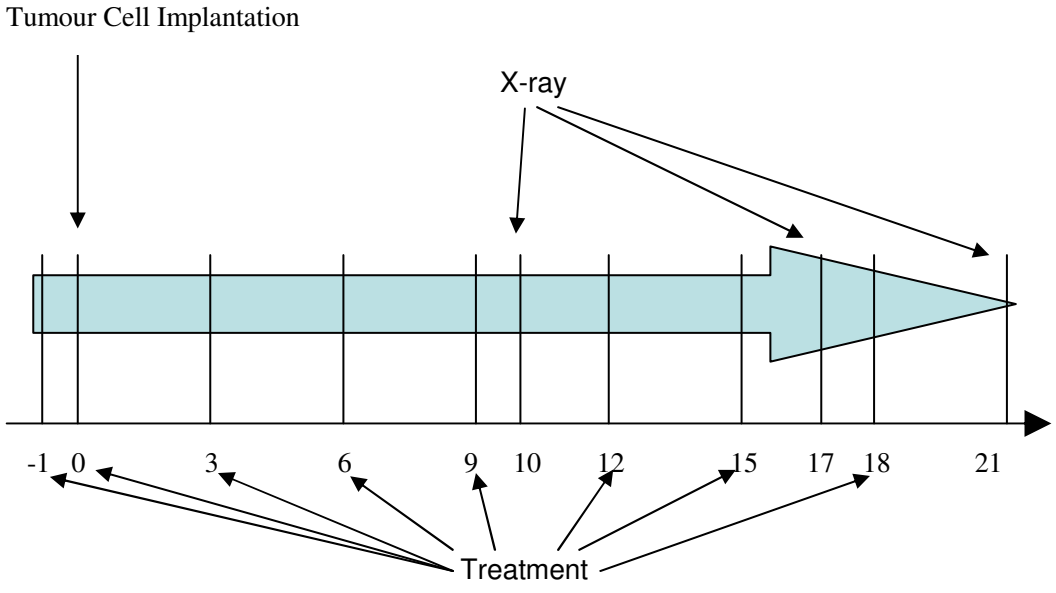

Figure 9: Outline of the experimental design for *in vivo* studies

	DOSAGE TESTING STUDY	TREATMENT STUDY	COMBINATION STUDY
Control (0.9% NaCl)	n=3	n=8	n=5
20mg/kg/3 days MR16-1	n=3	n=0	n=0
50mg/kg/3 days MR16-1	n=3	n=0	n=0
100mg/kg/3 days MR16-1	n=3	n=8	n=0
50mg/kg/3 days tocilizumab	n=3	n=8	n=0
100mg/kg/3 days tocilizumab	n=2	n=0	n=0
100mg/kg/3 days MR16-1 + 50mg/kg/3 days tocilizumab	n=0	n=8	n=6

Table 11: Treatment groups and numbers in the different *in vivo* studies

Mouse maintenance

Congenitally athymic female germ-free BALB/c nu/nu mice (Animal Resources Centre, Canning Vale, WA, Australia) were purchased at the age of 4 weeks and housed at the animal facilities of the ANZAC Research Institute. Animals were kept for at least one week in the facility before any experimental manipulation. Mice were maintained under specific pathogen-free conditions in cages bedded with sterilized soft wood granulate and were fed irradiated rat chow and autoclaved acidified tap water ad libitum. An artificial cycle of 12h light/ 12 h dark was created; room temperature was kept at 20 degrees. A maximum of five mice were housed in each box, all mouse manipulations were performed inside a laminar-flow hood ensuring aseptic conditions whilst maintaining general anaesthesia via i.p. injection of freshly prepared 0.75% ketamine/0.1% Xylazine (Sigma-Aldrich, St. Louis, MO, U.S.A.) administered at 10 mg/kg, unless otherwise stated. During all experiments, mice were monitored for changes in weight and behaviour at least every three days. All experimental procedures were approved by the Sydney Local Health District Animal Welfare Committee in accordance with the NHMRC animal ethics guidelines.

INSTRUMENTS, METHODS	MANUFACTURER, CITY, STATE, COUNTRY
Faxitron X-ray "MX-20 X-ray cabinet"	Faxitron, Wheeling, IL, U.S.A.
Image analysis software "ImageJ 1.42q"	National Institute of Health, U.S.A.
Micro CT "Skyscan 1172 scanner"	Skyscan, Kontich, Belgium
VG Studio MAX 1.2 software	Volume Graphics GmbH, Heidelberg, Germany

Table 12: Instruments and methods used for *in vivo* studies

MATERIALS	MANUFACTURER, CITY, STATE, COUNTRY
Ketamine 200mg/ml	Sigma-Aldrich, St. Louis, MO, U.S.A.
Xylazine 100mg/ml	Troy Laboratories Pty Ltd, Smithfield, NSW, Australia
Sodium Chloride 0.9%	Baxter Healthcare, Deerfield, IL, U.S.A.
Falcon tubes 15ml	BD Labware, Franklin Lakes, NJ, U.S.A.
Sterile filters 0.22µm	Millipore, Cork, Ireland
Insulin syringes 1ml for i.p. injections of anaesthesia and antibodies	BD Labware, Franklin Lakes, NJ, U.S.A.
Hamilton Syringe 25µl for intratibial injections	Hamilton Syringe Co., Reno, NV, U.S.A.
Rimadyl	Troy Laboratories Pty Ltd, Smithfield, NSW, Australia
26 gauge needles	BD Labware, Franklin Lakes, NJ, U.S.A.

Table 13: Materials used for *in vivo* experiments

Intratibial implantation of MDA cells

Hamilton Syringes were immersed in 100% ethanol overnight and dried completely before use. Mice were anaesthetised with ketamine/xylazine and additionally received 5mg/kg s.c. carprofen (Rimadyl) to prevent post-implantation pain. Once unconscious and not responding to stimuli such as twitching of the leg, animals were placed in a supine position before cleaning the hind legs with 70% ethanol. A 26 gauge needle was then inserted through the cortex of the anterior tuberosity of the tibia using a gentle drilling motion while holding the syringe at the correct angle so as to place the needle in the same orientation as the tibia, in order to avoid fracture of the latter. When the tip of the needle was positioned approximately 3-5mm deep into the diaphysis of the tibia, 10µl of the MDA-Tx-SA cell suspension ($5*10^6$ cells/ml) was injected. In all studies described in this thesis, both legs were injected with tumour cells. All intratibial implantations were performed by Dr. Yu Zheng.

Figure 10: Intratibial implantations. Photography kindly provided by Dr. Yu Zheng.

Antibody administration

The recombinant mAbs tocilizumab and MR16-1, were administered at doses ranging from 20mg/kg/3 days to 100mg/kg/3 days via i.p. injections, using 1-ml Insulin syringes fitted with 29 gauge needles. Appropriate dilutions of stock solutions of antibodies in DPBS were prepared beforehand to equalise volumes injected into the peritoneal cavity to about 10ml/kg body weight in all treatment groups. Both drugs were stored as stock concentrations, MR16-1 at -80°C, thawed immediately prior to use, tocilizumab at 4°C after reconstitution with PBS.

Radiological methods

Faxitron X-Ray

Employing Faxitron X-ray allowed *in vivo* imaging of developing osteolytic lesions in tibiae injected with MDA-Tx-SA cells. Mice were anaesthetised prior to taking digital radiography images on days 10, 17 and 21 after tumour cell inoculation. X-ray doses were standardised at 26kV for 10 seconds in order to obtain well-defined images of long bones with approximately 2x magnification.

Measuring osteolytic lesions

Osteolytic areas in tumour-cell injected tibiae were determined on digitally recorded radiographs using interactive image analysis software "ImageJ 1.42q", following careful identification and manual demarcation of lesion boarders that were observed as radiolucent lesions in hindlimbs. The size of each osteolytic lesion was calculated and presented as area mm^2 on days 10, 17 and 21 post tumour cell inoculation. Two-dimensional measurement of osteolytic bone areas using X-ray has limitations and may not reflect the actual size of lytic lesions. However, further analysis of tibiae was conducted and revealed similar results. Hence, X-ray data should be regarded in context with other evaluation techniques.

Micro-computerised tomography (μCT)

After tissue collection, representative μCT images of tibiae were obtained using Skyscan 1172. Scanning of each sample was performed at 100kV, 100μA using 1mm aluminium filters. In total, 1800 projections were collected at a resolution of 6.93 μm per pixel. Reconstruction of sections was performed by applying a modified Feldkamp cone-beam algorithm with beam hardening

correction set to 50%. All μCT scans were accomplished by Julian Kelly. VG Studio MAX 1.2 software was used to create three-dimensional visualization of tibiae from reconstructed sections.

Tissue Analysis

Tissue processing

Mice received an overdose of anaesthetics on day 21 post inoculation. After cardiac puncture for blood collection, cervical dislocation was performed and both hindlimbs were dissected. Collected tibiae were fixed in 4% paraformaldehyde buffered with 0.1M PBS (pH 7.4) for 48-72 hours and afterwards decalcified in 10% ethylenediaminetetraacetic acid (EDTA) pH 7.6, adjusted with Sodium hydroxide (NaOH) at 4°C for two weeks. EDTA solution was changed every two to three days. Tissues were then processed following a standardized protocol. Following fixation and processing, samples were paraffin-embedded for histological and immunohistochemical examination and in situ hybridization studies. All specimens were handled under sterile conditions to avoid contamination with foreign DNA. 5μm thick sections were cut, of which some were stained with hematoxylin and eosin for routine histological examination. To enhance adhesion of the bone sections, glass slides were pre-coated with 2% 3-Aminopropyl-triethoxysilane in acetone solution and dried overnight.

INSTRUMENTS, APPARATUS	**MANUFACTURER, CITY, STATE, COUNTRY**
Tissue processor "Leica TP1020"	Leica Microsystems GmbH, Nussloch, Germany
"Leica EG 1150G"	Leica Microsystems GmbH, Nussloch, Germany
"Leica EG 1120"	Leica Microsystems GmbH, Nussloch, Germany
Sterile containers	Sarstedt AG & Co, Nümbrecht, Germany
Embedding cassettes	Simport, Beioeil, QC, Canada
Microtome	Leica Microsystems GmbH, Nussloch, Germany
Microscopic slides ISO NORM 8037/1	HD Scientific Supplies Pty Ltd, Wetherill Park, NSW, Australia
Thermoblock	Liebisch, Bielefeld, Germany
Microscope	Olympus
OsteoMeasure System for histomorphometry	Osteometrics, Atlanta, GA, U.S.A.

Table 14: Instruments and materials for tissue analysis

CHEMICAL	MANIFACTURER, CITY, STATE, COUNTRY
Paraformaldehyde	Merck KGaA, Darmstadt, Germany
Ethylenediaminetetraacetic acid (EDTA) "Titriplex III"	Merck KGaA, Darmstadt, Germany
Sodium Hydroxide (NaOH) A.R.	Labscan Ltd, Dublin, Ireland
Tissue embedding medium	Tyco Healthcare Group LP, Mansfield, MA, U.S.A.
3-Aminopropyl-triethoxysilane (AES)	Sigma-Aldrich, St. Louis, MO, U.S.A.
Hematoxylin for H.E. staining " Lillie-Mayer's Haematoxylin"	Fronine, NSW, Australia
"Eosine Y" for H.E. staining	Fronine, NSW, Australia
Acetone A.R.	Fronine, NSW, Australia
Xylene	Fronine, NSW, Australia
Xylene-based mounting medium	Gurr, BDH, Poole, U.K.
Coverslips for microscopic slides	Gerhard Menzel Glasbearbeitungswerk GmbH & Co. KG , Braunschweig, Germany
Naphthol AS-BI phosphate	Sigma Chemical Co, St. Louis, MO, U.S.A.
Fast red violet Luria-Bertani salt	Sigma Chemical Co, St. Louis, MO, U.S.A.
20% Gill's hematoxylin for TRAcP and Ki67 counterstaining	Fronine, NSW, Australia
Hydrogen peroxide solution 30%	Sigma-Aldrich, St. Louis, MO, U.S.A.
Albumin bovine, Cohn Fraction V	Sigma-Aldrich, St. Louis, MO, U.S.A.
Triton® X for molecular biology	Sigma-Aldrich, St. Louis, MO, U.S.A.
Superblock® Blocking Buffer in TBS	Thermo Scientific, Rockford, IL, U.S.A.
Primary antibody to Ki67	Santa Cruz Biotechnology, Inc., Santa Cruz, CA, U.S.A.
Vectastain ABC reagent	Vector Laboratories Inc., Burlingame, CA, U.S.A.
Diaminobenzidine tetrahydrochloride (DAB)	Vector Laboratories Inc., Burlingame, CA, U.S.A.
ApopTaq® Peroxidase In Situ Apoptosis Detection Kit	CHEMICON International Inc., Billerica, MA, U.S.A.
Proteinase K, recombinant, PCR Grade	Roche Diagnostics GmbH, Mannheim, Germany
Harris' hematoxylin for TUNEL counterstaining	Fronine, NSW, Australia

Table 15: Chemicals for tissue processing

Pre-coating of glass slides

At the beginning, slides were washed in hot water containing detergent for 2 hours. After rinsing them thoroughly with distilled water, slides were soaked in 80% ethanol for another 2 hours and dried at 37°C overnight. 2% 3-Aminopropyl-triethoxysilane (AES) solution was prepared in acetone, and slides were dipped into this solution for 30 seconds before being rinsed briefly in two changes of acetone and one wash with distilled water. After drying slides completely overnight, they were used for collecting sections.

Hematoxylin and eosin staining

Wax was melted off paraffin sections on a hot plate at 60°C for ten minutes before samples were further cleaned in two changes of xylene, followed by serial rehydration in different dilutions of ethanol and water. Sections were then stained in Hematoxylin for 6 minutes, washed, dehydrated in 95% ethanol and further stained in eosin for 10 minutes. Finally, sections were dehydrated again in ascending concentrations of ethanol and two changes of xylene and mounted in depex with a coverslip.

Counting mitotic figures in H.E.-stained slides

In light microscopy at 4x0 magnification, cells undergoing mitosis can be recognised by hairy nuclear protrusions often seen as irregularities of the border of hyperchromatic centres of the cells, and basophilic cytoplasm [207]. Mitotic figures were counted in five fields of non-necrotic tumour area and afterwards related to the overall count in these five representative views of the section.

Histochemical examination for tartrate-resistant acid phosphatase (TRACP)

Histochemical examination of TRAcP [208] was performed by using naphthol AS-BI phosphate as substrate and fast red violet Luria-Bertani salt as stain for the reaction product. 5µm sections were dewaxed on a 60°C hot plate for ten minutes, followed by two five-minute incubations in xylene. After rehydration in descending concentrations of alcohol ranging from absolute ethanol for 2 x 5 minutes, followed by 95% ethanol and 70% ethanol for 3 minutes each, sections were washed briefly in distilled water before immersion in TRAcP solution (0.01% naphthol AS-MX phosphate, 50mM tartrate, 0.06% fast red violet Luria-Bertani salt in 0.1M acetate buffer, pH 5.0) took place for 30-60 minutes, depending on colour development, which was monitored every 5-10 minutes. Subsequent to histochemical reaction, sections were rinsed in distilled water before being counterstained in 20% Gill's hematoxylin (diluted in distilled water) for 1 minute. Afterwards, slides were rinsed in tap water and sections were air-dried overnight before being cleaned briefly in xylene and mounted in xylene-based mounting medium.

As a result, osteoclasts could be identified by microscopy as multinucleated cells adjacent to the resorbing surface of cortical or trabecular bone, displaying a general red to purple cytoplasmatic stain.

Ki67 Immunohistochemistry

As nuclear protein, Ki67 is expressed during most cell cycle phases except the G0 phase. Immunohistochemical staining of proliferating cells with Ki67 binding antibodies has widely replaced mitotic counting for assessing tumour cell proliferation. The mindbomb homolog (MIB) antibody has been developed as monoclonal antibody (mAb) that binds a recombinant fragment of the Ki67 antigen and has been demonstrated to work well in paraformaldehyde-fixed and paraffin-embedded tissue [209-210]. It involves indirect avidin-biotin-enhanced horseradish-peroxidase staining reaction.

In brief, 5µm sections were cut from paraffin-embedded samples and placed on AES-coated glass slides. Two sections were placed on each slide; one serving as immunohistochemical sample, the other representing a negative control. To begin with, wax was melted off by placing the sections on a hot plate at 60°C for 10 minutes. Then, samples were deparaffinized in xylene for 2 x 5 minutes. Subsequently, rehydration in descending concentrations of alcohol took place, starting from absolute ethanol for 3 x 3 minutes, continuing through 95% ethanol to 70% ethanol to sterile distilled water, each for 3 minutes. Endogenous peroxidase activity was blocked with 3% hydrogen peroxide solution for 15 minutes. Sections were then washed twice for 5 minutes in PBS/ 0.15% BSA/ 0.1% Triton X Buffer. In order to prevent non-specific binding, samples were incubated in normal-goat serum diluted 3:200 in superblock blocking solution for 30 minutes. The primary antibody binding Ki67 is a polyclonal rabbit antibody, raised against amino acids 2641-2940 at the C-terminus of human Ki67. It was diluted 1:50 [209] in superblock blocking solution and incubated in an incubation chamber at 4°C overnight. The next morning, primary antibody was washed away with two changes of PBS/BSA/Triton X buffer for 5 minutes each. Subsequently, the secondary antibody, a biotinylated goat anti-rabbit IgG diluted 1:200 in superblock blocking solution, was pipetted onto the sections and incubated in a humidified chamber for 1 hour at room temperature. Sections were then washed twice in PBS/BSA/Triton X Buffer. Vectastain ABC reagent was applied for 30 minutes to reveal fixed secondary antibodies. After incubation, sections were washed in PBS/BSA/Triton X buffer and diaminobenzidine tetrahydrochloride (DAB) solution was applied for 30 seconds to 4 minutes depending on the

intensity of colour development. Following washing in distilled water, nuclei were counterstained with Gill's hematoxylin diluted 1:20 in distilled water for 1 minute. Slides were then dipped in Tris buffer, ph 9.5, for 5 seconds and transferred through an ascending series of ethanol and xylene before being mounted with a xylene-based mounting medium.

Under the microscope, cells positive for Ki67 showed clearly detectable brown staining of the nucleus. Cytoplasmatic staining was considered non-specific and not taken into account. The index of Ki67-positive cells was then determined by counting positive cells and proportioning them to all cells counted in 5 random fields of non-necrotic areas of the tumour in representative sections in each bone specimen at 400x.

TUNEL staining

Apoptosis is characterized by degradation of DNA after activation of Ca^{2+}/Mg^{2+}-dependent endonucleases that cause strand breaks within the DNA. The identification of apoptotic cells by light microscopy relies chiefly on their morphological pattern, involving chromatin condensation as well as nuclear and cytoplasmatic fragmentation into apoptotic bodies. However, apoptotic cells are not easily distinguishable by light microscopy from other elements displaying condensed chromatin, such as mitotic cells in telophase. Moreover, nuclear morphology strongly depends on sample fixation, which influences both identification and interpretation of morphological aspects of apoptotic cells [211]. Therefore, in situ labelling of apoptotic cells compromises both high sensitivity and precise identification, with TUNEL (terminal deoxynucletidyl Transferase-mediated Biotin-dUTP Nick End Labeling) being the most commonly used method. It allows detection of apoptotic cells in situ at different stages of apoptosis by identifying apoptotic cells by transferring biotin-dUTP to strand breaks of cleaved DNA, using terminal deoxynucletidyl transferase (TdT). These biotin-labelled cleavage sites are then detected with horseradish peroxidase (HRP)-conjugated streptavidin and visualized by DAB [211].

Tumour cell apoptosis rates were assessed by TUNEL staining, employing an ApopTaq® Peroxidase In Situ Apoptosis Detection Kit, according to the manufacturer's protocol. Wax was melted off the sections on a hot plate at 60°C for 10 minutes. The 5µm specimens were then deparaffinized in two changes of xylene for 5 minutes each, rehydrated in gradual changes of ethanol starting at 100% ethanol for 2 x 5 minutes, then, to 95% ethanol to 70% ethanol for 3

minutes each. Afterwards, slides were washed in sterile distilled water and PBS. Subsequently, an antigen retrieval step was included in order to permeabilize the cells, which make the antigen more accessible for TdT enzyme, thus increasing sensitivity and specificity of the in situ hybridisation. Sections were treated with 1μg/ml proteinase K solution in 10mM Tris HCl ph7.4 in a humidified chamber at 37°C for 30 minutes [212]. After this, sections were washed in two changes of sterile distilled water and incubated in 3% H_2O_2 to block endogenous peroxidase activity. Following another washing step in sterile distilled water, equilibration buffer was pipetted onto the sections and left to incubate in a humidified chamber at room temperature for 10 minutes. Later, TdT enzyme solution diluted in reaction buffer was applied onto the sections and incubated at 37°C in a humidified chamber for one hour. This reaction was stopped by washing the slides in stop/wash buffer for ten minutes and in PBS for a further 3 minutes before applying the secondary antibody anti-digoxigenin for 30 minutes at room temperature. Before revealing immunoreactivity with DAB solution, slides were washed again in PBS. Colour development was assessed under 4x magnification and reactions were stopped when sufficient staining against low background staining appeared. Counterstaining was performed with 1:10 filtered Harris' hematoxylin for 3 minutes, then slides were dehydrated in ascending changes of ethanol and dipped into xylene before being mounted with a xylene-based mounting medium.

TUNEL-positive cells were identified as cells showing a dark-brown coloured nucleus. As with Ki67 quantification, 5 fields were counted in each stained section from areas showing non-necrotic tumour cells. The ratio between TUNEL-positive cells against all cells was then calculated.

Bone histomorphometry

Histomorphometric analysis of proximal tibial metaphysis was conducted in order to evaluate cortical bone area (BA) and tumour burden (TuA) at the endpoint of each experiment. All measurements were performed in longitudinal 5μm sections stained with haematoxylin and eosin or stained for TRAcP activity as described above, using the OsteoMeasure System. For determination of tumour area, representative sections were chosen displaying long bone with tumour inside. All tumour areas were measured at 4x magnification, surrounding soft tissue was included in case tumour should break through the bone, unless an independent tumour mass was visible caused by leakage during injection, which was rare. Total tumour area was measured in each section and the average tumour area in mm^2 of each group can be regarded as an index of

tumour burden. The cortical bone area was measured in the same sections at the same magnification (4x), here again, means of all samples in one treatment group were calculated and expressed as representative cortical bone mass of each group.

Osteoclasts were identified as TRAcP-positive multinucleated cells adherent to either trabecular or cortical bone surfaces. In brief, representative regions of interest were determined showing either trabecular- or cortical bone-tumour interface in each TRAcP-stained section using 12.5x magnification. The number of osteoclasts lining the bone-tumour interface was then counted in each section and osteoclasts per millimetre of either trabecular or cortical bone-tumour interface (TBTI or CBTI) were then calculated for each section. In cases where samples did not display any bone-tumour interface, they were excluded. Means for each group were calculated and compared. Moreover, CBTI and TBTI were combined in order to obtain a general value of osteoclasts per millimetre bone-tumour interface (BTI).

Serum biochemistry

Mouse N-terminal propeptide of type I collagen (P1NP) ELISA

An important step during the bone formation process is synthesis of type I collagen, the major organic component in bone matrix. During collagen synthesis, propeptides are released from both the amino- and the carboxy-terminal ends of the procollagen molecule, which can be detected in the circulation. Serum samples were collected on day 21 of *in vivo* experiments. Samples were spun at 13200 rpm for 5 minutes and serum was stored at -20°C until further analysis.

The ELISA kit used is a specific method to determine P1NP released during mouse and rat bone collagen synthesis. It is widely applied to determine bone formation rates from rat or mouse serum samples and shows no cross-reactivity with human P1NP. Basically, it is a competitive enzymeimmunoassay utilising a polyclonal rabbit snit-P1NP antibody coated on microtiter plates. Calibrators, controls and samples were added to the wells of the microtiter plate, followed by P1NP labelled with biotin and plates were incubated for one hour before aspiration and washing. Enzyme-labelled avidin (horseradish peroxidase) was added, binding selectively to complexed biotin and, following a further washing step, colour was developed after adding a chromogenic substrate (TMB). Absorbances were read by a microplate reader at 405nm with correction at 600nm, colour intensity developed being inversely proportional to concentrations of

P1NP. The sensitivity of the assay is defined as 7ng/ml serum equivalent, no cross-reactivity or interference is known.

Mouse tartrat- resistant acid phosphatase (TRAcP) assay

High amounts of TRAcP are expressed by bone-resorbing osteoclasts and activated macrophages. Two forms of TRAcP, known as TRAcP5a and TRAcP5b, circulate in the blood stream, whereas TRAcP5b is derived from osteoclasts only [213] and secreted into the blood circulation as active enzyme, which is inactivated and degraded to fragments before being removed from the circulation. Recent studies have shown that TRAcP5b indicates the quantity of osteoclasts rather than their activity [214]. The mouse TRACP assay is specific for determination of TRAcP5b activity in mouse serum samples. In the test, a polyclonal antibody directed against mouse TRAcP is incubated in anti-rabbit IgG-coated microtiter wells. After washing, standard, control and samples are incubated in the wells, and bound TRAcP5b activity is determined with a chromogenic substrate. The reaction is stopped, and absorbance is read with colour intensity being directly proportional to the amount and activity of TRAcP5b present in samples. The sensitivity of the assay is 0.1U/L, no cross-reactivity or interferences is mentioned by the supplier.

ELISA KITS FOR SERUM BIOCHEMISTRY	MANUFACTURER, CITY, STATE, COUNTRY
Rat/Mouse P1NP EIA	Immunodiagnostic Systems Ltd, Boldon, U.K.
Mouse TRACP Assay	Immunodiagnostic Systems Ltd, Boldon, U.K.

Table 16: ELISA kits for serum biochemistry

Statistical Analysis

All data are presented as mean ± SE. Statistics for *in vitro* experiments were calculated using one-way ANOVA, followed by Bonferroni's adjustment for when there were multiple comparisons by means of SPSS 17.0 for Windows (SPSS Inc., Chicago, IL, USA.). *In vivo* statistical analysis took into consideration that two samples originated from one organism. Therefore, a Fisher test was chosen in which the data were compacted.

Significance was accepted when $p < 0.05$.

Results

Pilot study to define the optimal dose of the Interleukin-6 receptor mAbs for in vivo studies

Since IL-6 exerts various functions, it was crucial to define optimal doses of both the human IL-6R mAb tocilizumab as well as of the murine IL-6R mAb MR16-1 before commencing the major *in vivo* experiments.

We took advantage of the differing specificities of the anti-human IL-6R antibody, tocilizumab, and the anti-mouse IL-6R antibody, MR16-1 (Figure 11 A-C). It is known that human IL-6 can bind and activate both the human and murine IL-6R, but murine IL-6 can only bind and activate the murine IL-6 receptor [215]. In our experimental setting, the cancer cells introduced into mice are of human origin. Subsequently, the hIL-6 produced by these cells will act both on the human (tumour) and the murine IL-6R, inducing downstream reactions in both cell types. In contrast, murine IL-6 only interacts with the mouse IL-6R and will affect only cells of the murine bone environment. As tocilizumab binds exclusively to the human IL-6 receptor expressed by the implanted cancer cells [216], it will only prevent signalling by human, i.e. cancer-derived IL-6, in tumour cells. Tocilizumab does not affect signalling by human or mouse IL-6 through the mouse IL-6R on host cells [215]. In contrast, the mouse-specific IL-6R antibody, MR16-1, inhibits human and murine IL-6 signalling in mouse cells only [194-195, 202, 215-218].

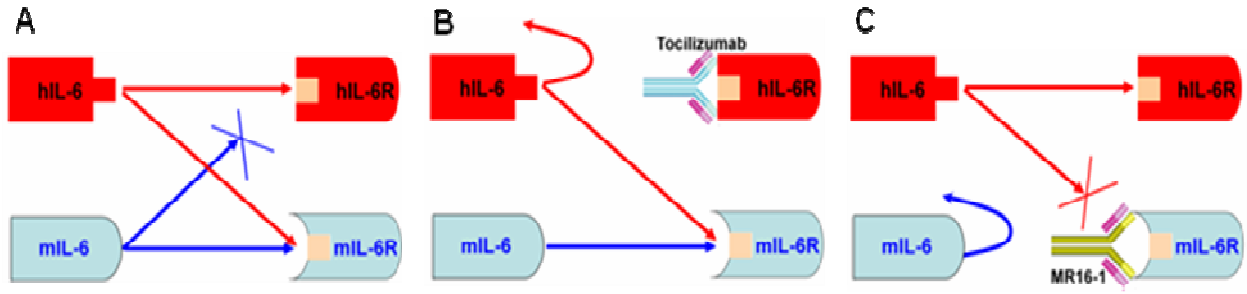

Figure 11: **A-C,** Schematic representation of IL-6 / IL-6 receptor interactions in human (tumour) and mouse (bone) cells. **A**, Tumour-derived human IL-6 (hIL-6) binds to both the human hIL-6R and the mouse IL-6R (mIL-6R). In contrast, bone cell-derived mouse IL-6 (mIL-6) binds only to the mIL-6R. **B**, Blocking the hIL-6R with Toclilizumab only blocks the autocrine effects of hIL-6 on the tumour, which expresses hIL-6R. However, hIL-6 is still able to act on the mIL-6R. **C**, Blocking the mouse IL-6R with MR16-1 inhibits endogenous mIL-6 and hIL-6 signalling in the host (murine bone) cells only.

As illustrated in figure 9 and table 11, female BALB C nu/nu mice were injected intratibially with MDA-MB-231 Tx-SA cells. One day prior to tumour cell inoculation, animals were assigned randomly to 6 groups (n=3) receiving either i.p. injections with PBS as placebo or treatment with 20mg/kg MR16-1, 50mg/kg MR16-1, 100mg/kg MR16-1, 50mg/kg tocilizumab or 100mg/kg tocilizumab i.p. respectively, as pre-dose before tumour cell implantation. From the day of intratibial injection onwards, mice were administered the respective antibody doses or placebo every three days via i.p. injection. During the study time, progression of osteolytic lesions was monitored through radiographic imaging on days 10, 17 and 21 post implantation. Endpoint analysis was conducted by micro-CT examination and histological evaluation of tibiae and the tumour masses that developed within the bone.

Radiographic analysis showed largest reduction of osteolytic areas in tibiae of mice treated with 50 or 100mg/kg/3 days MR16-1 or 50mg/kg/3 days tocilizumab

Quantifying sizes of osteolytic areas displayed in the X-ray pictures (Figure 13) revealed that treatment with both MR16-1 and tocilizumab inhibited progression of bone resorption throughout the whole study (Figure 13). Ten days after tumour cell implantation, lytic lesions could be detected in all animals, constantly growing during the course of the experiments. From day 10 onwards, mice treated with either 50mg/kg/3days or 100mg/kg/3days MR16-1, as well as animals receiving 50mg/kg/3 days or 100mg/kg/3 days tocilizumab exhibited smaller osteolytic areas. Greatest effects in terms of blocking bone resorption were seen in groups receiving either one of the two higher doses of MR16-1 and in mice injected with 50mg/kg/3 days tocilizumab. The 20mg/kg/3 days MR16-1 regimen only resulted in slightly smaller osteolytic areas on day 10 and day 17, though this inhibitory effect on bone resorption was not evident any more on day 21. Tibiae of mice treated with 50mg/kg/3 days MR16-1 displayed reduced osteolysis compared to placebo-treated mice on all three occasions; -34.67% on day 10, -22.01% on day 17 and -19.41% on day 21. Similar reductions in the size of osteolytic areas were achieved when mice were administered 100mg/kg/3 days MR16-1: -39.65% on day 10, -19.59% on day 17 and -24.34% on day 21 when juxtaposed to placebo tibiae. Even though these results are not significant, they define a strong trend towards impaired osteolysis in metastatic breast cancer growth in bone as a result of blocking the murine IL-6Rs of cells surrounding the tumour in contrast to placebo-treated mice.

Two other groups of mice were treated with the anti-human IL-6R mAb tocilizumab. Here, 50mg/kg/3days proved to be the most effective dose regarding decrease of breast cancer-mediated local bone resorption in tumour-inoculated tibiae. Determination of osteolytic areas revealed significant reductions of -56.11% on day 10, -47.22% on day 17 and -47.10% on day 21 compared to placebo. 100mg/kg/3 days tocilizumab treatment also revealed smaller osteolytic lesions, however, differences to placebo-treated mice were not as striking as with the lower dose. Here, divergences of -39.40% on day 10, -34.23% on day 17 and -33.83% on day 21 were determined (Figure 13).

Consequently, most distinguished impacts were detected in mice treated with 50mg/kg/3 days tocilizumab. Less striking effects were displayed in groups injected with either 50mg/kg/3 days or 100mg/kg/3 days MR16-1. The lowest dose of the anti-mouse IL-6R mAb did not reveal any hindrance concerning reduction of osteolytic processes caused by breast cancer cells in this metastatic xenograft model.

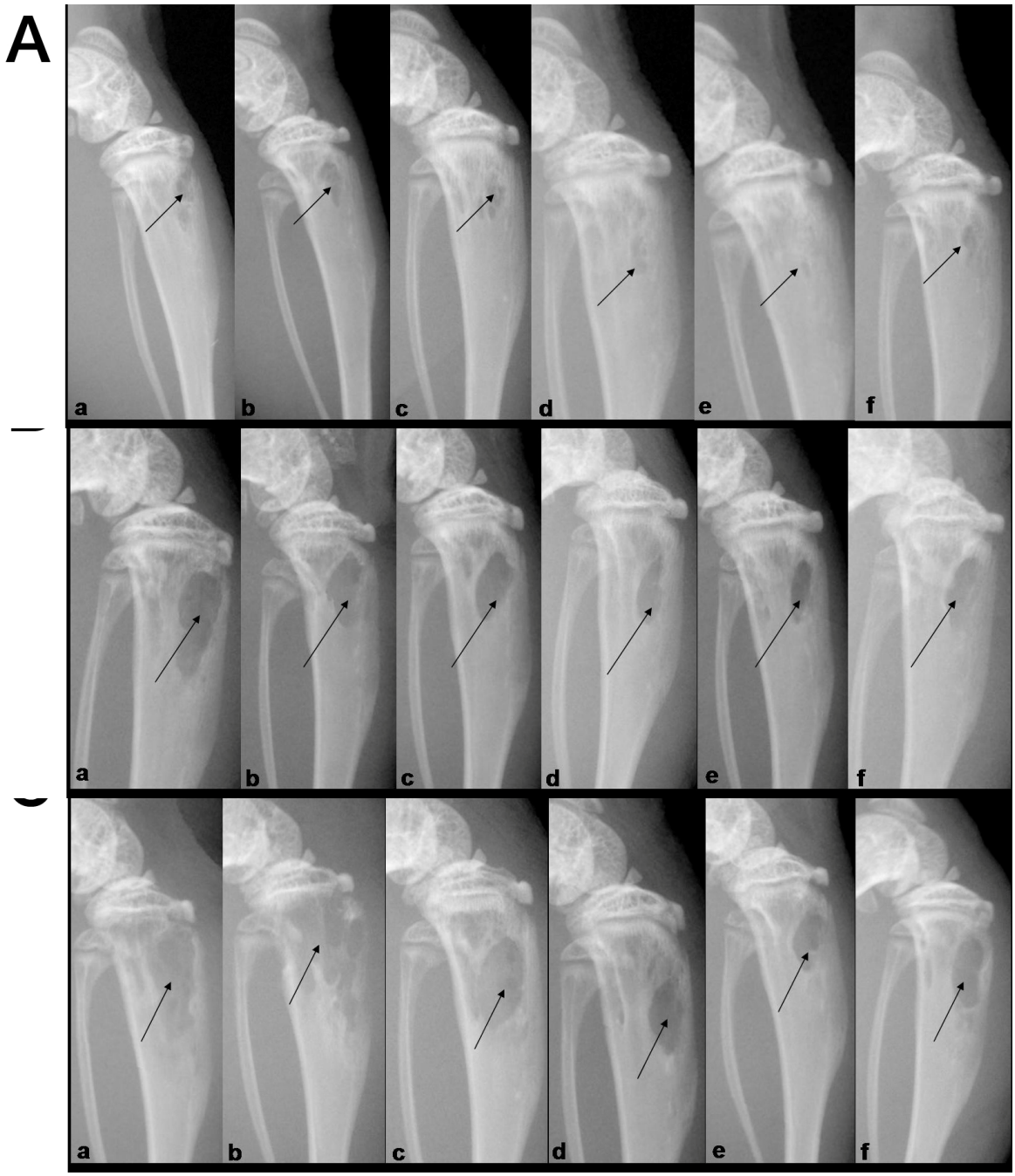

Figure 12: Radiographic images of osteolytic areas in tibiae on days 10 (A), 17 (B) and 21 (C) post tumour cell inoculation in the dose testing study. a = Placebo, b = 20mg/kg/3 days MR16-1, c = 50mg/kg/3 days MR16-1, d = 100mg/kg/3 days MR16-1, e = 50mg/kg/3 days tocilizumab, f = 100mg/kg/3 days tocilizumab.

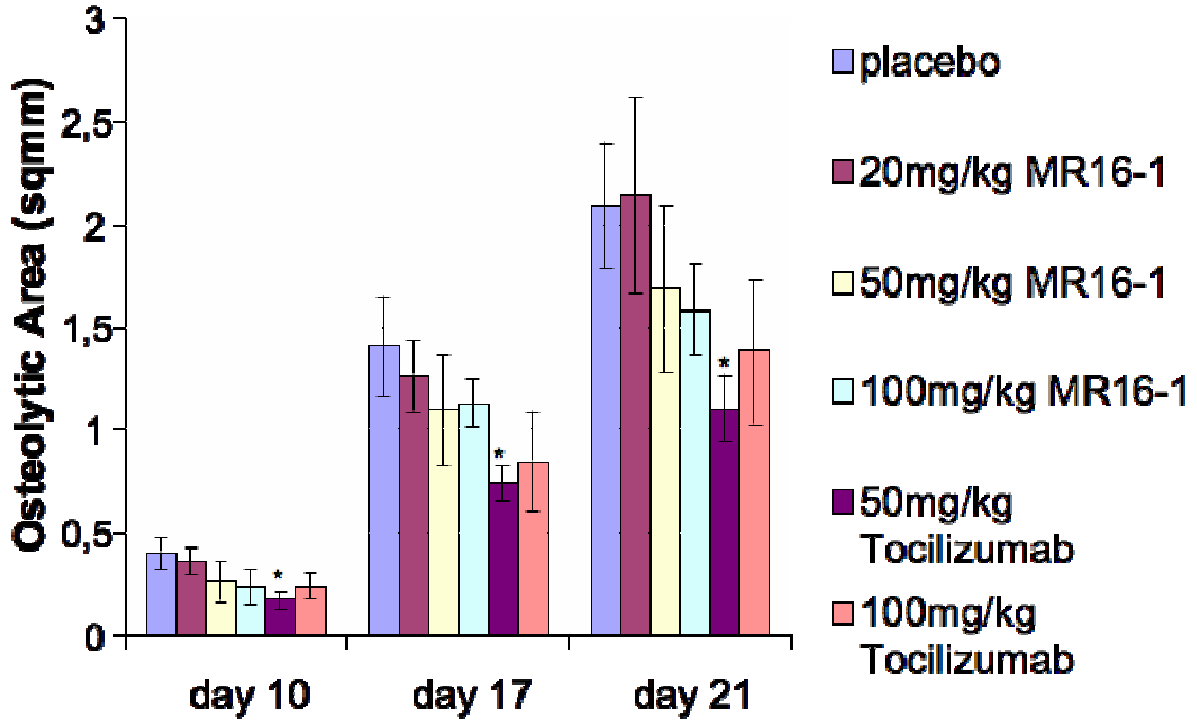

Figure 13: Osteolytic lesions on days 10, 17 and 21 post tumour cell inoculation in the dose testing study

Basic histomorphometry in tumour-bearing tibiae exhibited reduced tumour growth as well as less cortical bone destruction in mice treated with MR16-1 or tocilizumab

The cytokine IL-6 has been associated with tumour-induced osteoclast activation and bone resorption, causing typical osteolytic bone metastases of breast cancer cells that have spread to the skeleton [127]. Furthermore, tumour cell proliferation is promoted by IL-6, which activates its receptors in MDA-Tx-SA cells and in cells of the bone microenvironment, resulting in an augmented release of secondary growth factors and osteolysis-promoting agents. H.E-stained sections of tumour-bearing tibiae collected on day 21 were assessed for cortical bone area and tumour area in order to check whether osteolytic areas determined by X-ray analysis are associated with tumour growth within bone and whether they correlate with the size of the tumour (Figure 16).

As illustrated in Figure 15 andFigure 14, treatment with 20mg/kg/3 days MR16-1 resulted in neither smaller tumour areas within tibiae nor alteration of the amount of cortical bone present compared to placebo. Again, this dose of the antibody does not prove to be effective in terms of inhibited tumour growth of metastatic breast cancer in bone, or tumour-associated osteolysis. Mice treated with 50mg/kg/3 days also did not reveal augmented values of cortical bone area

compared to placebo-treated mice. On the other hand, analysis of tumour areas in these samples showed a slight decrease in the size of the tumours within the tibiae compared to placebo (3.308 mm^2 vs. 4.156 mm^2). In tibiae of mice injected every three days with the highest dose of the anti-mouse mAb MR16-1, not only a very similar reduction of tumour areas (3.209mm^2) as in mice treated with 50mg/kg MR16-1 was displayed, but also a trend towards greater cortical bone protection than in placebo-treated mice could be observed in these samples (2.1mm^2 vs. 1.7mm^2).

Blocking the human IL-6R with tocilizumab influenced both the tumour size as well as the cortical bone area in a preventive way, thus suggesting inhibition of tumour growth in bone and tumour-induced bone resorption. Again, the most distinct outcomes were seen in mice receiving 50mg/kg/3 days tocilizumab since augmented cortical bone area of 2.406mm^2 (+38.51% compared to controls) and significantly diminished tumour area of 1.987mm^2 (-52.19% compared to placebo, p=0.0478) were exhibited. The higher dose of 100mg/kg/3 days tocilizumab caused hardly any difference in the cortical bone area to controls (1.915mm^2 vs. 1.737mm^2) but still displayed reduced tumour areas (3.209mm^2 vs. 4.156mm^2). However, this difference was not as striking as in mice administered 50mg/kg/3 days tocilizumab.

Subsequently, histomorphometric observations support conclusions drawn from radiographic analysis: 100mg/kg/3 days MR16-1 and 50mg/kg/3 days tocilizumab are the most potent doses to inhibit proliferation of metastatic breast cancer cells in the tibiae and tumour-induced osteolysis.

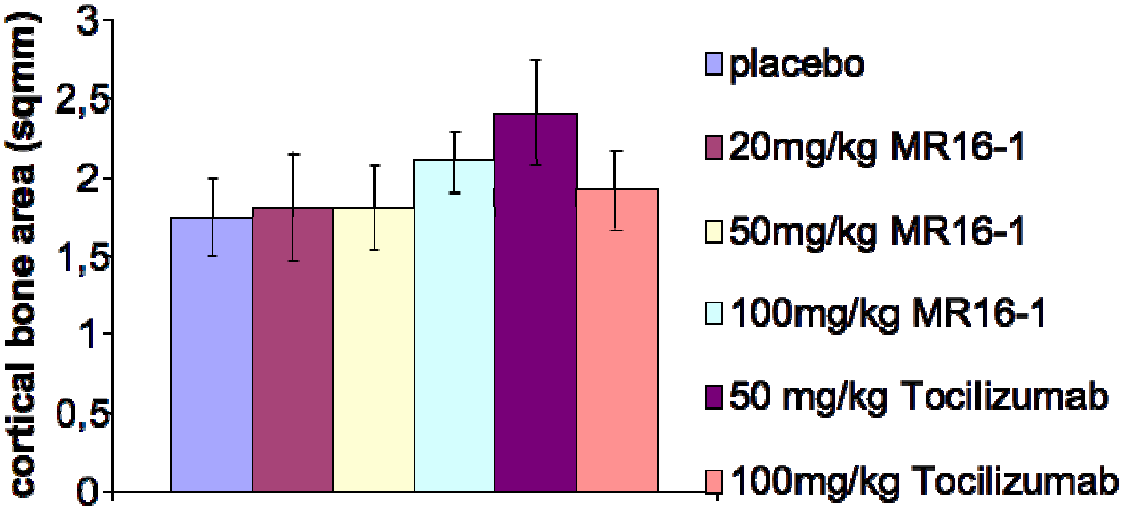

Figure 14: Cortical bone area in mm^2 +/- standard error in tumour-bearing tibiae 21 days post tumour cell inoculation in the dose testing study.

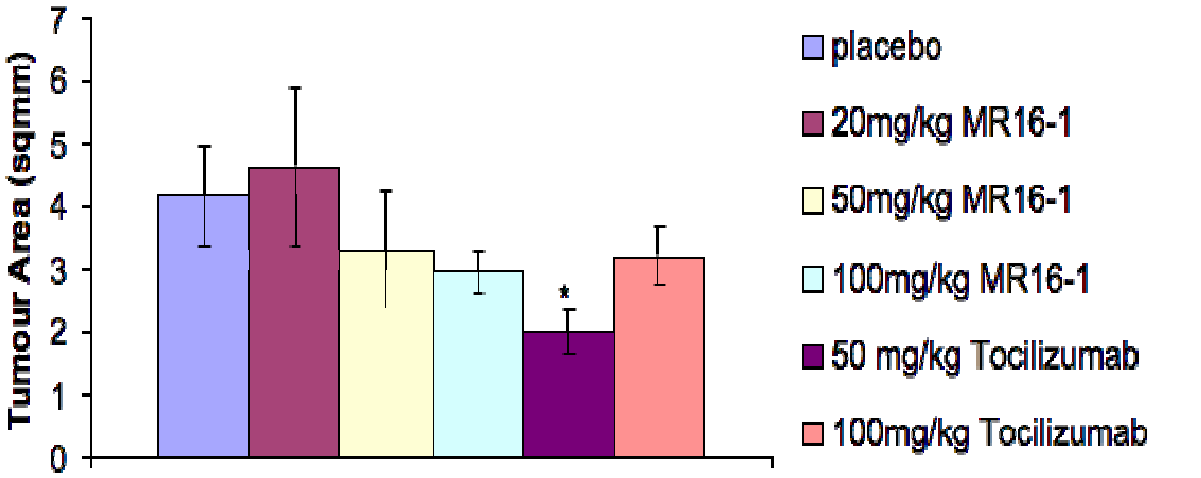

Figure 15: Tumour area in tibiae in mm^2 +/- standard error 21 days post tumour cell inoculation in the dose testing study, * $p<0.05$ vs. Placebo.

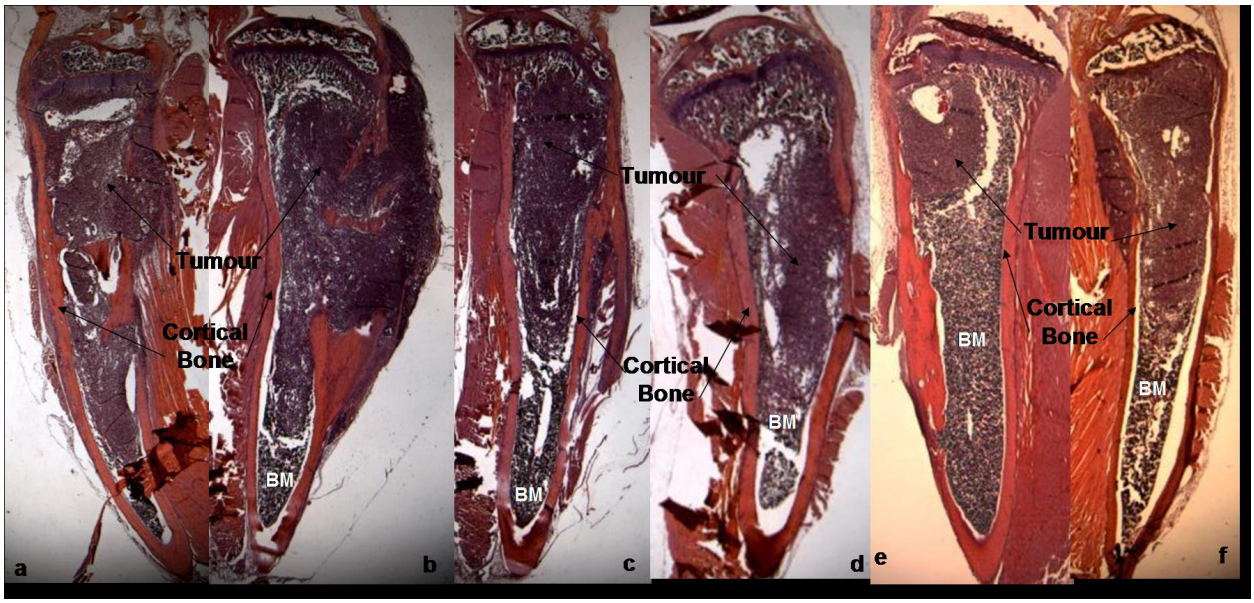

Figure 16: Histomorphometry in H.E.-stained sections in the dose testing study. a = placebo, b = 20mg/kg/3 days MR16-1, c = 50mg/kg/3 days MR16-1, d = 100 mg/kg/3 days MR16-1, e = 50mg/kg/3 days tocilizumab, f= 100mg/kg/3 days tocilizumab

Treatment with Interleukin-6R antibodies decreased the number of active osteoclasts at the bone-tumour interface

Since literature implies the cytokine IL-6 is involved in osteoclast formation and activation [127], the number of active osteoclastic cells at the bone-tumour interface was determined by staining sections of tumour-bearing tibiae for tartrate-resistant acid phosphatase 5b (TRAcP5b).

Being expressed exclusively in mature osteoclasts, this enzyme is considered the gold standard for detection of these cells. The number of osteoclastic cells was evaluated both at the growth-plate tumour interface as well as on the cortical bone-tumour interface, whenever the tumours were in direct contact to the former. Otherwise, samples were excluded from analysis. There were no substantial differences between the numbers of osteoclasts per mm at two sites within one treatment group. Afterwards, the mean of both values was calculated forming the osteoclast number per mm at the bone-tumour interface in general, which was applied for comparing the degree of osteoclast activity. Osteoclast activation involves both murine osteoclast precursor cells that differentiate into mature bone resorbing osteoclasts as well as murine osteoblastic cells. The latter are not only responsible for building up the organic bone matrix but also produce and secrete a brittle balance between RANKL and OPG that in turn is important for the extent of osteoclast activation and therefore the degree of bone resorption occurring. Both cell types mentioned above express the murine IL-6R, which is activated by both murine IL-6 and tumour derived hIL-6 and is antagonized by MR16-1. However, IL-6 is only one among many pro-resorptive factors capable of inducing a shift in favour of RANKL secretion by osteoblastic cells and therefore generating osteoclast-mediated bone resorption.

As indicated in Figure 17 and table 17, control mice exhibited a mean of 11.384 osteoclasts/mm bone-tumour interface. This number was insignificantly decreased to 9.489/mm in animals receiving 20mg/kg/3 days MR16-1. Even though the dose of 50mg/kg/3 days MR16-1 did reveal smaller osteolytic areas in the X-ray analysis, the number of active osteoclasts at the site of tumour-induced bone resorption was not different to the number defined in control mice (11.284 osteoclasts/mm). These observations seem contradictory, however, it is important to take into consideration that histological evaluation was only conducted at the endpoint of the study, whereas X-ray pictures represent a follow-up analysis. It is therefore possible that the number of osteoclasts only increases again towards the end of the study so that the lytic process itself has not yet kept up with this development. Hence, it would be of interest to examine the osteoclast number at earlier and the osteolytic area at later time points of the study. Treatment with 100mg/kg/3 days mouse IL-6R mAb MR16-1 significantly abated the number of active osteoclasts at the bone-tumour interface to 7.409/mm ($p=0.0144$). This again is in line with the findings of the radiographic and the histomorphometric examinations, since reduced numbers of active osteoclastic cells at the local site of tumour in the bone are only capable of breaking down less bone matrix and consequently causing smaller osteolytic areas and providing greater cortical

bone protection. Moreover, it becomes obvious that bone resorption and tumour growth seem to be coupled processes, since smaller tumour areas were detected in these samples.

Tocilizumab treatment impedes the auto- and paracrine IL-6 signalling loop on metastatic breast cancer cells by blocking human IL-6Rs expressed on the MDA tumour cells. As mentioned above, IL-6 is only one among many pro-resorptive factors produced and secreted by the tumour cells, but it is possible that auto- or paracrine IL-6 signalling may affect further production of secondary pro-resorptive factors by the tumour cells which then, in turn, might activate osteoblasts and hence promote a RANKL-induced osteoclast activation and differentiation. So by blocking human IL-6Rs on the tumour cells, it is still possible to influence the number of osteoclasts.

50mg/kg/3days of tocilizumab treatment suppressed the number of active osteoclasts at the bone-tumour interface significantly to 7.388/mm, compared to controls (p=0.0140). The higher dose of 100mg/kg/3 days tocilizumab did not show such a striking decrease of osteoclast numbers (9.475/mm). Although these observations mirror the results obtained by analysing osteolytic areas, it is not yet clear why the higher dose of the antibody does not lead to an even more apparent inhibition of osteoclast activity and consequent bone resorption.

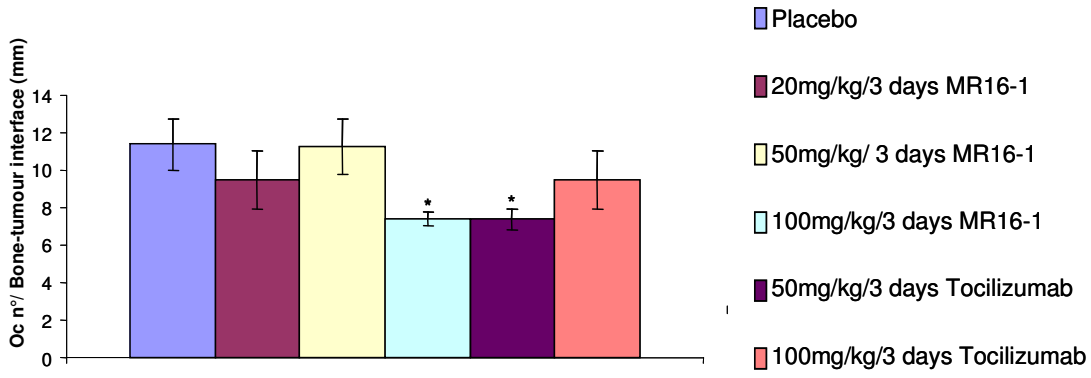

Figure 17: Osteoclast numbers per mm bone-tumour interface +/- standard error in the dose testing study. * p<0.05.

	Oc n°/TBTI (mm)	Oc n°/ CBTI (mm)
Placebo	11.515 +/- 1.824	11.253 +/- 1.264
20mg/kg/3 days MR16-1	9.374 +/- 1.404	9.604 +/- 2.329
50mg/kg/3 days MR16-1	10.849 +/- 1.119	11.634 +/- 1.823
100mg/kg/ 3 days MR16-1	7.364 +/- 0.643 *	7.557 +/- 0.568
50mg/kg/ 3 days tocilizumab	6.83 +/- 0.824 *	7.984 +/- 0.63

100mg/kg/ 3 days tocilizumab	8.161 +/- 1.391	9.43 +/- 1.71

Table 17: Osteoclast numbers per mm trabecular bone-tumour interface and at cortical bone-tumour interface +/- standard error in the dose testing study. * = $p<0.05$ vs. placebo.

Blocking Interleukin-6 signalling in host cells by MR16-1 or in tumour cells by tocilizumab administration influenced the tumour vitality in the bone metastatic xenograft model

IL-6 is known to exert actions on the tumour cells in an auto- or paracrine manner and thus to generate a more aggressive phenotype of the tumour with enhanced expression of pro-proliferative and anti-apoptotic genes [174-176]. When considering the vicious cycle model of bone metastases explained above, release of growth factors stored in the bone matrix is a consequence of increased bone resorption and osteoclast activation. Hence, by blocking IL-6 signalling in host cells, the vicious cycle lacks one of its many activators, which might result in less growth factors promoting tumour cell proliferation. Taking these theories into consideration, the viability of the tumour in terms of the ratio of proliferating cells within the bone metastases, as well as the rate of cells undergoing apoptosis, was assessed by either counting mitotic figures in H.E.-stained sections or by employing immunohistochemistry for detecting apoptotic tumour cells.

The anti-mouse mAb MR16-1 inhibited proliferation and enhanced apoptosis of the tumour cells in a dose-dependent manner. Mice treated with 20mg/kg/3days MR16-1 show a significant decline in the ratio of mitotic cells within the tumour, compared to mice injected with PBS (5% vs. 6.9%, $p=0.0214$). This effect became even more evident in mice treated with the higher doses of MR16-1 (4.2% in 50mg/kg/3 days MR16-1, $p=0.0011$ and 2.1% in 100mg/kg/3 days MR16-1, $p<0.0001$ vs. placebo). Evaluating the rate of apoptotic cells in these treatment groups also showed a dose-dependent effect that became significant at a dose of 100mg/kg/3days MR16-1 (1% in 20mg/kg/3 days MR16-1, 1.7% in 50mg/kg/3 days MR16-1, 2.8% in 100mg/kg/3 days MR16-1 vs. 0.8% in placebo-treated mice).

Tumour vitality in tocilizumab-treated mice was also affected in a way that implied inhibitory effects of the antibody treatment on tumour growth in bone. As with the anti-mouse mAb treatment, dose-dependent effects could be observed with significant decreases in the ratio of mitotic figures (2.4% in 50mg/kg/3 days tocilizumab, $p<0.0001$ and 2.1% in 100mg/kg/3 days tocilizumab treated mice, $p=0.0005$) and substantial augmentations regarding the apoptotic index

(2.8% for 50mg/kg/3 days tocilizumab, p=0.0013 and 3.5% for 100mg/kg/3 days tocilizumab, p=0.0009) compared to placebo-treated mice.

In conclusion, the greatest impact on the tumour vitality was provoked by administration of either 100mg/kg/3 days MR16-1 or 100mg/kg/3 days tocilizumab.

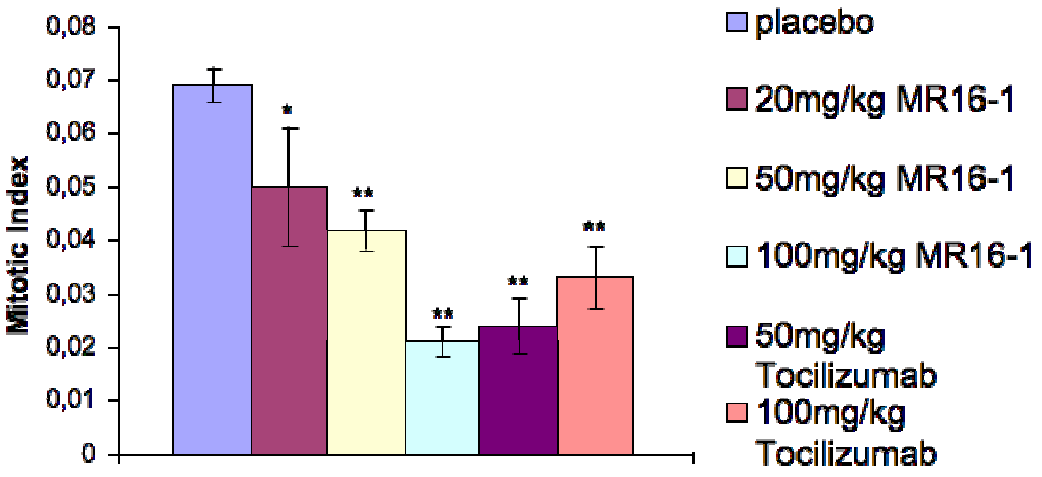

Figure 18: Mitotic Index +/- standard error in tumours in tibiae 21 days post tumour cell inoculation in the dose testing study. * p<0.05. ** p<0.001.

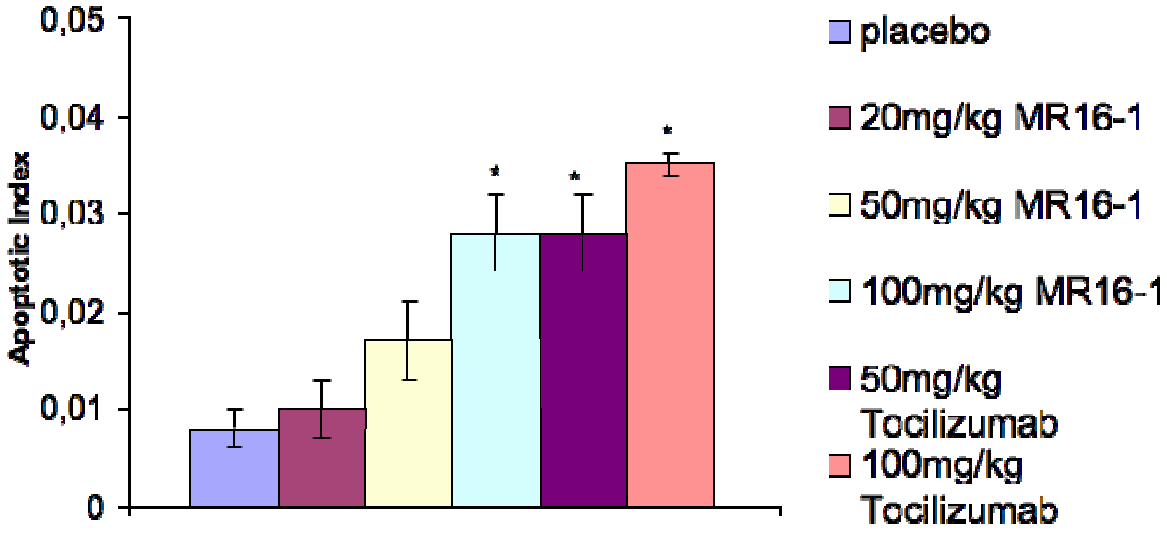

Figure 19: Apoptotic Index +/- standard error in tumours in tibiae 21 days post tumour cell inoculation in the dose testing study. * p<0.05.

100mg/kg/3 days MR16-1 and 50mg/kg/3 days tocilizumab affected bone biology and the tumour vitality in the metastatic breast cancer model to the greatest extent

The pilot study was conducted primarily to evaluate the most potent doses of single antibody treatments with either the anti-mouse IL-6R mAb MR16-1 or the anti-human IL-6R mAb tocilizumab, in terms of reducing the tumour growth in the metastatic breast cancer model as well as impeding associated bone resorption.

As for MR16-1, 100mg/kg/3 days consistently showed the greatest effects. Even though radiographic analysis suggested that the lower dose of 50mg/kg/3 days MR16-1 might prevent tumour-induced bone resorption to a similar extent, histological evaluations of tumour-bearing tibiae exhibited stronger inhibition by the higher dose of the antibody that antagonizes the murine IL-6Rs on host cells. The lowest dose tested, 20mg/kg/3 days MR16-1, showed hardly any effect on tumour growth or bone resorption.

Tocilizumab blocks the human IL-6Rs and therefore affects primarily tumour cells themselves, consecutively modulating their gene expression patterns and hence the amount of tumour-derived osteolytic factors secreted into the bone microenvironment. Throughout the study, 50mg/kg/3 days tocilizumab continually impressed with greater inhibition of bone resorption and tumour growth, apart from apoptotic and mitotic counts. Since the differences between these two dose regimens are not significant and the overall beneficial effect of the antibody treatment favours the lower dose administered, further experiments were conducted with 50mg/kg/3 days as the treatment of choice.

Treatment study

After having defined the most efficient dose regimens for treatment with either the anti-mouse IL-6R mAb MR16-1 or the anti-human IL-6R mAb tocilizumab in the pilot study, experiments with increased numbers of animals were conducted. Consequently, 100mg/kg/3 days MR16-1 and 50mg/kg/3 days tocilizumab were chosen as doses for further evaluation in this treatment study including 8 mice in each group inoculated with tumour cells into both tibiae so that the number of samples added up to 16. The design of the study was the same as the protocol applied in the previous one in order to obtain comparable data. However, only four different groups were included: a placebo group of mice injected i.p. with PBS, a second set of animals received 100mg/kg/3 days MR16-1 i.p., another group was administered 50mg/kg/3 days tocilizumab i.p. and a fourth group of mice was injected with a newly introduced treatment regimen in order to

evaluate the effects of combined treatment with both 100mg/kg/3 days MR16-1 plus 50mg/kg/3 days tocilizumab i.p. As before, radiographic imaging of osteolytic lesions within the tumour-bearing tibiae was conducted on days 10, 17 and 21 post tumour cell inoculation and endpoint analysis included basic histomorphometry of tumour area and cortical bone area, TRAcP5b staining of active osteoclastic cells at the bone-tumour interface, as well as evaluation of tumour vitality by means of immunohistochemical staining for Ki67 and TUNEL.

Radiographic analysis revealed attenuated progression of osteolytic lesions in mice treated with single antibody injections

X-ray images were taken on days 10, 17 and 21 after tumour cell inoculation in order to monitor the progression of tumour-induced osteolytic lesions within the tibiae (Figure 20). Once again, areas of pathological bone resorption were visible in most samples already on day 10, increasing throughout the study in all treatment groups. Results are illustrated in Figure 20 andFigure 21.

Mice treated with 100mg/kg/3 days MR16-1 exhibited significant reductions of bone resorption on all three occasions on which X-ray images were taken. Ten days after tumour implantation, the mean lytic area was diminished by 35.79% compared to placebo-treated mice (p=0.036). This relative difference remained on day 17 (-34.37%, p=0.0115), but abated to only a reduction of 24.90% vs. control on day 21 (p=0.0492). This might suggest that the inhibitory properties of the anti-mouse IL-6R mAb MR16-1 are depleted towards the end of the treatment study and other factors might override the effects of MR16-1 treatment on tumour-mediated bone resorption.

Treatment with 50mg/kg/3 days tocilizumab also diminished the size of osteolytic areas in the tibiae. A significant abatement of 38.13% compared to placebo-treated mice was detected on day 10 (p=0.0185). Osteolytic areas measured on day 17 were 24.91% smaller than lesions exhibited by control mice (p=0.0554) and on day 21 post tumour cell implantation, osteolysis in tocilizumab-treated animals reached 76.92% of the size of bone resorption in placebo mice (p=0.0575). Whilst these results are not significant, it is important to acknowledge that they nevertheless define a very strong trend, indicating reduction of bone resorption in tumour-bearing tibiae.

Animals injected with both antibodies simultaneously every three days, did not reveal a more pronounced or even similar effect in terms of suppressed bone resorption compared to single antibody regimens. On all three occasions, osteolytic areas shown were larger in size than those in mice receiving either of the two mAbs. However, slightly reduced bone resorption was observed on day 10 (-16.39%), day 17 (-9.76%) and day 21 (-15.27%) when compared with tibiae of placebo-treated mice.

To sum up, substantially diminished pathological breast-cancer cell related bone resorption was detected in mice treated with single antibody injections of 100mg/kg/3 days MR16-1 or 50mg/kg/3 days tocilizumab. The combination of both antibodies which impedes IL-6 signalling in both host and cancer cells does not prove to be more effective than the single antibody, but rather displays less ramification of bone resorption in breast cancer bone metastases.

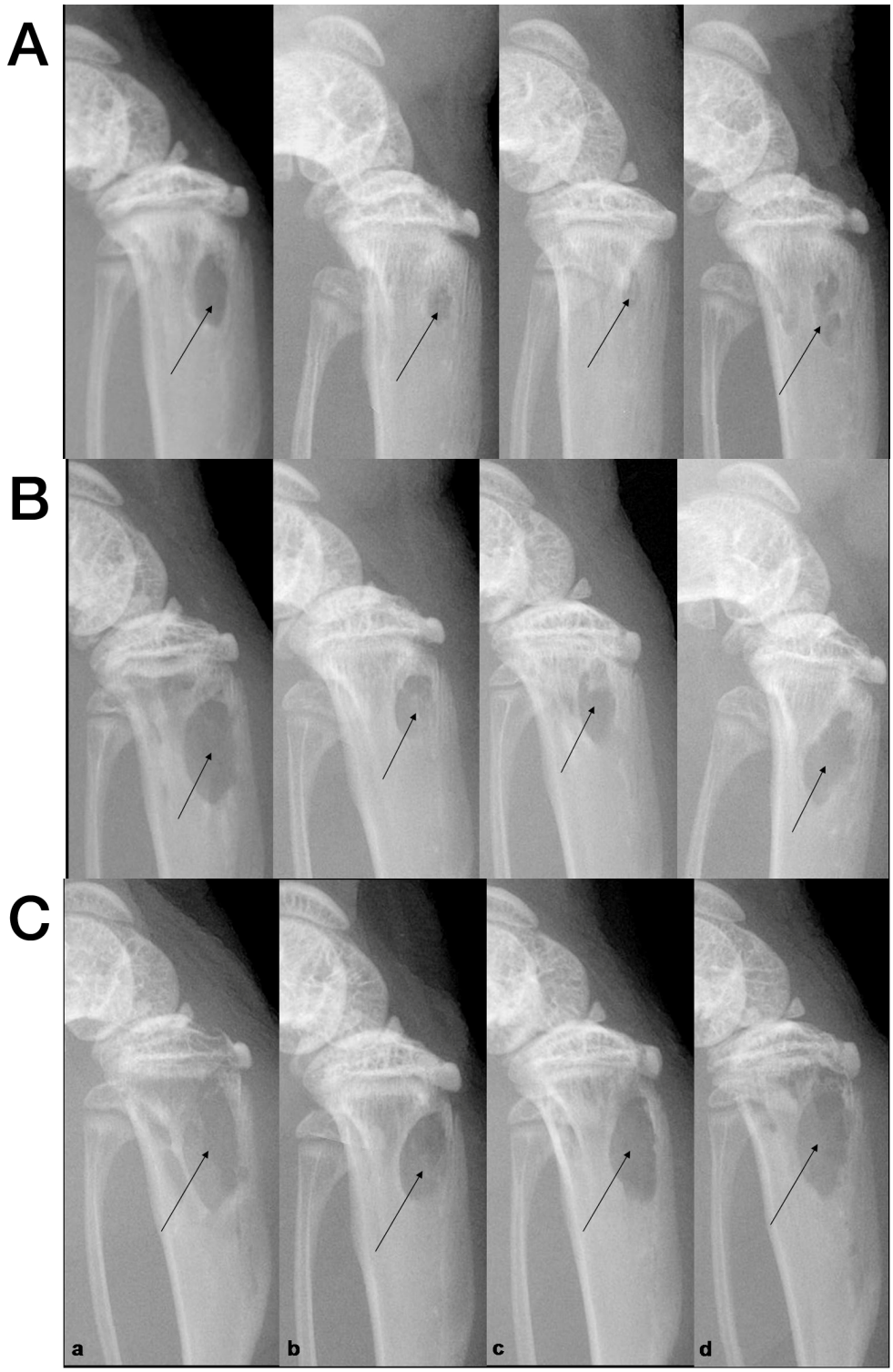

Figure 20: X-ray images of treatment study taken on days 10, 17 and 21 post tumour cell implantation into tibiae of 5-week old nude mice. A = day 10, B = day 17, C = day 21, a = placebo, b = 100mg/kg/3 days MR16-1, c = 50mg/kg/3 days tocilizumab, d = 100mg/kg/3 days plus 50mg/kg/3 days tocilizumab

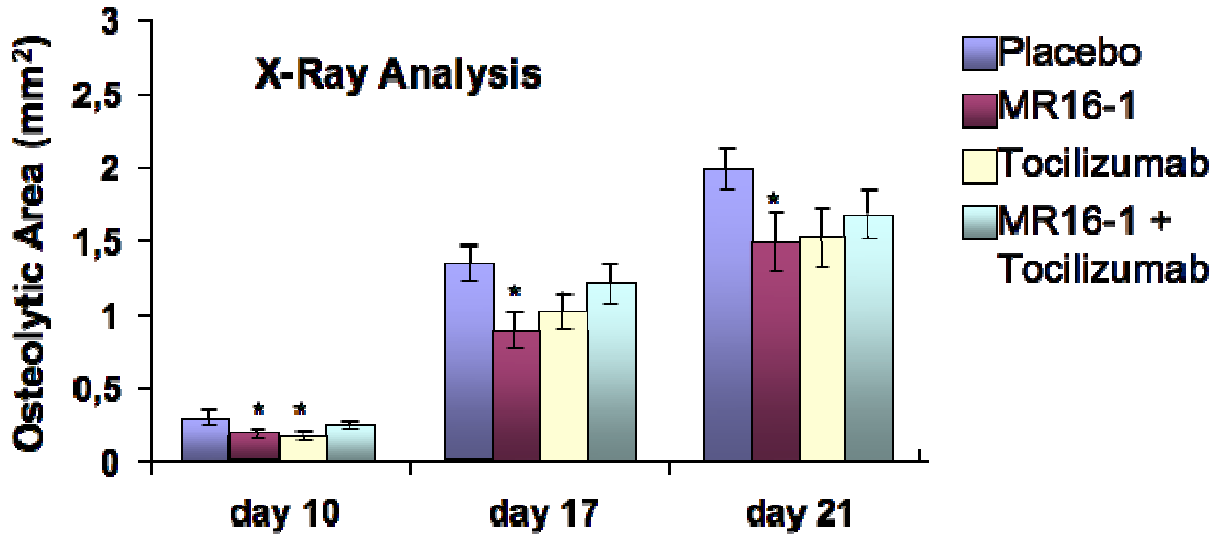

Figure 21: Osteolytic lesions in mm^2 +/- standard error on days 10, 17 and 21 in the treatment study. * $p<0.05$.

Animals treated with 100mg/kg/3 days MR16-1 and/or 50mg/kg/3 days tocilizumab displayed smaller tumour areas and less cortical bone destruction

Histomorphometric analysis of H.E.-stained sections was conducted to define the area of cortical bone as well as the size of the tumour within the tibiae collected 21 days post intratibial tumour cell implantation. The cortical bone area (CBA) differed in all treatment groups from the cortical bone area measured in tibiae of placebo-treated mice (Figure 22).

100mg/kg/3 days of MR16-1 administration prevented tumour-induced resorption of cortical bone significantly (CBA of $1.762mm^2$ vs. $1.324mm^2$ in placebo-treated mice, $p=0.0016$). Similar effects were observed in animals treated with 50mg/kg/3 days tocilizumab (CBA of $1.793m^2$, $p=0.0005$). Furthermore, the combination treatment of the human and the murine antibody proved to be effective in this set of experiments, displaying a smaller extent of cortical bone resorption than in the placebo group (CBA of $1.820mm^2$, $p=0.0002$). These results correlate with smaller osteolytic lesions detected by radiographic imaging. Still, the combination treatment does not exert enhanced effects. This is most possibly due to the fact that tumour-secreted pro-resorptive factors exert actions on the neighbouring bone first, in this case trabecular bone in the bone cavity. As tumour growth progresses, the amount of pro-resorptive factors increases and exerts its actions on the more distant cortical bone as well. Hence, it is likely that this process was only about to start and differences could not be distinguished yet. On the other hand, it is obvious that lytic lesions are visible in radiographic images due to lysis of the cortical bone.

Therefore, differences in the cortical bone volume are evident. Moreover, one has to take into consideration that histomorphometric analysis of the cortical bone area is confined to a two-dimensional analysis. Hence, it is also possible that the sections do not correspond to an area of representative bone resorption.

Measuring tumour areas (TuA) in these H.E.-stained samples revealed very distinct differences in tumour sizes (Figure 23). Tibiae of mice administered 100mg/kg/3 days MR16-1 contained tumours only 47.5% the size of tumours in mice injected with PBS (TuA of 2.669mm^2 vs. 5.619mm^2, $p<0.001$). A similarly convincing deterioration of tumour sizes was found in mice receiving 50mg/kg/3 days of the anti-human IL-6R mAb tocilizumab (TuA of 2.166mm^2, 38.55% of control tumour size, $p<0.0001$).
Although blocking both IL-6Rs by combining the human and the murine IL-6R mAb caused a significant reduction of the size of the tumour compared to placebo (TuA of 3.120mm^2 vs. 5.619mm^2, $p=0.0003$), simultaneous treatment with both antibodies, once again, does prove to be less effective than the treatment with either single antibody alone.

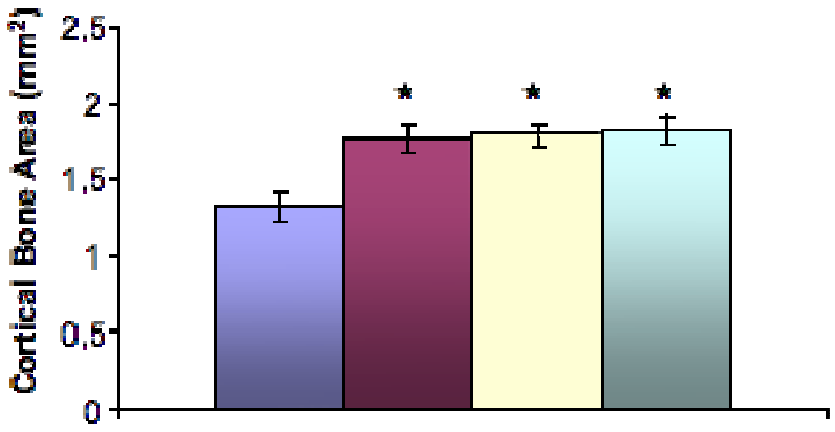

Figure 22: Cortical bone area in mm^2 +/- standard error in long-sections of tibiae 21 days post tumour cell inoculation in the treatment study, * $p<0.05$.

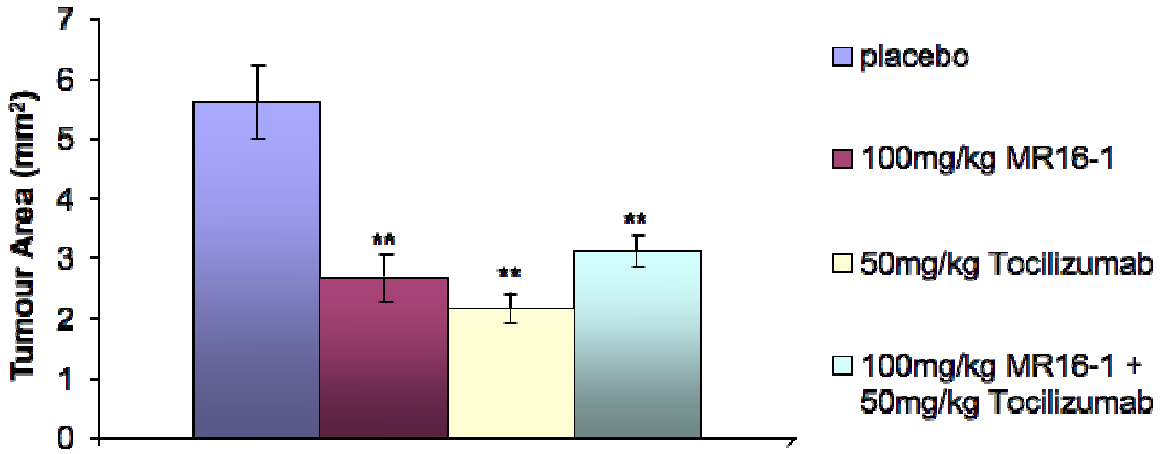

Figure 23: Tumour area in mm^2 +/- standard error in tibiae 21 days post tumour cell inoculation in the treatment study. * $p<0.05$.

Only treatment with the anti-human IL-6R mAb tocilizumab and the combination treatment decreased the number of active osteoclasts at the bone-tumour interface

The number of active osteoclasts was determined by staining sections for tartrate-resistant acid phosphatase, which reveals osteoclasts as pink multinucleated cells lined up along the bone-tumour interface. Osteoclast numbers were counted on the border of the growth plate and the tumour as trabecular bone-tumour interface (Oc n°/mm TBTI), as well as at the cortical bone-tumour interface (Oc n°/mm CBTI). The numbers obtained here were then referred to the osteoclast number per mm overall bone-tumour interface (Oc n°/mm BTI).

In this experiment, there were no significant differences between the treatment groups in the osteoclast count at the growth plate tumour interface (Table 18). However, significant discrepancies were seen in the number of osteoclastic cells at the cortical bone-tumour interface, which account for variations of osteoclast numbers at the overall bone-tumour interface.

Whereas blocking the mouse IL-6R with 100mg/kg/3 days MR16-1 did not decrease osteoclast numbers in general compared to placebo treated mice (11.245/mm vs. 10.910/mm), a significant change in the number of active osteoclast at the bone-tumour interface was determined by injecting mice with either 50mg/kg/3 days tocilizumab (8.520/mm, p=0.0052) or a combination of both antibodies (9.095/mm, p=0.0348).

In this context it is apparent that the anti-human IL-6R mAb tocilizumab can be responsible for these effects in the combination treatment group. Consequently, these results suggest that IL-6R activation on the tumour cells stimulates osteoclast activation by means of secondary effectors,

which are produced and secreted in response to para- or autocrine IL-6 signalling in tumour cells and consecutively exert actions on host cells. These secondary effectors are probably other pro-resorptive factors exerting an even greater effect on osteoclast activation than IL-6. By blocking the tumour cells' response to IL-6 with tocilizumab, the amount of these other pro-resorptive factors released into the bone microenvironment is decreased and therefore osteoclast activation is reduced in these tibiae. MR16-1 antagonizes IL-6 signalling in host cells. Even though IL-6 is widely recognized to support osteoclast precursor cell differentiation and activation of mature osteoclasts [127, 219], it is important to take into consideration that IL-6 is only one of many pro-resorptive factors and among these certainly not the most potent one. So, by blocking solely the response to IL-6 in host cells, but allowing other osteolytic factors to exert actions on the former and thus promote osteoclast differentiation and activation, no inhibition of osteoclast activity is achieved.

Nevertheless, there are smaller osteolytic lesions as shown in the radiographic images on days 10, 17 and 21. Moreover, the pilot study showed significantly decreased osteoclast numbers at the bone-tumour interface for mice treated with 100mg/kg/3 days MR16-1, too. A possible explanation might be that MR16-1 only inhibits bone resorption and tumour growth in bone in the early stages of application. If therapy continues, effects wear off and osteoclasts are increasingly activated and start resorbing bone with consequent promotion of tumour growth. In this case, treatment with the anti-mouse IL-6R mAb would only attenuate the development/onset of osteolytic breast cancer bone metastases but not inhibit it. When comparing the two experiments with each other, it is possible that the end point of both studies was defined on day 21 post tumour cell inoculation, but that the tumour model appeared to be in different stages due to unknown influences. But the bone metastases model in the dose finding experiment still showed suppressed numbers of osteoclast and reduced tumour growth. Animals treated with 100mg/kg/3 days MR16-1 already passed his stage of tumour growth and inhibitory effects of host IL-6R blockage are overridden by other pro-resorptive factors, or even accumulation of IL-6 due to a delayed clearance rate. In this case, the osteoclast number would be the first factor to increase again, followed by bone resorption and lastly, tumour growth and tumour biology. Therefore, if this model is correct, the early stages of mAb being overridden are just occurring. Moreover, this implies that most of the tumour-derived hIL-6 binds to the murine receptors expressed on the host cells. When these are blocked, the clearance is affected to a greater extent than it is by blocking the human IL-6R with tocilizumab. For the combination treatment, the wearing-off effects would occur even earlier, which might explain why the combination of both antibodies is not as efficient in the first place.

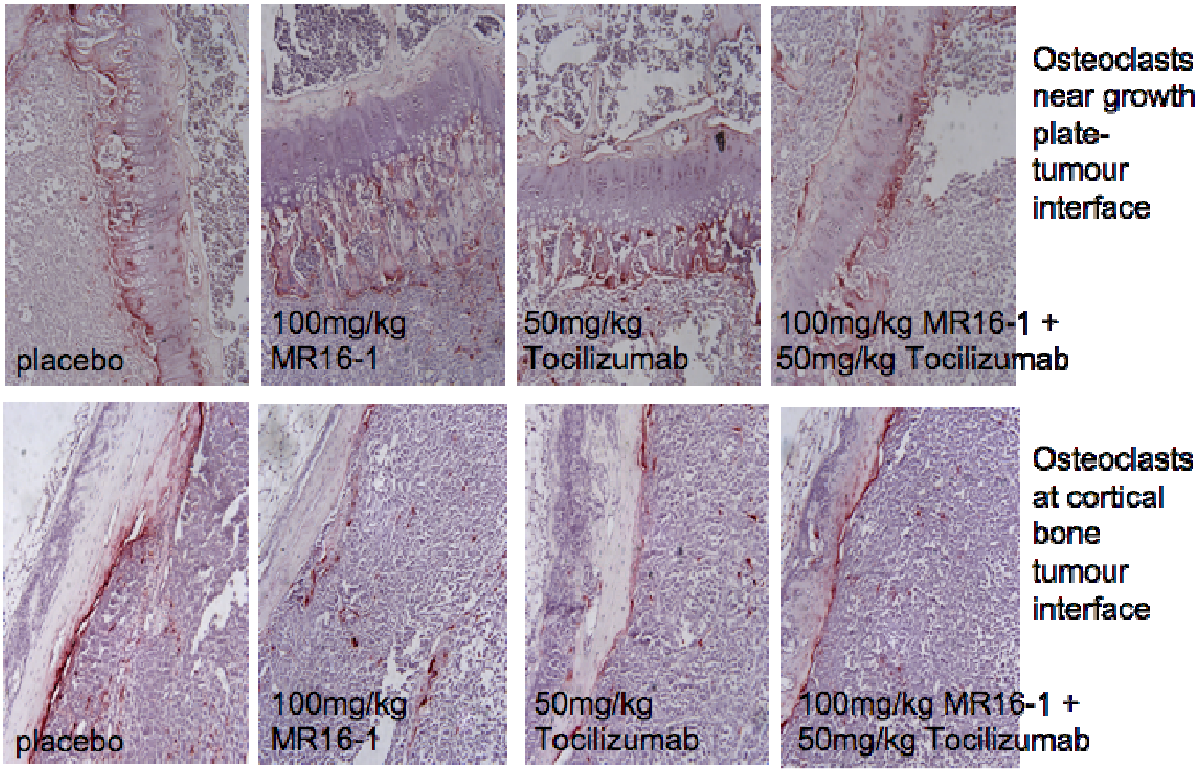

Figure 24: TRAcP stain of breast cancer cell-containing tibiae 21 days post tumour cell inoculation in the treatment study.

	Oc n°/mm TBTI	Oc n°/mm CBTI	Oc n°/m BTI
Placebo	10.85 +/- 0.638	11.55 +/- 0.730	10.91 +/- 0.619
100mg/kg/3 days MR16-1	9.95 +/- 0.864	12.77 +/- 0.707	11.24 +/- 0.897
50mg/kg/3 days tocilizumab	8.83 +/- 0.633	8.84 +/- 0.757 *	8.52 +/- 0.473 *
100mg/kg/3days MR16-1 + 50mg/kg/3 days tocilizumab	9.12 +/- 0.976	9.06 +/- 0.599*	9.09 +/- 0.456 *

Table 18: Osteoclast number at the TBTI, CBTI and overall BTI per mm bone-tumour interface +/- standard error in the treatment study. OC n°/ mm TBTI = Osteoclast number per mm trabecular bone-tumour interface, Oc n°/mm CBTI = Osteoclast number per mm cortical bone-tumour interface, Oc n°/mm BTI = Osteoclast number per mm overall bone-tumour interface. * $p < 0.05$ vs. Placebo.

Analysis of serum markers of bone turnover P1NP and TRAcP5b did not mirror observations concerning bone turnover made locally at the site of tumour-induced bone resorption

It is widely recognized that bone resorption and bone formation always occur together, hence, the imbalance between these two processes dooms the phenotype of bone metastases as osteolytic or osteosclerotic. Therefore, levels of serum markers of bone formation, P1NP, and bone resorption, TRAcP5b, were determined by means of commercially available ELISA kits for both molecules.

Serum of mice receiving placebo treatment contained TRAcP5b values of 6.98U/L and P1NP levels of 56.71pg/ml. A literature search showed that serum TRAcP5b in 8-week-old nude mice not injected with breast cancer cells, reaches values of around 1 U/L and P1NP levels of 400pg/ml [169, 171, 220]. Consequently, it is obvious that implanting the human breast cancer cell line MDA-Tx-SA into tibiae of nude mice induces a great increase in osteolysis and a substantial decrease in bone formation, correlating with the phenotype of osteolytic bone metastases.

Administration of 100mg/kg/3 days MR16-1 resulted in an increase in both TRAcP5b (8.53U/L) and P1NP (72.15pg/ml) in the serum of these mice 21 days post tumour cell inoculation, compared to placebo treated animals. Even though these changes are not significant when compared to placebo treated mice, a trend towards accelerated bone turnover can be established here. This correlates with the theory that mAb effects are just overridden on day 21 and thus, enhanced tumour-induced osteolysis is just taking place.

On the other hand, treatment with either 50mg/kg/3 days tocilizumab or the combination of both antibodies resulted in hardly any changes regarding the serum markers of bone turnover (5.68U/L TRAcP5b and 58.97pg/ml P1NP in the group receiving 50mg/kg/3 days tocilizumab and 7.24U/L TRAcP5b and 66.68pg/ml P1NP in the serum of mice treated with both antibodies). Data are shown in Figure 25 andFigure 26.

These data do not only mirror the observations acquired in terms of osteoclast numbers at the local site, but also suggest that MR16-1 is not capable of preventing a general increase of bone turnover in response to the tumour in the mouse organism. However, it is important to take into consideration that serum biochemistry was only conducted at the endpoint of the study. No values were obtained for any earlier time point. Moreover, serum biochemistry includes processes occurring within the whole organism and might therefore not display results as striking

as does assessment at the local site by means of histology. Also, all values obtained are very far from those considered normal in healthy mice.

Nevertheless, it becomes obvious that MR16-1 does not inhibit osteoclast activation and consequent bone resorption, followed by reactive bone formation. On the contrary, tocilizumab shows reduced osteoclast numbers, as well as slightly reduced values of TRAcP5b in the serum. Again, the effects of combination treatment are not as strong as those of treatment with the single antibody tocilizumab. Still, it is likely that tocilizumab can be responsible for beneficial effects in the combination treatment group, regarding the number of active osteoclasts and attenuation of bone turnover.

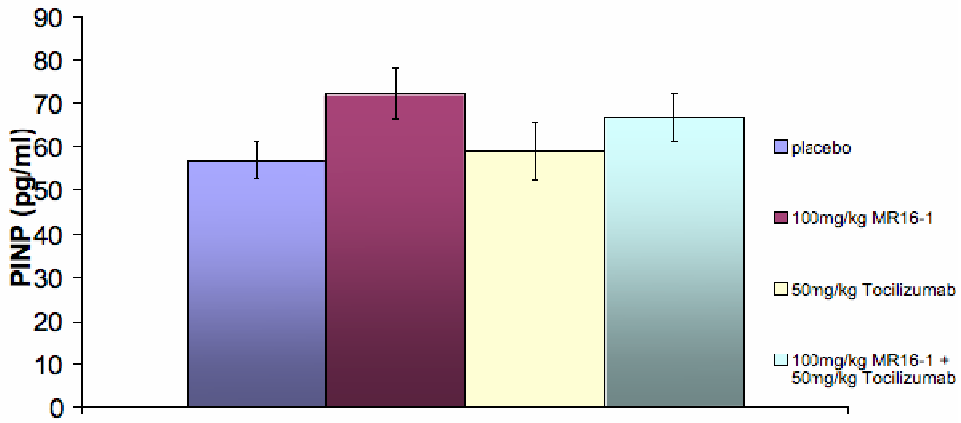

Figure 25: P1NP concentrations in pg/ml +/- standard error in serum of mice 21 days post tumour cell inoculation in the treatment study.

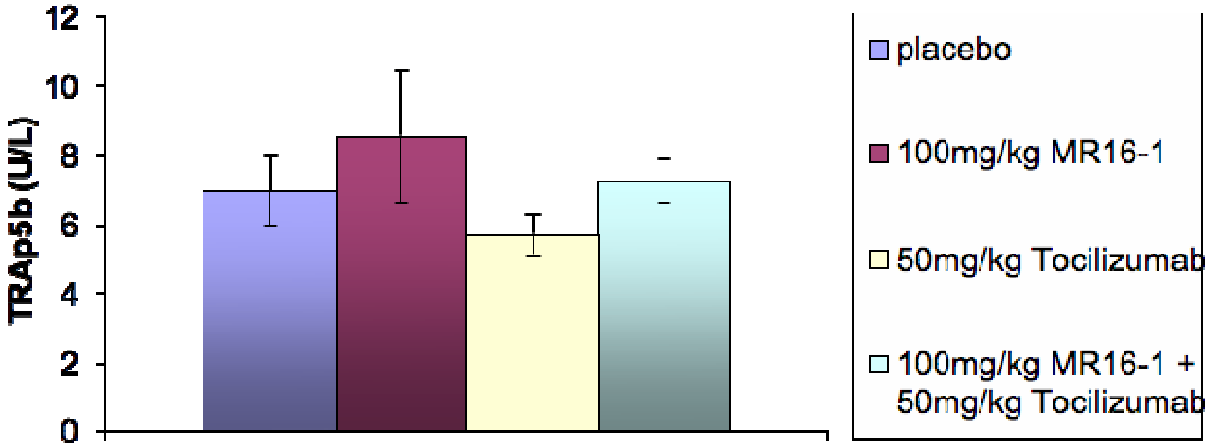

Figure 26: TRAcP5b concentrations in pg/ml +/- standard error in serum of mice 21 days post tumour cell inoculation in the treatment study.

MR16-1 and/or tocilizumab-treated tumours contained fewer proliferating cells and higher apoptotic ratios

The tumour biology was assessed by employing immunohistochemical staining techniques for both proliferation (Ki67) and apoptosis (TUNEL). Positive cells were counted and the index of cells undergoing proliferation or apoptosis was calculated.

Ki67 staining revealed a significant decrease of the fraction of proliferating cells within the tumour when treated with either therapeutic regimen. Whereas in the control samples, an average of 8.24% of cells resided outside the resting G0 phase, this number dropped to only 3.27% in tumours of mice receiving 100mg/kg/3 days MR16-1 treatment ($p<0.001$) and 4.04% in tumours of 50mg/kg/3 days tocilizumab treated mice ($p<0.001$). Very similar reductions were observed in tumours of mice administered the combination treatment (3.75% Ki67 positive cells, $p<0.001$ compared to placebo treatment). Results are shown in Figure 28.

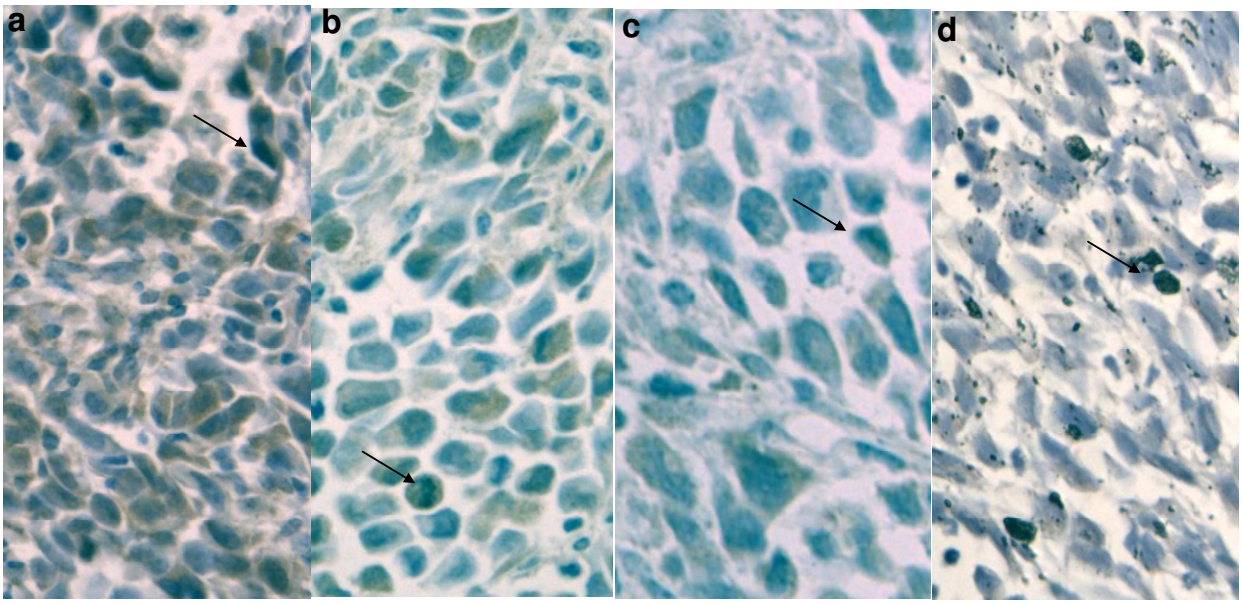

Figure 27: Ki67 immunohistochemistry in breast cancer cell-containing tibiae 21 days post tumour cell inoculation in the treatment study a= control, b = 100mg/kg/3 days MR16-1, c= 50mg/kg/3 days tocilizumab, d= 100mg/kg/3 days MR16-1 + 50mg/kg/3 days tocilizumab, → Ki67 positive cells

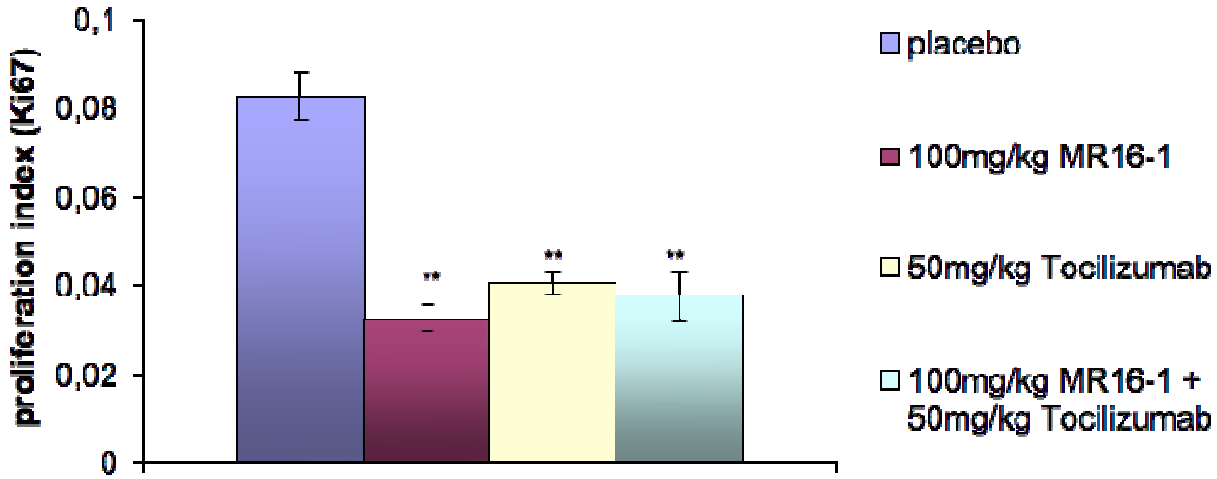

Figure 28: Index of Ki67 positive cells in tumours in tibiae 21 days post tumour cell inoculation +/- standard error in the treatment study. ** $p<0.001$.

Along with diminished proliferation of tumour cells, the rate of cells undergoing apoptosis was significantly increased in tumours of mice treated with antibodies. 100mg/kg/3 days MR16-1 raised the apoptotic ratio from 1.71% in placebo-treated mice to 2.93% ($p=0.004$). Greatest effects were determined in the group receiving 50mg/kg/3 days tocilizumab, displaying 3.54% positive cells for apoptosis within the tumours ($p<0.001$). The combination treatment with 100mg/kg/3 days MR16-1 and 50mg/kg/3 days tocilizumab increased the rate of apoptotic cells to 3.08% ($p=0.0002$). When juxtaposing these results with the apoptotic ratios obtained in the pilot study, it becomes obvious that percentages in positive cells in the tumours receiving either 100mg/kg/3 days MR16-1 or 50mg/kg/3 days tocilizumab are very similar.

Thus, treatment with 100mg/kg/3 days MR16-1, 50mg/kg/3 days tocilizumab or the combination of the two, significantly decreased proliferation and increased the apoptotic ratio within the metastatic breast cancer cells located in the bone microenvironment (Figure 30).

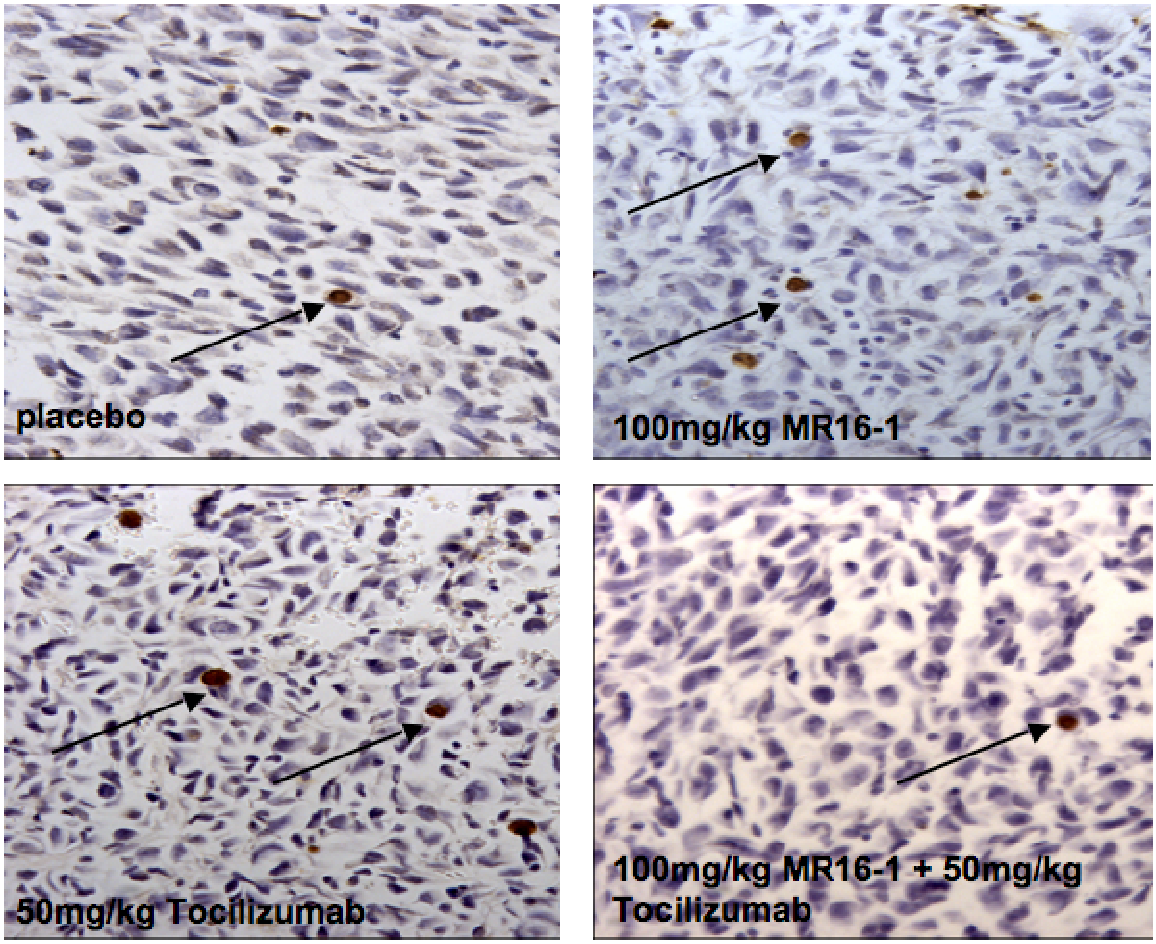

Figure 29: TUNEL staining in breast cancer cell containing tibiae 21 days post tumour cell inoculation in the treatment study. Cells positive for apoptosis are staining brown.

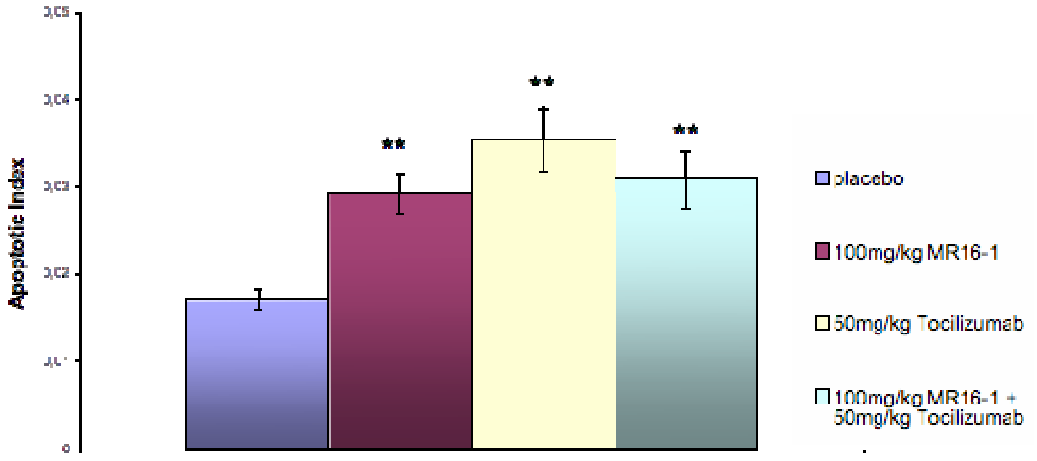

Figure 30: Apoptotic Rate (%) in tumours in tibiae 21 days post tumour cell inoculation +/- standard error in the treatment study. ** $p<0.001$.

Confirming the results with the combinations of both antibodies

In the previously described study, treatment with the murine IL-6R mAb MR16-1 and the human IL-6R mAb tocilizumab simultaneously manifested beneficial effects that were not only not greater but even smaller in terms of abating growth of breast cancer bone metastases in the murine xenograft model. In order to confirm these results once more, we conducted a further study in which only a placebo group, injected with PBS i.p., as well as mice receiving the combination treatment with 100mg/kg MR16-1 and 50mg/kg tocilizumab were included. The study protocol complies with the protocol applied in the former experiments.

Administration of 100mg/kg/3 days MR16-1 + 50mg/kg/3 days tocilizumab initially decreased tumour-induced bone resorption, but effects vanish at later time points

Radiographic images were taken on days 10, 17 and 21 post tumour cell inoculation into the tibiae of 5-week old nude mice. Measurement of the osteolytic areas revealed that administration of the combination treatment reduced pathological bone resorption to a small extent on day 10 (-13.79%) compared to placebo treatment, but this effect disappeared almost entirely towards the end of the study, since only a decrease of the resorptive area of -4.55% on day 17 and 1.65% on day 21 could be determined (Figure 31).

Therefore, it can be stated that the lessened benefits already observed in the treatment study are not due to the injection of another preparation of MDA-Tx-SA cells but rather verify the data obtained before. Thus, the combination treatment with both antibodies does not prove to be as effective as treatment with the anti-mouse or the anti-human IL-6R mAb alone, nor does it produce additional effects. This raises the questions whether this is due to an interaction between these two antibodies, that in the end, results in an activation instead of a blockage of an IL-6R, or whether this prevents binding of the two antibodies to their appropriate receptors, or, whether the impaired clearance of IL-6 from the serum and bone micro-environment leads to the antibody effect being overridden at early stages already. The effect that great concentrations of IL-6 prevent beneficial effects of IL-6R mAb was already described [193].

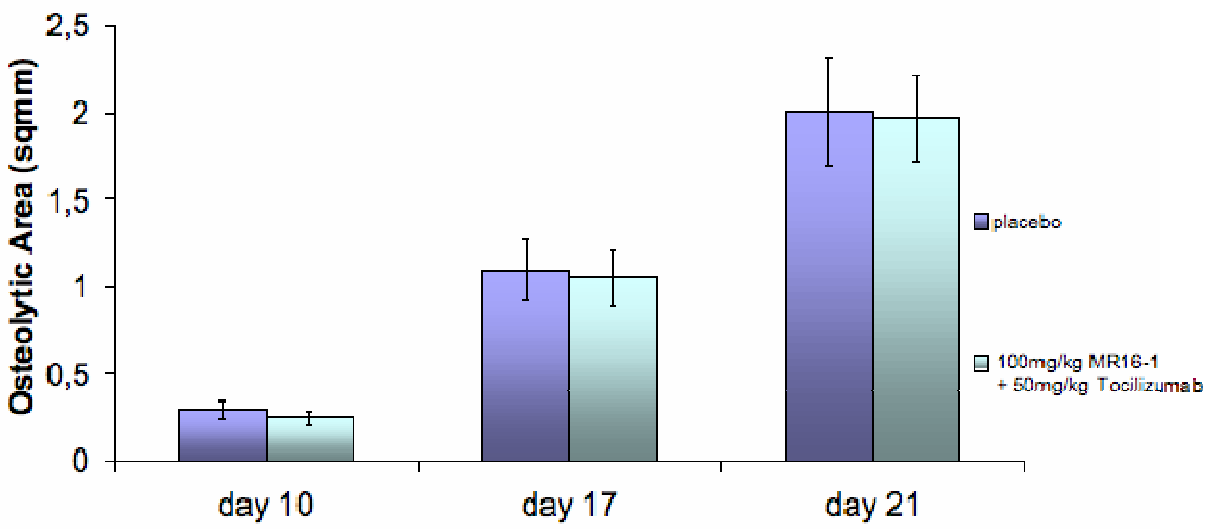

Figure 31: Osteolytic areas in mm^2 +/- standard error in tibiae on days 10, 17 and 21 post tumour cell inoculation in the confirmation study.

Effects of tocilizumab on hIL-6 and human IL-6R mRNA expressions and hIL-6 protein secretion by MDA-Tx-SA cells in vitro

Expression of the pleiotropic cytokine IL-6 plays an important role in numerous cancers, such as mammary, prostate and lung cancer. It has been associated with both pro- and anti-tumour effects in mammary epithelial cell lines and is known to influence the degree of gene expression of numerous genes via activation of the STAT3 signalling pathway. Moreover, IL-6 plays a major role in inducing and maintaining osteolytic bone metastases by stimulating the activity of mature osteoclasts, as well as the maturation of precursor cells of the bone microenvironment. However, whether IL-6 signalling in the human breast cancer cell line MDA-Tx-SA also affects gene transcription of the cytokine itself or expression of its cognate receptor is not yet clear. A hypothetical autocrine loop could function as a feedback or feed-forward mechanism, meaning that hIL-6 might either result in promotion or reduction of its own expression.

In order to determine the influence of IL-6 signalling on the expression of the cytokine itself and its receptor, MDA-Tx-SA cells were seeded with $1*10^5$ cells/ml for RNA isolation and $2.5*10^4$ cells/ml for protein detection and incubated overnight in supplemented DMEM, before media was removed and changed to serum-free DMEM supplemented with 0.1% BSA. This stimulates the transcription and secretion of hIL-6 by these cells, providing perfectly sufficient amounts of this cytokine to exert actions on the cells via activation of the hIL-6R expressed on the latter. Simultaneously with serum-free medium, antibodies were added into the wells. Treatment

groups included control, 50µg/ml tocilizumab and 100µg/ml tocilizumab. All experiments were run in triplicate. Treatment was carried out for 12 hours before cell lysates were harvested for RNA isolation and supernatants were collected for protein level determination.

Treatment of MDA-Tx-SA cells with tocilizumab influences hIL-6 and human IL-6R transcription levels by these cells

RNA isolation, cDNA synthesis and following qPCR were performed with cell lysates. Assessing the levels of hIL-6 mRNA expression by these cells after treatment revealed that 50µg/ml tocilizumab marginally suppressed hIL-6 gene expression (82.6% +/- 28.9%). On the other hand, adding the higher dose of the human IL-6R antibody, 100µg/ml, to MDA-Tx-SA cells did significantly interfere with hIL-6 gene expression levels, decreasing them to 66.85% +/- 32.3% compared to cells incubated without tocilizumab.

In the same samples, gene expression levels of human IL-6Rs were determined. By altering the expression of its cognate cytokine receptor, MDA-Tx-SA cells would be capable of modifying their responsiveness to hIL-6. Increasing or diminishing receptor expression on the cells could hence lead to corresponding modifications in the downstream signalling pathway activity. As shown in Figure 32, cells incubated with 50µg/ml or 100µg/ml exhibit diminished levels of human IL-6R mRNA expression compared to placebo-treated control samples (74.55% ($p=0.015$) and 58% ($p<0.001$)). Consequently, blocking the human IL-6R on MDA-Tx-SA cells by applying tocilizumab affects downstream signalling and hIL-6 induced gene expression in a dose-dependent manner.

While hIL-6 transcription rates are only diminished when large amounts of IL-6Rs are inhibited by tocilizumab, the expression of human IL-6Rs by MDA-Tx-SA cells seem to react in a more sensitive way. Already, lower doses of tocilizumab decrease rates of receptor gene transcription. Thus, active hIL-6 signalling pathways enhance the expression of hIL-6Rs and therefore, augment the responsiveness of the cells to the cytokine.

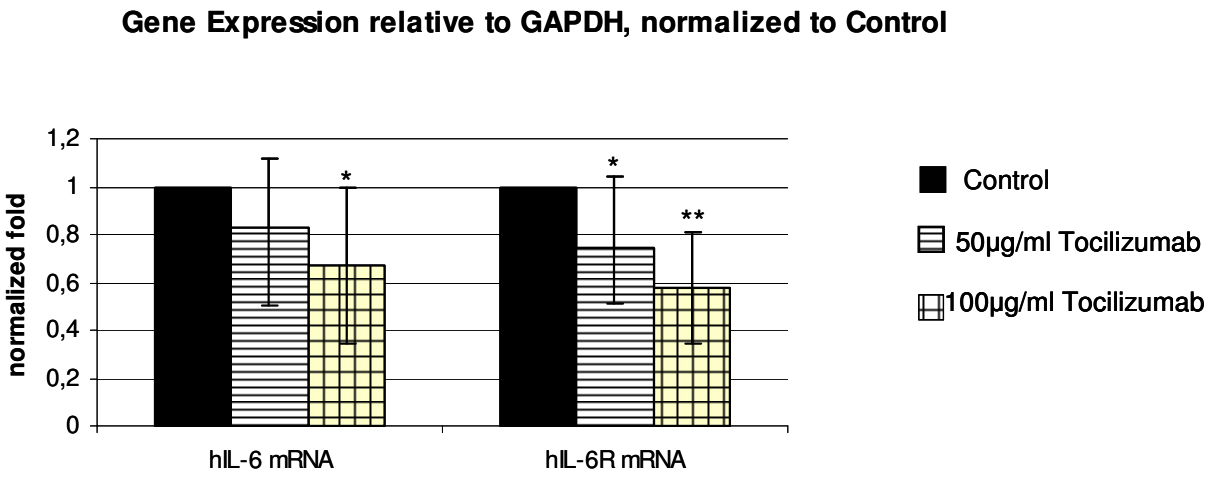

Figure 32: Levels of hIL-6 and hIL-6R mRNA expression *in vitro*. Cells were cultured overnight before hIL-6 expression was induced by changing the culture medium to serum-free DMEM, supplemented with 0.1% BSA. Antibody treatment was added immediately into this medium for a further 12 hours. RNA was extracted after this incubation time from all samples and levels of hIL-6 and hIL-6R mRNA were measured with qPCR SYBR Green technique. All values were normalized to GAPDH expression of each sample and are expressed as relative value, compared to control treated samples. All data are shown as mean (n=10) +/- standard deviation. * $p<0.05$, ** $p<0.001$.

Treatment of MDA-Tx-SA cells with tocilizumab does not alter the level of hIL-6 protein secretion by these cells

Since there are many ways to alter gene expression later than on the transcriptional level, hIL-6 protein concentrations were determined in supernatants obtained from cells treated for 12 hours with 50µg/ml or 100µg/ml of the anti-human IL-6R mAb tocilizumab, while inducing hIL-6 secretion via nutrient-depletion in serum-free BSA-containing medium. This can be considered an endpoint analysis, since the product of the signalling pathway – the protein – is measured. A commercially available ELISA kit employing the so-called sandwich ELISA technique was used for determination of hIL-6 levels in supernatants. Furthermore, the monoclonal antibody tocilizumab, itself diluted in serum-free DMEM, but without any previous contact to MDA-Tx-SA cells, was tested for cross-reactivity with the ELISA kit. No increase of absorption at 450nm was observed due to tocilizumab only. Therefore, the IL-6 antibody bound to the wells of the microtiter plate and tocilizumab do not interfere with each other and thus, do not influence the analysis (data not shown).

Concerning levels of hIL-6 protein secreted by MDA-Tx-SA cells, no significant differences were found between any of the groups, compared to control samples. Incubation with 50µg/ml tocilizumab still showed 78.33%, 100µg/ml tocilizumab 84.86% hIL-6 protein expression (Figure 33). These results suggest that stimulation with hIL-6 does not alter the hIL-6 protein production and secretion itself and, moreover, confirm the findings described above concerning the mRNA transcription levels of hIL-6. Inhibiting IL-6 signalling in MDA-Tx-SA cells by blocking human IL-6Rs with tocilizumab therefore does not affect concentrations of hIL-6 in the supernatants of cells treated with this antibody.

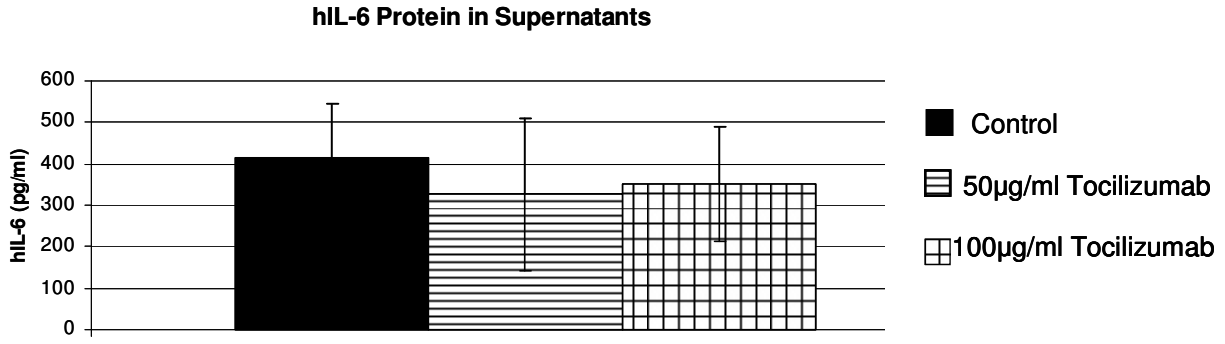

Figure 33: hIL-6 protein levels in supernatants of MDA-Tx-SA cells. Cells were seeded with $2.5*10^4$ cells/ml. After incubation in supplemented DMEM overnight, hIL-6 expression was induced by serum-free DMEM, supplemented with 0.1% BSA. Antibodies were added directly into the wells and lasted for 12 hours with either control or 50µg/ml or 100µg/ml of the anti-human IL-6R antibody tocilizumab (n=3). Supernatants were then collected and hIL-6 concentrations were measured using a commercially available ELISA kit. All data are shown as means +/- standard deviation.

Discussion

High circulating levels of IL-6 have been associated with adverse clinical outcomes in patients with metastatic breast and prostate cancer. For example, survival rates are significantly shorter in cancer patients with persistently high serum IL-6 levels [174-175, 221-222]. The pleiotropic cytokine IL-6 has been associated with increased osteolysis and tumour progression in breast cancer bone metastases [100, 160]. Tocilizumab is a monoclonal anti-human IL-6R antibody approved for the treatment of inflammatory autoimmune conditions. Human studies have demonstrated tocilizumab to be effective in the treatment of IL-6-related disorders, such as rheumatoid arthritis or Crohn's disease [39, 47, 223]. Furthermore, targeting the IL-6R may show clinical benefit in certain malignancies such as multiple myeloma and oral squamous cell carcinoma [224-225]. However, the use of tocilizumab in human metastatic bone disease has not been studied yet.

Using the species-specific features of the anti-human IL-6R mAb, tocilizumab, to block IL-6 signalling in human breast cancer cells and the anti-mouse IL-6R mAb, MR16-1, to impede IL-6R activation in host cells of the bone microenvironment in a xenograft model, we established that both antibodies inhibit metastatic breast cancer progression in murine bone to a similar extent, indicating that IL-6 signalling to both cancer *and* host cells promotes tumour growth. However, due to its specificity for the human IL-6R, tocilizumab in our setting can only inhibit auto- and paracrine IL-6 signalling between human (i.e. cancer) cells, while permitting human IL-6 to activate the murine IL-6R on the host (i.e. bone) cells [215] (Figure 11). Nevertheless, we have observed that tocilizumab treatment strongly inhibits tumour growth within the murine bone environment. This suggests a biologically relevant auto- and paracrine IL-6 signalling pathway in cancer cells. On the other hand, MR16-1 inhibited skeletal tumour growth, likely due to its combined action on both autocrine and paracrine signalling in and between bone cells. Our finding that disruption of IL-6 signalling in cancer cells strongly inhibits tumour growth in mice, provides experimental evidence for a causal relationship between IL-6 expression and these adverse clinical outcomes.

Discussion of methods

Five-week-old BALB c nu/nu mice were inoculated intratibially with MDA-Tx-SA cells: the bone-seeking clone of the ER-negative human breast cancer cell line MDA-MB-231. One day

prior to tumour cell inoculation, on the day of tumour inoculation and from then on every three days during the twenty-one days of experiments, animals were injected intraperitoneally with different doses of the mAbs tocilizumab or MR16-1, in order to define the most promising dose regimen for each antibody in a pilot study (Figure 9). As a result, administration of either 50mg/kg/3 days tocilizumab or 100mg/kg/3 days MR16-1 showed most beneficial effects in terms of reduced tumour-induced osteolysis and vitality of human MDA-Tx-SA cells within tibiae at the end of this set of experiments.

Afterwards, larger experiments were conducted in which only the most effective doses of each antibody, as mentioned above, and a combination of both antibodies were administered in the same manner as in the first set of experiments. In a last set of *in vivo* experiments, we, once more, confirmed the data obtained for the combined administration of the two antibodies simultaneously.

X-ray analysis

Effects of IL-6R mAb treatment in this study were monitored by radiographic imaging on days 10, 17 and 21 post tumour cell inoculation during the experiments, followed by endpoint analysis of histological sections and serum parameters. Even though X-ray analysis revealed significant reduction of osteolytic bone destruction on all three occasions, it is important to note that by means of this technique only lesions are detected, in which more than 30-75% of the bone mineral content is lost already [153]. Thus, bone metastases with a smaller degree of bone destruction cannot be identified. This observation might also explain some of the differences observed between radiographic measurement of the tumour area on day 21 and the tumour size determined in the H.E.-stained sections (Figure 13 vs. Figure 15 and Figure 21 vs. Figure 23). Furthermore, X-ray analyses of the size of bone metastases only reveals osteolytic types of metastases. Even though osteolytic bone metastases are most common in patients suffering from breast cancer, there are about 15% who develop osteoblastic bone metastases which cannot be as easily detected by X-ray alone [143].

The mouse model and its impairments and limitations

Athymic nude (nu/nu) mice are widely employed for the heterotransplantation of human tumour cell lines established *in vitro* and tumour cells directly grafted from patients. The lack of T cells prevents repelling of the xenograft human tumour cells by the murine organism. Hence, tumour growth and its behaviour in response to varying conditions can be studied. By comparing groups

of mice injected with either the placebo treatment or the specific antibody treatments, but keeping the rest of the conditions standardized, it is possible to account for the differences found in the study to the differing conditions, in this case the antibody treatment.

However, this model may only serve as a basic model, since human tumour cells are inoculated into a xenograft organism which is devoid of functioning mature T cells. T cells play a major role in cell-mediated immune response and tumour defence [226]. In addition to this, T cells are also affected by IL-6 signalling in various ways [227]. It has been reported that IL-6 supports differentiation of cytotoxic T cells from immature thymocytes, fuels the activation of T cells and NK-cells, and up-regulates the expression of chemokines and adhesion molecules [199, 228-229]. Furthermore, Interleukin-6 enhances the cytolytic capability of NK-cells [13]. Taking these effects of Interleukin-6 on T cells into consideration, it becomes obvious that Interleukin-6 also has an anti-tumour effect, which is neglected in the model using T-cell deficient BALB c nu/nu mice.

In order to obtain a model of breast cancer bone metastases, mice were inoculated directly intratibially with the bone-seeking clone of the ER-negative human breast cancer cell line MDA-MB-231, MDA-Tx-SA. This enables us to observe processes of tumour growth and development in this particular microenvironment and the influences of IL-6R mAbs. By injecting the tumour cells directly into the tibiae of nude mice, the process of tumour development and progression at the orthotopic site, as well as the process of metastasising to different sites of the organism, was neglected. An ideal animal model of human cancers that metastasize to bone would also reproduce the genetic and phenotypic changes that occur within cancer cells during the metastasizing process. These include invasions, vascular spread to bone and proliferation and survival in the bone microenvironment with subsequent modifications of bone structure [230]. Hence, in order to monitor the whole metastatic process, mammary fat pad injections should be used [231].

In other words, this model does not represent earlier stages of bone metastases but only late events in the metastatic process. Nevertheless, it is suited to monitor the effects of bone resorption inhibitors, as well as effects of breast cancer bone metastases in the bone microenvironment [231].

Antibody doses

In the pilot study, the most effective doses of both the anti-human and the anti-mouse IL-6R mAb were determined. Thus, the following experiments were run with these doses revealing only partly significant effects. In humans, between 4mg/kg to 8 mg/kg tocilizumab is the recommended dose for treating RA [232-233], also showing beneficial effects in the bones and joints of patients suffering from this disease. When comparing the amount of antibody we injected weight-adjusted intraperitoneally into nude mice to doses recommended for the treatment of RA in humans, the doses necessary in our studies appear to be substantially higher. In former studies, it has been described that saturation of the sIL-6R by tocilizumab is achieved already with doses of 0.1µg/ml and complete inhibition was found at 4µg/ml [39, 193]. However, the main effector organs in these former studies were all characterized by a very good blood supply, implying that concentrations of the antibody within the effector organ were similar to systemic blood concentrations. Bone is a tissue within the organism, which is reached by therapeutic agents admitted systemically in much lower concentrations than, for example, the heart or the liver. The dose testing study revealed that much higher doses are needed in order to obtain effects in the bone microenvironment. This might be due to the fact that bone is an exclusive compartment within the organism, which is only reached by a fraction of the antibody dose administered systemically. Thus, blood concentrations and concentrations of the monoclonal antibody within the bony compartment are not equal, and much higher systemic antibody concentrations might be needed in order to attain significant effects in bone. Hence, it becomes obvious that higher doses need to be administered in order to obtain similar effects in bone than in tissues with a high blood supply. One also has to take into consideration that it has been reported that maintenance of high levels of tocilizumab was important to achieve clinical efficacy [234]. It is worth noticing that mice usually exhibit a much faster metabolism of tocilizumab via the RES than humans [234-235] so that higher weight-adjusted doses in preclinical trial with animals might be justified.

Ki67 vs. mitotic index

In order to analyse the index of tumour cells undergoing apoptosis, the mitotic index was applied in the pilot study, whereas in the treatment study, cells undergoing mitosis were marked with immunohistochemistry for Ki67. Previous studies have shown that the immunohistochemically determined Ki67 fraction and the number of mitotic figures are positively correlated and clearly associated with breast cancer prognosis. [210] This is understandable, since both Ki67 and

mitotic activity are markers of cell proliferation. It is well known that Ki67 is expressed in all cell cycle phases except in the resting cell (G0 phase). Although the correlation between cells positive for Ki67 and mitotic figures is obvious, not all Ki67+ cells enter mitosis [210]. This might be a possible explanation of why the index of cells positive for Ki67 in the tumours of the treatment study is generally higher than the index of cells found positive when counting the mitotic index in the pilot study (Figure 18 and 28).

Confirmation study

Since data obtained for the combined administration of both antibodies did show less promising effects than the administration of a single antibody, a further set of experiments was carried out, in which radiographic results obtained earlier for the combination treatment with the anti-human and the anti-murine IL-6R mAbs were once more verified. In retrospect, we found that this group of mice was injected intratibially with the same batch of cells in the treatment study, but these cells were prepared for intratibial implantation separately from the other injections due to the high number of animals in the prior experiment. This practice was applied to ensure vitality of cells injected into the tibiae of nude mice. On the other hand, it is possible that during the cell preparation, other circumstances might have influenced the growth of tumour cells in the bone micro-environment. Hence, another study was conducted in which only a control group injected with PBS intraperitoneally and a treatment group receiving 100mg/kg MR16-1 + 50mg/kg tocilizumab were included. The experimental design was the same as the ones applied before to obtain reproducible results. However, only analysis of X-ray images was conducted on days 10, 17 and 21 to check for similar results first. In case major differences to the treatment experiment conducted before would have been found, further histological examinations would have been carried out.

Up to now, there is no literature available on testing the efficacy of the combination of both a human IL-6R mAb and a mouse IL-6R mAb. However, it has been reported that after regular injections of MR16-1, a tolerance to this monoclonal antibody due to auto-antibody development was observed [236]. In addition to this, since both MR16-1 as well as tocilizumab include an antigen-binding domain and an IgG domain, there might be interferences between the two different antibodies, which consequently might explain the lack of effect the combination of both antibodies displayed. Further experiments are needed in this field.

Interleukin-6 and the metastasising process

As stated above, establishing metastases is a sequential multi-step process. Tumour cells at the primary site acquire properties tha allow them to invade the surrounding stroma and vasculature, to gain access to the blood stream and to survive in the circulation; to home to specific secondary sites and to establish secondary growth at the metastatic site [237]. This study only concentrates on the endpoint of this process, since tumour cells were injected directly, in considerably high quantities, into tibiae of nude mice. Interleukin-6 however is a cytokine which exerts actions systemically and locally in numerous organs and compartments of the organism, and not only the bone microenvironment (Figure 1). Thus, treatment with IL-6R mAbs might possibly also diminish the number of breast cancer bone metastases by blocking certain steps in the metastasising process. It is known that IL-6 signalling enhances VEGF expression which then promotes CXCR4 expression on endothelial cells of the bone marrow, an important molecule for homing breast cancer cells to bone [153]. Thus, blocking the IL-6R with mAbs might prevent breast cancer cells in the circulation from extravasating into the bone marrow and forming metastases there.

Bone of inferior quality seems to be more prone to acquiring bone metastases than healthy, stable bone [237]. Furthermore, it was shown that administration of bisphosphonates prior to intra-osseous tumour cell inoculation of MDA-MB-231 cells decreased the number as well as the progression of bone metastases, even though there was no consistent effect on the establishment of bone metastases in general [150]. In our study, IL-6R mAbs were only injected intraperitoneally into nude mice one day prior to tumour cell inoculation, leaving no time for exerting any significant effects on bone structure before tumour cells inoculation. Thus leaving the question whether suppression of bone resorption early in the course of malignant disease and while cancer cells are still dormant might prevent the development of macro-metastases?

Serum analysis of P1NP and TRAcP5b

Serum levels of markers of bone formation, P1NP, and bone resorption, TRAcP5b, were determined at the endpoint of the study. Here, no significant differences between the placebo-treated animals, animals receiving 50mg/kg tocilizumab, 100mg/kg MR16-1 or the combination of the two antibodies, were found (Figure 25 andFigure 26). However, in the literature, in all tumour-bearing animals these markers of both bone resorption and bone formation are strongly elevated in contrast to reference levels of serum markers in healthy animals [169, 171]. This

indicates that the brittle balance between bone formation and bone resorption is disrupted in all tumour-bearing animals. However, it would be of interest to determine serum levels of P1NP and TRAcP5b at earlier stages of the experiment in order to define whether antibody treatment might have a protective effect on bone in early stages of bone metastases.

In vitro

For the *in vitro* experiments, we only focused on effects of IL-6R blockage in MDA-Tx-SA cells on hIL-6 and hIL-6R mRNA expression and hIL-6 protein production. We found that application of tocilizumab to human breast cancer cells *in vitro* decreased the levels of hIL-6 and hIL-6R mRNA expression dose-dependently, but did not show a significant effect on hIL-6 protein levels in supernatants (Figure 32 andFigure 33). However, IL-6 exerts actions on various genes [39], so it is crucial to determine influences of IL-6 and IL-6R mAbs on mRNA expression levels of other secondary messengers. We could show in further experiments conducted in our laboratory that stimulation of MDA-MB 231 cells with IL-6 increased RANK mRNA production by the human breast cancer cells significantly [238]. Consequently, the effect of IL-6R mAb administration on the gene transcription of further genes involved in bone resorption and tumour progression needs to be examined.

Discussion of results

In Vivo

In the pilot study, administration of 100mg/kg/3 days MR16-1 displayed most beneficial effects in MR16-1 treated mice. This dose regimen marks a trend towards smaller osteolytic lesions on all three occasions on which radiographic images were taken, compared to placebo-treated animals (Figure 13). There was also greater cortical bone protection and smaller tumour areas than in tibiae of mice treated with 20mg/kg MR16-1, 50mg/kg MR16-1 or placebo (Figure 14 andFigure 15). The fact that mice treated with 100mg/kg/3 days MR16-1 exhibited significantly lower numbers of active osteoclasts at the bone-tumour interface than placebo-treated animals or those injected with lower doses of MR16-1, supports the thesis that activation of osteoclasts can be considered as one of the first crucial steps leading to tumour-induced osteolysis (Table 17). Moreover, significant changes of tumour vitality were observed with increased rates of cells undergoing apoptosis and fewer proliferating cells within the tumours in the tibiae of animals

receiving 100mg/kg MR16-1 compared to other doses of MR16-1 or placebo (Figure 18 andFigure 19).

Regarding the anti-human IL-6R mAb tocilizumab, the lower dose of 50mg/kg was more beneficial in almost all analyses undertaken than administering 100mg/kg tocilizumab to mice inoculated intratibially with human MDA-Tx-SA breast cancer cells. It caused significant reductions of the osteolytic areas on all three occasions that radiographic images were taken (Figure 13) and also resulted in diminished numbers of active osteoclasts at the bone-tumour interface compared to placebo-treated animals (Table 17). Furthermore, significantly smaller tumour areas could be determined in the tibiae of animals receiving 50mg/kg tocilizumab at the end of the experiment compared to placebo-treated mice (Figure 15). The tumour biology of tumours in tibiae of mice treated with 50mg/kg tocilizumab varied strongly with significantly fewer cells undergoing mitosis and an enhanced number of tumour cells undergoing apoptosis compared to placebo treated animals (Figure 18 andFigure 19). In general, application of 50mg/kg tocilizumab is proposed to be slightly more efficient than the 100mg/kg MR16-1 treatment in the pilot study. This might be due to the fact that tocilizumab inhibits IL-6R activation on tumour cells, whereas MR16-1 blocks IL-6R activation on cells of the bone microenvironment.
To further validate these data, we conducted larger experiments. Consequently, 100mg/kg/3 days MR16-1 and 50mg/kg/3 days tocilizumab were chosen as suitable dose regimens and were administered in further experiments.

The larger treatment study included these two dose regimens and, additionally, the combination of 100mg/kg MR16-1 plus 50mg/kg tocilizumab, in order to determine whether additional effects can be achieved by blocking both the human and the murine IL-6Rs. As for 100mg/kg MR16-1, positive trends observed in the pilot study could be validated: areas of tumour-related bone resorption were significantly smaller on all three occasions (Figure 21), remaining cortical bone areas present at the end of the experiment were significantly larger than in placebo-treated animals (Figure 22) and tumour areas determined on H.E.-stained sections were substantially reduced (Figure 23). Tumours themselves contained significantly less proliferating and more apoptotic cells than tumours of the placebo group, as assessed by immunohistochemistry for Ki67 and TUNEL (Figure 28 andFigure 30). However, the number of active osteoclasts at the bone-tumour interface was just as high as the one determined in samples of placebo-treated animals 21 days post tumour cell inoculation (Table 18), even though there was no other

evidence of increased tumour-related osteolysis, like diminished cortical bone areas, larger radiographically visible osteolytic lesions or greater tumour areas in samples of animals receiving 100mg/kg MR16-1. As mentioned above, activation of osteoclasts can be considered the first step towards initiation of osteolysis [76, 239]. Thus, it is possible that protective effects of the antibody treatment, in terms of bone protection, will be overcome after a certain time and the endpoint of the study did just correlate with this switch. Yoshida et al. even described an auto-antibody provoked tolerance to MR16-1 in mice [236]. We did not determine MR16-1 auto-antibodies in the serum of mice at the end of the experiments. However, due to the fact that nude, T-cell deficient mice were used in our experiments, antibody levels can be expected to be quite low compared to fully immunocompetent mice. Systemic markers of bone turnover in serum of mice at the endpoint of the study did not reveal any significant differences between animals receiving 100mg/kg MR16-1 and placebo-treated mice (Figure 25 and Figure 26).

Blocking the human IL-6R expressed on MDA-Tx-SA breast cancer cells with 50mg/kg tocilizumab in the treatment study, once again, resulted in significant reduction of tumour size in samples of tumour-bearing tibiae, as already seen in the pilot study (Figure 23). Even though the number of active osteoclasts at the bone-tumour interface compared to placebo treated animals was diminished to a similar extent as in the pilot study (Table 18), osteolytic lesions within tumour-bearing tibiae were significantly smaller on day 10 post tumour cell inoculation, but advanced up to around 75% of the size of lesions observed in the placebo group on day 17 and day 21 (Figure 21). Cortical bone areas remained reproducibly larger in animals treated with 50mg/kg tocilizumab (Figure 22). The percentage of cells undergoing apoptosis in bone-residing tumours was significantly higher compared to tibiae of placebo-treated animals (Figure 30), nevertheless, the results were not as impressive as in the pilot study. P1NP and TRAcP5b in the serum of mice on day 21, can be considered systemic markers for bone turnover, whereas the number of osteoclasts at the actual site of bone metastasis mark the local rate of activated bone resorption. For P1NP and TRAcP5b no significant differences between placebo-injected animals and animals receiving monoclonal antibody treatment with 50mg/kg tocilizumab were seen (Figure 25 and Figure 26). Even though the mitotic index and Ki67 do not render exactly the same cells as positive [210], both parameters verify that fewer cells within bone metastases treated with 50mg/kg tocilizumab are subject to proliferation than in control tumours (Figure 28). Another parameter, which was evaluated for vitality of the tumour marked cells undergoing apoptosis via TUNEL staining. Here, a significant increase in cells undergoing apoptosis could

be revealed when comparing tumours of mice injected with 50mg/kg tocilizumab and placebo (Figure 30).

Surprisingly, the combination of both antibodies did not reveal enhanced effects at any time during the course of the experiment. Even more, benefits observed in groups receiving single antibody treatments were diminished when animals were administered both antibodies simultaneously. Radiographically determined osteolytic lesions showed less reduction of bone resorption compared to placebo than single antibody treatment on days 10, 17 and 21 post tumour cell inoculation (Figure 21). Correspondingly, greater tumour areas were determined in H.E.-stained sections (Figure 23). However, cortical bone areas, osteoclast numbers at the bone-tumour interface, as well the percentage of $Ki67^+$ and $TUNEL^+$ cells within the bone metastases did not differ significantly from tumours in tibiae of animals treated with 50mg/kg tocilizumab only (Figure 22, Table 18, Figure 28 and Figure 30). It is worth noting that there are no significant differences between groups administered 50mg/kg tocilizumab or 50mg/kg tocilizumab plus 100mg/kg MR16-1. Consequently, only a trend towards smaller effects by the combined treatment compared to the single antibody administration could be determined.

Within the whole study it becomes obvious that inhibiting IL-6 signalling in human tumour cells with tocilizumab as well as blocking IL-6 signalling in murine cells by applying MR16-1 has beneficial effects in terms of impaired tumour growth and reduced bone destruction. The combination of both antibodies did not exhibit enhanced effects, but rather proved to be less beneficial than the application of either antibody alone. In literature it has been reported that the complex formed of IL-6R mAbs and IL-6 molecules impairs the clearance of IL-6 from the serum which is facilitated by internalization of the IL-6/IL-6R complex. Impaired clearance, in turn, causes elevated serum levels of IL-6 [198, 202, 240]. Furthermore, it has to be taken into consideration that the IL-6R mAbs serve as competitive inhibitors of IL-6 signalling. With rising serum levels, inhibition will be overridden and onset of IL-6 signalling might take place again [197]. Hence, the combination of both antibodies might result in excess concentrations of IL-6 within the serum and therefore reversed inhibition of IL-6 signalling which, in turn, results in greater tumour growth and accelerated bone resorption. This fact might also explain why the higher dose of 100mg/kg tocilizumab tested in the pilot study was less effective than 50mg/kg tocilizumab.

In addition to this, Yoshida et al. found that mice injected regularly with MR16-1 produce antibodies directed against the rat IgG component of MR16-1 [236]. It has not yet been reported

whether tocilizumab induces auto-antibody production in mice treated with this antibody as well. However, since tocilizumab is a humanized monoclonal antibody, this is likely to be the case. Auto-antibody production might therefore be another explanation why higher doses or the combination of both antibodies show less clinical effect.

Moreover, one can conclude that binding of tumour-produced hIL-6 to murine IL-6Rs on host cells is an important paracrine signalling way. This pathway is interrupted by applying MR16-1 to the xenograft model used in our studies. Hence, we found that in MR16-1 treated mice, tumour growth in bone was diminished compared to placebo-treated animals. This finding is supported by literature. For instance Chang et al. found that tumour-produced IL-6 leads to activation of STAT3 and IL-6 production in cancer-associated fibroblasts, endothelial cells and myeloid cells, facilitating tumour promotion and metastases [241].

One of the first effects of hIL-6 signalling in the bone microenvironement can be observed in activation of osteoclast precursor cells, which induce bone resorption. Tanaka et al. found that, correspondingly to our results, treatment with MR16-1 reduced osteoclast activation due to IL-6 stimulation in mice suffering from RA. Moreover, they also found that inhibitory effects of MR16-1 treatment, visible on day 14 of their experiments, vanished on day 35 [242]. Again, these finding correspond to our results. Tanaka et al. showed that serum IL-6 in mice on day 35 was still inhibited by MR16-1. They stated that factors other than IL-6 are therefore responsible for osteoclast activation and induction of osteolysis in later phases [242].

In all cases during our experiment, osteoclastic cells at the bone-tumour interface are activated and start bone resorption. Osteolysis can, in turn, be determined by osteolytic lesions and diminished cortical bone areas. Further effects of bone resorption are the release of growth factors stored within the bone matrix that affect tumour growth, thus influencing the rates of proliferating cells, apoptotic cells and, finally, the tumour size in general, which in turn leads to enhanced activation of osteoclastic cells. This fuels the so-called vicious cycle of bone resorption [100]. Since only the number of osteoclasts at the bone-tumour interface, but not the secondary parameters like P1NP and TRAcP5b, were affected, yet in animals receiving 100mg/kg MR16-1 it is likely that endpoint analysis on tibiae 21 days post tumour cell inoculation shows the state in which osteoclastic cells are activated, starting the cascade of increased bone resorption and augmented tumour growth. This also implies that hIL-6, tumour-derived IL-6, plays a more important role in progressing breast cancer bone metastases than host cell-derived murine IL-6,

since the amount of hIL-6 secreted by tumour cells increases substantially with the number of tumour cells.

In the experiments it was shown that inhibition of IL-6 signalling reduced bone destruction. This process is mediated by osteoclasts. The osteoclast numbers at both the trabecular and the cortical bone-tumour interface were reduced in histological images of tumours of mice treated with either 100mg/kg MR16-1 or 50mg/kg tocilizumab (Table 17 and Table 18). However, in the pilot study significant reductions of osteoclast numbers were only seen in at the trabecular bone-tumour interface in tumours of mice administered with either 100mg/kg MR16-1 or 50mg/kg tocilizumab (Table 17), whereas in the treatment study, significant reductions occurred only at the cortical bone-tumour interface of mice receiving 50mg/kg tocilizumab (Table 18). It is also worth mentioning, that osteoclast numbers are slightly higher in the treatment study than in the pilot study. The cortical bone area in sections obtained from mice in the pilot study appears to be larger after 21 days than in sections of tibia from the treatment study. Hence, it might be possible that osteoclast activation following tumour-derived interleukin-6 secretion may only start after a certain threshold of IL-6 is overcome. Since IL-6 modulates trabecular and endochondral bone turnover in nude mice by stimulating osteoclast differentiation [127], it is possible that IL-6 affects trabecular bone first, before starting to act on osteoclastic cells of the cortical bone. IL-6 has been identified to act as an auto- and paracrine mediator of bone resorption, mainly stimulating osteoclast development from precursor cells [219]. It has been proven in former studies that the IL-6R mAb MR16-1 influences inflammatory osteoclast formation required for structural damage in bone [195].

Moreover, the cytokine IL-6 enhances osteoblast differentiation, but lowers proliferation of osteoblast precursors and induces apoptosis in differentiated osteoblasts [123]. Zheng et al. reported that PTHrP expression in human MDA-MB 231 cells is crititcal for tumour growth and survival and osteoblast inhibition [243]. Moreover, we found in further experiments conducted in our laboratory that IL-6 induced RANK expression in MDA-MB 231 cells *in vitro* [244]. It needs to be examined in further experiments as to how far PTHrP production and secretion by MDA-MB 231 cells is influenced by IL-6R activation in these cells.

In osteoporotic conditions, IL-6 is produced and released by stromal cells and osteoblastic cells in response to PTH, PTHrP, 1,25 Vitamin D_3, TGF-β, IL-1 and TNF-α [71]. In our model, IL-6 itself is also produced and secreted by the MDA-Tx-SA cells inoculated into tibia of nude mice,

which explains the local bone destruction around the tumour. Moreover, it was shown that mice suffering from high bone turnover due to a low calcium diet are more prone to develop metastases of breast cancer to bone [156]. Whether also a general loss of bone mass occurs in the mice suffering from bone metastases due to a systemic elevation of IL-6 levels in mice suffering from localized osteolytic breast cancer bone metastases needs to be investigated.

When looking closely at the results obtained in our experiments, it becomes obvious that blocking IL-6 signalling in tumour cells or host cells by applying the respective IL-6R mAbs only exhibits inhibitory effects on bone resorption and tumour growth in stages in which bone metastases are still small in size. Once they exceed a critical threshold in volume, and consequently also in the amount of tumour-produced hIL-6 released from the tumour cells, these benefits are overridden and not detectable any more. Furthermore, it has been reported that IL-6 concentrations in femurs of mice inoculated intra-femurally with MDA-Tx-SA cells were significantly higher early (11 days) after tumour cell inoculation and declined again during the course of metastatic growth in femurs [245]. Chang et al. reported that IL-6 levels in metastatic breast cancer cells are especially high on the edge of the tumours, implying that IL-6 is especially important in inducing metastases, but not in further enhancing the growth of already established metastases [241]. These data also support the thesis that IL-6 is especially important in early stages of breast cancer bone metastases.

In Vitro

IL-6 regulates transcription rates of a variety of genes, mainly via activation of STAT3 [241, 246]. Activation of these genes is believed responsible for proliferation, inhibition of apoptosis, increased mobility of cells and enhanced angiogenesis [241, 246]. While many of these effector genes are already known, the influence of autocrine human IL-6R activation in human MDA-Tx-SA breast cancer cells has not been determined yet. We hypothesized that an autocrine feed-forward loop exists, meaning that after IL-6 stimulation of MDA-Tx-SA cells, the IL-6 production by these cells is enhanced. It has been described in literature that IL-6 itself stimulates the IL-6 production in rat osteoblastic cells [219]. Moreover, up-regulation of growth and survival pathways in breast cancer cells after autocrine IL-6 stimulation have been reported [183]. Effects of IL-6 signalling on the transcription of the cytokine itself in MDA-Tx-SA cells have not been studied before. Taking the pro-tumourigenic effects attributed to IL-6 into consideration, enhanced IL-6 transcription and secretion after autocrine IL-6 stimulation would

feed these pro-tumourigenic features and therefore render the tumour even more aggressive. In a set of *in vitro* experiments, we could show that such a mechanism exists. MDA-Tx-SA cells were cultured and treated with placebo, 50µg/ml or 100µg/ml tocilizumab for 12 hours before levels of hIL-6 mRNA and human IL-6R mRNA expressions were determined. While treatment with 50µg/ml tocilizumab only decreased human IL-6R mRNA transcription rates significantly compared to controls, but not levels of hIL-6 mRNA, 100µg/ml tocilizumab diminished either value significantly (Figure 32). Thus, IL-6 acts as autocrine stimulation for enhanced mRNA production in these cells. However, when trying to confirm these observations by hIL-6 ELISA on protein levels for hIL-6, no significant alterations in hIL-6 protein secretion were found (Figure 33). This might be due to the fact that supernatants might have been collected too early, when protein synthesis and secretion was not yet finished.

Autocrine IL-6 signalling has a less pronounced impact on transcription levels on the cytokine itself, but rather amplifies human IL-6R mRNA which subsequently results in elevated receptor expression on the cell surface, rendering the cells more sensitive to IL-6 signalling. Hence, an autocrine feed-forward mechanism in IL-6 signalling seems to exist. However, this is not due to increased transcription and production of the cytokine itself in response to its receptor activation, but rather to an enhanced production of human IL-6Rs once IL-6 signalling has been initiated. By providing a greater amount of receptors, downstream signalling can be potentiated and hence, greater phenotypic changes due to IL-6 signalling can be observed. However, it is possible that changes in mRNA transcription rates are already detectable after 12 hours' incubation with tocilizumab, but protein levels need longer until detectable increase. Thus, it might be possible that changes will only become measurable at later time points. Moreover, no further evaluation of protein levels of the hIL-6R was carried out in this study to confirm decreased rates of human IL-6R gene transcription on a phenotypic level.

Future directions

As mentioned above, the effects of IL-6 on T cells as a major part of the immune system have not been investigated in this study on account of the study design employing T-cell deficient BALB c nu/nu mice. T cells also play a crucial role in tumour-defence [232]. Consequently, it is very important to evaluate the response of an anti-IL-6R treatment on tumour progression in a fully immunocompetent model first, before predicting its possible beneficial effects on humans suffering from breast cancer bone metastases.

Metastasis as a multi-step process

Tumourigenesis and forming metastases is a complex multi-step process including constant cell growth, resistance to hypoxia, invasion and angiogenesis [183]. IL-6R activation in tumour cells not only enhances local tumour growth, angiogenesis and immune evasion of breast cancers [184], but also promotes the development of metastases, induces migration via disruption of cell-cell adhesion, increases mobility of breast cancer cells and conveys multi-drug resistance of breast carcinomas [13, 38, 191]. Inhibition of STAT3 signalling in MDA-MB-231 cells has been associated with smaller orthotopic tumours in the mammary fat pad, fewer metastases and a significantly lower tumour-associated angiogenesis via suppression of transcription of VEGF [180, 191].

Another point worth evaluating in future studies is the effect that an IL-6R blockade exerts on the metastasising process, which is initiated and maintained by acquiring and accumulating several mutations. These changes enable a tumour cell to abandon the formation of primary cancer cells, enter the circulation and start residing and proliferating at secondary sites of the organism [237]. There are several genes such as VEGF and survivin that are considered crucial for establishing metastatic [159]. It is still unclear what specific role IL-6 plays in the context of initiating the metastases process to different tissues. Zinonos et al. reported that MDA-MB 231 cells overexpressing OPG showed smaller osteolytic metastases in bone, however, breast cancer cell metastases to soft tissues, in this case lung metastases, were promoted [247]. Since our studies solely concentrated on the bone metastatic growth model, the effects of IL-6R mAb treatment on the growth and metastasizing capabilities of orthotopic breast cancers need to be determined in future experiments. Thus, further experiments need to be conducted with either injection of mammary breast cancer cells into the mammary fat pad as orthotopic site or intracardially in order to determine the effect of IL-6 signalling blockade on the affinity of tumour cells to certain tissues, as well as their ability to proliferate and form significant cancers.

We were able to demonstrate that both murine and human IL-6R mAb inhibit the progression of breast cancer metastases in bone. Most likely, it is not blocking the IL-6R itself that can account for these beneficial effects but rather its influence on the production and secretion of other molecules affecting bone turnover and susceptibility for bone metastases in response to IL-6R activation, such as RANKL or PTHrP. Thus, murine autocrine IL-6 signalling between host cells will contribute to tumour growth via changes in secondary messenger expression like RANKL and PTHrP by osteoblasts and other cells of the osteoblast lineage [81]. Furthermore,

MR16-1 prevents human IL-6 from activating the murine IL-6R on cells within the bone environment. In further experiments conducted in our laboratory, we found that serum RANKL levels were significantly lower in tumour-bearing mice treated with either tocilizumab or MR16-1 [248]. This observation provides further evidence that cells of the osteoblast lineage are able to directly communicate with cancer cells via a RANKL/IL-6 dependent pathway, which is distinct from the osteoclast-mediated signalling pathway of the established vicious cycle [76, 78, 249]

Heterogeneous tumour cells

For intratibial inoculation, the bone-seeking clone MDA-Tx-SA of the ER-negative human breast cancer cell line MDA-MB-231 was used. Since spontaneous neoplasias in mammal organisms always consist of cells with different mutations and gene expression patterns, such as for example the hormone receptor status, it needs to be clarified whether inhibitory effects of IL-6R mAbs on breast cancer bone metastases can be observed in other human mammary cell lines, or if these effects are exclusive to the MDA-Tx-SA human breast cancer cells. In literature, it has been reported that IL-6 exerts different effects on different types of tumours: It functions as an autocrine growth factor in renal cell carcinoma, prostate carcinoma, oesophageal carcinoma, multiple myeloma and leukaemia cells [13, 185, 250]. By activating STAT3 in breast carcinoma cells, IL-6 signalling mediates cell growth and the onset of survival genes, but also prevents further differentiation of breast carcinoma cells, thus maintaining the cells in a continuous state of proliferation [246]. Constitutive activation of STAT3 has been associated with increased transformation of tumour cells, as well as increased angiogenesis, blocking of STAT3 signalling resulted in induction of apoptosis [251]. We could prove increased rates of apoptotic cells in tumours with disrupted IL-6R activation in our study by showing an elevated number of apoptotic cells in sections stained for TUNEL in mice treated with either tocilizumab or MR16-1 (Figure 30).

Furthermore, high levels of STAT3 in breast cancer cells were correlated with resistance to chemotherapy [180, 251]. Hence, it needs to be clarified whether treatment with IL-6R mAbs might be a possible additional treatment to augment conventional chemotherapy, hormone blocking therapy and already evaluated targeted therapies in patients suffering from breast cancer, rendering the cells more sensitive to chemotherapeutic agents or radiotherapy. Hence, it is necessary to observe the effects of IL-6R mAbs on the growth of heterogeneous tumours and

widen the experiments on various human breast cancer cells lines, especially also ER-positive breast cancer cell lines.

When treating women suffering from systemic breast cancer disease with bone metastases, it is important to target as many neoplastic cells as possible and not to target certain malignant cells only and thus possibly provide improved growth conditions for slightly different breast cancer cells, which might even accelerate disease progression.

Adverse effects of tocilizumab and MR16-1

Tocilizumab is a mAb approved for the treatment of RA and JIA [234]. There have been several reported adverse effects in response to treatment with tocilizumab, ranging from mild and transient liver function changes, modulation of the immune system with increased risk of infection of the upper respiratory tract, headache, nasopharyngitis and gastrointestinal events [39, 234]. Since IL-6 plays an important role in triggering the immune system, as it induces APP synthesis in hepatocytes, organisms treated with IL-6R mAbs are likely to be more prone to systemic infections. Furthermore, hypersensitivity reactions to tocilizumab injections have been reported [39, 192]. In some cases, elevated plasma lipids, such as TAG and cholesterol levels, neutropenia and thrombocytopenia have been reported [234]. During the course of the study conducted in this thesis, adverse events were not observed nor monitored in particular. Additionally, one also has to take into consideration that BALB c nu/nu mice are T-cell deficient and were housed in standardized conditions. Thus, infections were rare. Nevertheless, adverse effects in immunocompetent organisms have to be assessed in future experiments. Especially due to the fact that the dose of antibody needed in order to reach the bone microenvironment is much higher than the dose administered to patients treated for RA with tocilizumab. Hence, it is possible that with higher doses the rate of adverse events of a treatment with tocilizumab might rise and the benefits might be cancelled.

Conclusion

Breast cancer is not only the most common malignant disease in women, but it is also responsible for most cancer-related deaths in women. Once metastasized to bone, the treatment is usually palliative. It has been shown in former research that most bone metastases of breast cancer display osteolytic features. Elevated serum levels of the cytokine IL-6 in women suffering from metastatic breast cancer are associated with poor prognosis, disease progression and increased number of metastatic sites. Furthermore, IL-6 production by breast cancer cells has been attributed to more aggressive types of tumours.

However, the exact role of IL-6 in the progress of tumour progression and its influence on breast cancer bone metastases has not yet been understood to a great extent. Thus, the research of this thesis was aimed at understanding the mechanisms of IL-6 in breast cancer bone metastases and to examine the effects of blocking IL-6 signalling in a xenograft model of human breast cancer bone metastases in mice.To this end, both the anti-human IL-6 receptor antibody tocilizumab and the anti-mouse IL-6 receptor antibody MR16-1 were administered intraperitoneally in different doses to athymic nude mice which were injected intratibially with the human breast cancer cell line MDA-Tx-SA in order to determine the influence of blocking IL-6 signalling in either tumour cells and/or host cells by the respective antibody *in vivo*. The main hypothesis of this work was therefore that blocking IL-6 signalling in either tumour cells or in cells of the bone microenvironment reduces growth and vitality of breast cancer metastases in bone.

A minor hypothesis in this study was that IL-6 initiates a feed-forward mechanism in human MDA-Tx-SA breast cancer cells, resulting in augmented IL-6 production by these cells after stimulation with IL-6. To prove this hypothesis, *in vitro* experiments with MDA-Tx-SA cells stimulated with IL-6 and treated with either placebo or the IL-6 receptor antibody tocilizumab were conducted and IL-6 mRNA, IL-6R mRNA and IL-6 protein levels were measured after a certain time span in both groups.

The *in vivo* experiments were preceded by a dose-finding study, in which the most effective doses of both the anti-human IL-6 receptor mAb tocilizumab as well as of the anti-murine IL-6 receptor mAb MR16-1 were defined. It became obvious that 50mg/kg/3 days of tocilizumab and 100mg/kg/3 days MR16-1 displayed the most pronounced effects in terms of reduced bone resorption and changes of tumour biology. Therefore, experiments with an appropriate number

of animals were conducted with these two doses, with a group of animals receiving a combination of both antibodies. Again, treatment with 50mg/kg/3 days tocilizumab or with 100mg/kg/3 days MR16-1 showed significant effects considering the degree of tumour-induced osteolysis and immunohistochemical evaluation of tumour vitality. However, it is worth noting that the combination of both antibodies resulted in less striking effects.

As a consequence, the major hypothesis of the study could be proven correct: Inhibition of IL-6 signalling in breast cancer cells or in cells of the bone microenvironment by the respective antibody leads to a reduced degree of tumour-induced osteolysis as well as diminished tumour vitality.

The *in vitro* experiments showed that IL-6 mRNA and IL-6R mRNA production rates were reduced, however these results could not be shown when measuring IL-6 protein levels in supernatants of these cells. Therefore, autocrine stimulation of MDA-Tx-SA cells with IL-6 seems to have an effect on IL-6 gene expression, though whether or not this feed-forward mechanism is of great significance for maintaining and enhancing malignant features of theses cells is a point still to be elucidated.

The mAb tocilizumab is already approved for treatment of rheumatoid arthritis in humans. When taking the findings of this study into consideration, tocilizumab might also be useful in the treatment of metastasized breast cancer. However, further research concerning the safety and adequate doses for treatment of human beings is needed in this field.

Bibliography

1. Bauer, J., et al., *Regulation of interleukin-6 expression in cultured human blood monocytes and monocyte-derived macrophages.* Blood, 1988. **72**(4): p. 1134-40.
2. Cicco, N.A., et al., *Inducible production of interleukin-6 by human polymorphonuclear neutrophils: role of granulocyte-macrophage colony-stimulating factor and tumor necrosis factor-alpha.* Blood, 1990. **75**(10): p. 2049-52.
3. Sironi, M., et al., *IL-1 stimulates IL-6 production in endothelial cells.* J Immunol, 1989. **142**(2): p. 549-53.
4. Loppnow, H. and P. Libby, *Proliferating or interleukin 1-activated human vascular smooth muscle cells secrete copious interleukin 6.* J Clin Invest, 1990. **85**(3): p. 731-8.
5. Mantovani, L., et al., *Differential regulation of interleukin-6 expression in human fibroblasts by tumor necrosis factor-alpha and lymphotoxin.* FEBS Lett, 1990. **270**(1-2): p. 152-6.
6. Guerne, P.A., D.A. Carson, and M. Lotz, *IL-6 production by human articular chondrocytes. Modulation of its synthesis by cytokines, growth factors, and hormones in vitro.* J Immunol, 1990. **144**(2): p. 499-505.
7. Yasukawa, K., et al., *Structure and expression of human B cell stimulatory factor-2 (BSF-2/IL-6) gene.* EMBO J, 1987. **6**(10): p. 2939-45.
8. Ishimi, Y., et al., *IL-6 is produced by osteoblasts and induces bone resorption.* J Immunol, 1990. **145**(10): p. 3297-303.
9. Kirnbauer, R., et al., *IFN-beta 2, B cell differentiation factor 2, or hybridoma growth factor (IL-6) is expressed and released by human epidermal cells and epidermoid carcinoma cell lines.* J Immunol, 1989. **142**(6): p. 1922-8.
10. Hirano, T., et al., *Interleukin 6 and its receptor in the immune response and hematopoiesis.* Int J Cell Cloning, 1990. **8 Suppl 1**: p. 155-66; discussion 166-7.
11. Frei, K., et al., *On the cellular source and function of interleukin 6 produced in the central nervous system in viral diseases.* Eur J Immunol, 1989. **19**(4): p. 689-94.
12. Bender, S., et al., *Interleukin-1 beta induces synthesis and secretion of interleukin-6 in human chondrocytes.* FEBS Lett, 1990. **263**(2): p. 321-4.
13. Bauer, J. and F. Herrmann, *Interleukin-6 in clinical medicine.* Ann Hematol, 1991. **62**(6): p. 203-10.
14. Hirano, T., et al., *Human B-cell differentiation factor defined by an anti-peptide antibody and its possible role in autoantibody production.* Proc Natl Acad Sci U S A, 1987. **84**(1): p. 228-31.
15. Akira, S., T. Taga, and T. Kishimoto, *Interleukin-6 in biology and medicine.* Adv Immunol, 1993. **54**: p. 1-78.
16. Heinrich, P.C., J.V. Castell, and T. Andus, *Interleukin-6 and the acute phase response.* Biochem J, 1990. **265**(3): p. 621-36.
17. Van Snick, J., *Interleukin-6: an overview.* Annu Rev Immunol, 1990. **8**: p. 253-78.
18. Akira, S., et al., *Biology of multifunctional cytokines: IL 6 and related molecules (IL 1 and TNF).* FASEB J, 1990. **4**(11): p. 2860-7.
19. Bauer, J., *Interleukin-6 and its receptor during homeostasis, inflammation, and tumor growth.* Klin Wochenschr, 1989. **67**(14): p. 697-706.
20. Hirano, T., et al., *Biological and clinical aspects of interleukin 6.* Immunol Today, 1990. **11**(12): p. 443-9.
21. Kishimoto, T., et al., *Interleukin-6 family of cytokines and gp130.* Blood, 1995. **86**(4): p. 1243-54.

22. Xing, Z., et al., *IL-6 is an antiinflammatory cytokine required for controlling local or systemic acute inflammatory responses.* J Clin Invest, 1998. **101**(2): p. 311-20.
23. Schindler, R., et al., *Correlations and interactions in the production of interleukin-6 (IL-6), IL-1, and tumor necrosis factor (TNF) in human blood mononuclear cells: IL-6 suppresses IL-1 and TNF.* Blood, 1990. **75**(1): p. 40-7.
24. Tilg, H., et al., *Interleukin-6 (IL-6) as an anti-inflammatory cytokine: induction of circulating IL-1 receptor antagonist and soluble tumor necrosis factor receptor p55.* Blood, 1994. **83**(1): p. 113-8.
25. Saito, M., et al., *Molecular cloning of a murine IL-6 receptor-associated signal transducer, gp130, and its regulated expression in vivo.* J Immunol, 1992. **148**(12): p. 4066-71.
26. O'Brien, C.A., et al., *Expression levels of gp130 in bone marrow stromal cells determine the magnitude of osteoclastogenic signals generated by IL-6-type cytokines.* J Cell Biochem, 2000. **79**(4): p. 532-41.
27. Gao, Y., et al., *Expression of IL-6 receptor and GP130 in mouse bone marrow cells during osteoclast differentiation.* Bone, 1998. **22**(5): p. 487-93.
28. Rose-John, S., et al., *Interleukin-6 biology is coordinated by membrane-bound and soluble receptors: role in inflammation and cancer.* J Leukoc Biol, 2006. **80**(2): p. 227-36.
29. Horiuchi, S., et al., *Soluble interleukin-6 receptors released from T cell or granulocyte/macrophage cell lines and human peripheral blood mononuclear cells are generated through an alternative splicing mechanism.* Eur J Immunol, 1994. **24**(8): p. 1945-8.
30. Heinrich, P.C., et al., *Interleukin-6-type cytokine signalling through the gp130/Jak/STAT pathway.* Biochem J, 1998. **334 (Pt 2)**: p. 297-314.
31. Jones, S.A., et al., *The soluble interleukin 6 receptor: mechanisms of production and implications in disease.* FASEB J, 2001. **15**(1): p. 43-58.
32. Tamura, T., et al., *Soluble interleukin-6 receptor triggers osteoclast formation by interleukin 6.* Proc Natl Acad Sci U S A, 1993. **90**(24): p. 11924-8.
33. Heinrich, P.C., et al., *Principles of interleukin (IL)-6-type cytokine signalling and its regulation.* Biochem J, 2003. **374**(Pt 1): p. 1-20.
34. Scheller, J., N. Ohnesorge, and S. Rose-John, *Interleukin-6 trans-signalling in chronic inflammation and cancer.* Scand J Immunol, 2006. **63**(5): p. 321-9.
35. Stahl, N., et al., *Association and activation of Jak-Tyk kinases by CNTF-LIF-OSM-IL-6 beta receptor components.* Science, 1994. **263**(5143): p. 92-5.
36. Ihle, J.N. and I.M. Kerr, *Jaks and Stats in signaling by the cytokine receptor superfamily.* Trends Genet, 1995. **11**(2): p. 69-74.
37. Zhong, Z., Z. Wen, and J.E. Darnell, Jr., *Stat3: a STAT family member activated by tyrosine phosphorylation in response to epidermal growth factor and interleukin-6.* Science, 1994. **264**(5155): p. 95-8.
38. Hong, D.S., L.S. Angelo, and R. Kurzrock, *Interleukin-6 and its receptor in cancer: implications for Translational Therapeutics.* Cancer, 2007. **110**(9): p. 1911-28.
39. Sebba, A., *Tocilizumab: the first interleukin-6-receptor inhibitor.* Am J Health Syst Pharm, 2008. **65**(15): p. 1413-8.
40. Montero-Julian, F.A., *The soluble IL-6 receptors: serum levels and biological function.* Cell Mol Biol (Noisy-le-grand), 2001. **47**(4): p. 583-97.
41. Harris, E.D., Jr., *Rheumatoid arthritis. Pathophysiology and implications for therapy.* N Engl J Med, 1990. **322**(18): p. 1277-89.
42. Hirano, T., et al., *Excessive production of interleukin 6/B cell stimulatory factor-2 in rheumatoid arthritis.* Eur J Immunol, 1988. **18**(11): p. 1797-801.

43. Dasgupta, B., et al., *Serial estimation of interleukin 6 as a measure of systemic disease in rheumatoid arthritis.* J Rheumatol, 1992. **19**(1): p. 22-5.
44. Madhok, R., et al., *Serum interleukin 6 levels in rheumatoid arthritis: correlations with clinical and laboratory indices of disease activity.* Ann Rheum Dis, 1993. **52**(3): p. 232-4.
45. Nishimoto, N., et al., *Treatment of rheumatoid arthritis with humanized anti-interleukin-6 receptor antibody: a multicenter, double-blind, placebo-controlled trial.* Arthritis Rheum, 2004. **50**(6): p. 1761-9.
46. Hosokawa, T., et al., *Interleukin-6 and soluble interleukin-6 receptor in the colonic mucosa of inflammatory bowel disease.* J Gastroenterol Hepatol, 1999. **14**(10): p. 987-96.
47. Ito, H., et al., *A pilot randomized trial of a human anti-interleukin-6 receptor monoclonal antibody in active Crohn's disease.* Gastroenterology, 2004. **126**(4): p. 989-96; discussion 947.
48. Horii, Y., et al., *Involvement of IL-6 in mesangial proliferative glomerulonephritis.* J Immunol, 1989. **143**(12): p. 3949-55.
49. Grossman, R.M., et al., *Interleukin 6 is expressed in high levels in psoriatic skin and stimulates proliferation of cultured human keratinocytes.* Proc Natl Acad Sci U S A, 1989. **86**(16): p. 6367-71.
50. Luger, T.A., et al., *Interleukin-6 is produced by epidermal cells and plays an important role in the activation of human T-lymphocytes and natural killer cells.* Ann N Y Acad Sci, 1989. **557**: p. 405-14.
51. Nishimoto, N., et al., *Improvement in Castleman's disease by humanized anti-interleukin-6 receptor antibody therapy.* Blood, 2000. **95**(1): p. 56-61.
52. Yoshizaki, K., et al., *Pathogenic significance of interleukin-6 (IL-6/BSF-2) in Castleman's disease.* Blood, 1989. **74**(4): p. 1360-7.
53. Beck, J.T., et al., *Brief report: alleviation of systemic manifestations of Castleman's disease by monoclonal anti-interleukin-6 antibody.* N Engl J Med, 1994. **330**(9): p. 602-5.
54. Ludwig, H., et al., *Interleukin-6 is a prognostic factor in multiple myeloma.* Blood, 1991. **77**(12): p. 2794-5.
55. Seymour, J.F., et al., *Serum interleukin-6 levels correlate with prognosis in diffuse large-cell lymphoma.* J Clin Oncol, 1995. **13**(3): p. 575-82.
56. Berek, J.S., et al., *Serum interleukin-6 levels correlate with disease status in patients with epithelial ovarian cancer.* Am J Obstet Gynecol, 1991. **164**(4): p. 1038-42; discussion 1042-3.
57. Plante, M., et al., *Interleukin-6 level in serum and ascites as a prognostic factor in patients with epithelial ovarian cancer.* Cancer, 1994. **73**(7): p. 1882-8.
58. Twillie, D.A., et al., *Interleukin-6: a candidate mediator of human prostate cancer morbidity.* Urology, 1995. **45**(3): p. 542-9.
59. Blay, J.Y., et al., *Serum level of interleukin 6 as a prognosis factor in metastatic renal cell carcinoma.* Cancer Res, 1992. **52**(12): p. 3317-22.
60. Conze, D., et al., *Autocrine production of interleukin 6 causes multidrug resistance in breast cancer cells.* Cancer Res, 2001. **61**(24): p. 8851-8.
61. Kurzrock, R., et al., *Serum interleukin 6 levels are elevated in lymphoma patients and correlate with survival in advanced Hodgkin's disease and with B symptoms.* Cancer Res, 1993. **53**(9): p. 2118-22.
62. Strassmann, G., et al., *Evidence for the involvement of interleukin 6 in experimental cancer cachexia.* J Clin Invest, 1992. **89**(5): p. 1681-4.
63. Taichman, R.S., *Blood and bone: two tissues whose fates are intertwined to create the hematopoietic stem-cell niche.* Blood, 2005. **105**(7): p. 2631-9.

64. Clarke, B., *Normal bone anatomy and physiology.* Clin J Am Soc Nephrol, 2008. **3 Suppl 3**: p. S131-9.
65. Hock, J.M., M. Centrella, and E. Canalis, *Insulin-like growth factor I has independent effects on bone matrix formation and cell replication.* Endocrinology, 1988. **122**(1): p. 254-60.
66. Hauschka, P.V., et al., *Growth factors in bone matrix. Isolation of multiple types by affinity chromatography on heparin-Sepharose.* J Biol Chem, 1986. **261**(27): p. 12665-74.
67. Bonewald, L.F. and G.R. Mundy, *Role of transforming growth factor-beta in bone remodeling.* Clin Orthop Relat Res, 1990(250): p. 261-76.
68. Locklin, R.M., R.O. Oreffo, and J.T. Triffitt, *Effects of TGFbeta and bFGF on the differentiation of human bone marrow stromal fibroblasts.* Cell Biol Int, 1999. **23**(3): p. 185-94.
69. Hill, P.A., *Bone remodelling.* Br J Orthod, 1998. **25**(2): p. 101-7.
70. Malaval, L., et al., *Cellular expression of bone-related proteins during in vitro osteogenesis in rat bone marrow stromal cell cultures.* J Cell Physiol, 1994. **158**(3): p. 555-72.
71. Manolagas, S.C. and R.L. Jilka, *Bone marrow, cytokines, and bone remodeling. Emerging insights into the pathophysiology of osteoporosis.* N Engl J Med, 1995. **332**(5): p. 305-11.
72. Zhou, H., et al., *Osteoblasts directly control lineage commitment of mesenchymal progenitor cells through Wnt signaling.* J Biol Chem, 2008. **283**(4): p. 1936-45.
73. Logan, C.Y. and R. Nusse, *The Wnt signaling pathway in development and disease.* Annu Rev Cell Dev Biol, 2004. **20**: p. 781-810.
74. Otto, F., et al., *Cbfa1, a candidate gene for cleidocranial dysplasia syndrome, is essential for osteoblast differentiation and bone development.* Cell, 1997. **89**(5): p. 765-71.
75. Komori, T., et al., *Targeted disruption of Cbfa1 results in a complete lack of bone formation owing to maturational arrest of osteoblasts.* Cell, 1997. **89**(5): p. 755-64.
76. Guise, T.A., et al., *Basic mechanisms responsible for osteolytic and osteoblastic bone metastases.* Clin Cancer Res, 2006. **12**(20 Pt 2): p. 6213s-6216s.
77. Mundy, G.R., et al., *Growth regulatory factors and bone.* Rev Endocr Metab Disord, 2001. **2**(1): p. 105-15.
78. Mundy, G.R., *Metastasis to bone: causes, consequences and therapeutic opportunities.* Nat Rev Cancer, 2002. **2**(8): p. 584-93.
79. Mundy, G.R., *Cytokines and local factors which affect osteoclast function.* Int J Cell Cloning, 1992. **10**(4): p. 215-22.
80. Girasole, G., et al., *Interleukin-11: a new cytokine critical for osteoclast development.* J Clin Invest, 1994. **93**(4): p. 1516-24.
81. Kudo, O., et al., *Interleukin-6 and interleukin-11 support human osteoclast formation by a RANKL-independent mechanism.* Bone, 2003. **32**(1): p. 1-7.
82. Aarden, E.M., E.H. Burger, and P.J. Nijweide, *Function of osteocytes in bone.* J Cell Biochem, 1994. **55**(3): p. 287-99.
83. Plotkin, L.I., S.C. Manolagas, and T. Bellido, *Transduction of cell survival signals by connexin-43 hemichannels.* J Biol Chem, 2002. **277**(10): p. 8648-57.
84. Rubin, C.T. and L.E. Lanyon, *Kappa Delta Award paper. Osteoregulatory nature of mechanical stimuli: function as a determinant for adaptive remodeling in bone.* J Orthop Res, 1987. **5**(2): p. 300-10.
85. Xing, L. and B.F. Boyce, *Regulation of apoptosis in osteoclasts and osteoblastic cells.* Biochem Biophys Res Commun, 2005. **328**(3): p. 709-20.

86. Kurihara, N., et al., *Identification of committed mononuclear precursors for osteoclast-like cells formed in long term human marrow cultures.* Endocrinology, 1990. **126**(5): p. 2733-41.
87. Hattersley, G., J.A. Kerby, and T.J. Chambers, *Identification of osteoclast precursors in multilineage hemopoietic colonies.* Endocrinology, 1991. **128**(1): p. 259-62.
88. Kodama, H., et al., *Essential role of macrophage colony-stimulating factor in the osteoclast differentiation supported by stromal cells.* J Exp Med, 1991. **173**(5): p. 1291-4.
89. Yasuda, H., et al., *Osteoclast differentiation factor is a ligand for osteoprotegerin/osteoclastogenesis-inhibitory factor and is identical to TRANCE/RANKL.* Proc Natl Acad Sci U S A, 1998. **95**(7): p. 3597-602.
90. Lacey, D.L., et al., *Osteoprotegerin ligand is a cytokine that regulates osteoclast differentiation and activation.* Cell, 1998. **93**(2): p. 165-76.
91. Laitala, T. and H.K. Vaananen, *Inhibition of bone resorption in vitro by antisense RNA and DNA molecules targeted against carbonic anhydrase II or two subunits of vacuolar H(+)-ATPase.* J Clin Invest, 1994. **93**(6): p. 2311-8.
92. Teitelbaum, S.L., et al., *Cellular and molecular mechanisms of bone resorption.* Miner Electrolyte Metab, 1995. **21**(1-3): p. 193-6.
93. Hill, P.A., et al., *The effects of selective inhibitors of matrix metalloproteinases (MMPs) on bone resorption and the identification of MMPs and TIMP-1 in isolated osteoclasts.* J Cell Sci, 1994. **107 (Pt 11)**: p. 3055-64.
94. Hill, P.A., et al., *Inhibition of bone resorption in vitro by selective inhibitors of gelatinase and collagenase.* Biochem J, 1995. **308 (Pt 1)**: p. 167-75.
95. Boyle, W.J., W.S. Simonet, and D.L. Lacey, *Osteoclast differentiation and activation.* Nature, 2003. **423**(6937): p. 337-42.
96. Baron, R., R. Tross, and A. Vignery, *Evidence of sequential remodeling in rat trabecular bone: morphology, dynamic histomorphometry, and changes during skeletal maturation.* Anat Rec, 1984. **208**(1): p. 137-45.
97. de Vernejoul, M.C., *Dynamics of bone remodelling: biochemical and pathophysiological basis.* Eur J Clin Chem Clin Biochem, 1996. **34**(9): p. 729-34.
98. Frost, H.M., *A new direction for osteoporosis research: a review and proposal.* Bone, 1991. **12**(6): p. 429-37.
99. Kroger, H., et al., *Histomorphometry of periarticular bone in rheumatoid arthritis.* Ann Chir Gynaecol, 1994. **83**(1): p. 56-62.
100. Guise, T.A., *The vicious cycle of bone metastases.* J Musculoskelet Neuronal Interact, 2002. **2**(6): p. 570-2.
101. Kakonen, S.M. and G.R. Mundy, *Mechanisms of osteolytic bone metastases in breast carcinoma.* Cancer, 2003. **97**(3 Suppl): p. 834-9.
102. Burr, D.B., *Targeted and nontargeted remodeling.* Bone, 2002. **30**(1): p. 2-4.
103. Meikle, M.C., et al., *Human osteoblasts in culture synthesize collagenase and other matrix metalloproteinases in response to osteotropic hormones and cytokines.* J Cell Sci, 1992. **103 (Pt 4)**: p. 1093-9.
104. Parfitt, A.M., *The coupling of bone formation to bone resorption: a critical analysis of the concept and of its relevance to the pathogenesis of osteoporosis.* Metab Bone Dis Relat Res, 1982. **4**(1): p. 1-6.
105. Mundy, G.R., *Peptides and growth regulatory factors in bone.* Rheum Dis Clin North Am, 1994. **20**(3): p. 577-88.
106. Martin, T.J. and K.W. Ng, *Mechanisms by which cells of the osteoblast lineage control osteoclast formation and activity.* J Cell Biochem, 1994. **56**(3): p. 357-66.
107. Rodan, G.A. and T.J. Martin, *Role of osteoblasts in hormonal control of bone resorption--a hypothesis.* Calcif Tissue Int, 1981. **33**(4): p. 349-51.

108. Takahashi, N., et al., *Osteoblastic cells are involved in osteoclast formation.* Endocrinology, 1988. **123**(5): p. 2600-2.
109. Suda, T., N. Takahashi, and T.J. Martin, *Modulation of osteoclast differentiation.* Endocr Rev, 1992. **13**(1): p. 66-80.
110. Khosla, S., *Minireview: the OPG/RANKL/RANK system.* Endocrinology, 2001. **142**(12): p. 5050-5.
111. Nakagawa, N., et al., *RANK is the essential signaling receptor for osteoclast differentiation factor in osteoclastogenesis.* Biochem Biophys Res Commun, 1998. **253**(2): p. 395-400.
112. Hsu, H., et al., *Tumor necrosis factor receptor family member RANK mediates osteoclast differentiation and activation induced by osteoprotegerin ligand.* Proc Natl Acad Sci U S A, 1999. **96**(7): p. 3540-5.
113. Simonet, W.S., et al., *Osteoprotegerin: a novel secreted protein involved in the regulation of bone density.* Cell, 1997. **89**(2): p. 309-19.
114. Yasuda, H., et al., *Identity of osteoclastogenesis inhibitory factor (OCIF) and osteoprotegerin (OPG): a mechanism by which OPG/OCIF inhibits osteoclastogenesis in vitro.* Endocrinology, 1998. **139**(3): p. 1329-37.
115. Cohen, M.M., Jr., *The new bone biology: pathologic, molecular, and clinical correlates.* Am J Med Genet A, 2006. **140**(23): p. 2646-706.
116. Pottratz, S.T., et al., *17 beta-Estradiol inhibits expression of human interleukin-6 promoter-reporter constructs by a receptor-dependent mechanism.* J Clin Invest, 1994. **93**(3): p. 944-50.
117. Bellido, T., et al., *Regulation of interleukin-6, osteoclastogenesis, and bone mass by androgens. The role of the androgen receptor.* J Clin Invest, 1995. **95**(6): p. 2886-95.
118. Poli, V., et al., *Interleukin-6 deficient mice are protected from bone loss caused by estrogen depletion.* EMBO J, 1994. **13**(5): p. 1189-96.
119. Bellido, T., et al., *Detection of receptors for interleukin-6, interleukin-11, leukemia inhibitory factor, oncostatin M, and ciliary neurotrophic factor in bone marrow stromal/osteoblastic cells.* J Clin Invest, 1996. **97**(2): p. 431-7.
120. Erices, A., et al., *Gp130 activation by soluble interleukin-6 receptor/interleukin-6 enhances osteoblastic differentiation of human bone marrow-derived mesenchymal stem cells.* Exp Cell Res, 2002. **280**(1): p. 24-32.
121. Franchimont, N., S. Wertz, and M. Malaise, *Interleukin-6: An osteotropic factor influencing bone formation?* Bone, 2005. **37**(5): p. 601-6.
122. Udagawa, N., et al., *Interleukin (IL)-6 induction of osteoclast differentiation depends on IL-6 receptors expressed on osteoblastic cells but not on osteoclast progenitors.* J Exp Med, 1995. **182**(5): p. 1461-8.
123. Li, Y., et al., *IL-6 receptor expression and IL-6 effects change during osteoblast differentiation.* Cytokine, 2008. **43**(2): p. 165-73.
124. Desbois, C. and G. Karsenty, *Osteocalcin cluster: implications for functional studies.* J Cell Biochem, 1995. **57**(3): p. 379-83.
125. Franchimont, N., et al., *Interleukin-6 and its soluble receptor cause a marked induction of collagenase 3 expression in rat osteoblast cultures.* J Biol Chem, 1997. **272**(18): p. 12144-50.
126. Guillen, C., A.R. de Gortazar, and P. Esbrit, *The interleukin-6/soluble interleukin-6 receptor system induces parathyroid hormone-related protein in human osteoblastic cells.* Calcif Tissue Int, 2004. **75**(2): p. 153-9.
127. Rozen, N., et al., *Interleukin-6 modulates trabecular and endochondral bone turnover in the nude mouse by stimulating osteoclast differentiation.* Bone, 2000. **26**(5): p. 469-74.

128. Yoshitake, F., et al., *Interleukin-6 directly inhibits osteoclast differentiation by suppressing receptor activator of NF-kappaB signaling pathways.* J Biol Chem, 2008. **283**(17): p. 11535-40.
129. Palmqvist, P., et al., *IL-6, leukemia inhibitory factor, and oncostatin M stimulate bone resorption and regulate the expression of receptor activator of NF-kappa B ligand, osteoprotegerin, and receptor activator of NF-kappa B in mouse calvariae.* J Immunol, 2002. **169**(6): p. 3353-62.
130. Kurihara, N., C. Civin, and G.D. Roodman, *Osteotropic factor responsiveness of highly purified populations of early and late precursors for human multinucleated cells expressing the osteoclast phenotype.* J Bone Miner Res, 1991. **6**(3): p. 257-61.
131. Black, K., I.R. Garrett, and G.R. Mundy, *Chinese hamster ovarian cells transfected with the murine interleukin-6 gene cause hypercalcemia as well as cachexia, leukocytosis and thrombocytosis in tumor-bearing nude mice.* Endocrinology, 1991. **128**(5): p. 2657-9.
132. al-Humidan, A., et al., *Interleukin-6 does not stimulate bone resorption in neonatal mouse calvariae.* J Bone Miner Res, 1991. **6**(1): p. 3-8.
133. de la Mata, J., et al., *Interleukin-6 enhances hypercalcemia and bone resorption mediated by parathyroid hormone-related protein in vivo.* J Clin Invest, 1995. **95**(6): p. 2846-52.
134. Zhang, X., et al., *Evidence for a direct role of cyclo-oxygenase 2 in implant wear debris-induced osteolysis.* J Bone Miner Res, 2001. **16**(4): p. 660-70.
135. Zhang, X., et al., *Cyclooxygenase-2 regulates mesenchymal cell differentiation into the osteoblast lineage and is critically involved in bone repair.* J Clin Invest, 2002. **109**(11): p. 1405-15.
136. Liu, X.H., et al., *Interactive effect of interleukin-6 and prostaglandin E2 on osteoclastogenesis via the OPG/RANKL/RANK system.* Ann N Y Acad Sci, 2006. **1068**: p. 225-33.
137. Kopf, M., et al., *Impaired immune and acute-phase responses in interleukin-6-deficient mice.* Nature, 1994. **368**(6469): p. 339-42.
138. Gaillard, J.P., et al., *Increased and highly stable levels of functional soluble interleukin-6 receptor in sera of patients with monoclonal gammopathy.* Eur J Immunol, 1993. **23**(4): p. 820-4.
139. Klein, B., et al., *Interleukin-6 in human multiple myeloma.* Blood, 1995. **85**(4): p. 863-72.
140. Bataille, R., D. Chappard, and B. Klein, *The critical role of interleukin-6, interleukin-1B and macrophage colony-stimulating factor in the pathogenesis of bone lesions in multiple myeloma.* Int J Clin Lab Res, 1992. **21**(4): p. 283-7.
141. Roodman, G.D., et al., *Interleukin 6. A potential autocrine/paracrine factor in Paget's disease of bone.* J Clin Invest, 1992. **89**(1): p. 46-52.
142. Kato, A., et al., *Early effects of tocilizumab on bone and bone marrow lesions in a collagen-induced arthritis monkey model.* Exp Mol Pathol, 2008. **84**(3): p. 262-70.
143. Casimiro, S., T.A. Guise, and J. Chirgwin, *The critical role of the bone microenvironment in cancer metastases.* Mol Cell Endocrinol, 2009. **310**(1-2): p. 71-81.
144. Ferlay, J., D.M. Parkin, and E. Steliarova-Foucher, *Estimates of cancer incidence and mortality in Europe in 2008.* Eur J Cancer, 2010. **46**(4): p. 765-81.
145. Yang, L., et al., *Wogonin induces G1 phase arrest through inhibiting Cdk4 and cyclin D1 concomitant with an elevation in p21Cip1 in human cervical carcinoma HeLa cells.* Biochem Cell Biol, 2009. **87**(6): p. 933-42.
146. Ferlay, J., et al., *Estimates of worldwide burden of cancer in 2008: GLOBOCAN 2008.* Int J Cancer, 2010.
147. Ferlay, J., et al., *Cancer incidence and mortality patterns in Europe: estimates for 40 countries in 2012.* Eur J Cancer, 2013. **49**(6): p. 1374-403.
148. Jemal, A., et al., *Cancer statistics, 2007.* CA Cancer J Clin, 2007. **57**(1): p. 43-66.

149. Loberg, R.D., et al., *The lethal phenotype of cancer: the molecular basis of death due to malignancy.* CA Cancer J Clin, 2007. **57**(4): p. 225-41.
150. Buijs, J.T., et al., *Inhibition of bone resorption and growth of breast cancer in the bone microenvironment.* Bone, 2009. **44**(2): p. 380-6.
151. Paget, S., *The distribution of secondary growths in cancer of the breast. 1889.* Cancer Metastasis Rev, 1989. **8**(2): p. 98-101.
152. Fidler, I.J. and G. Poste, *The "seed and soil" hypothesis revisited.* Lancet Oncol, 2008. **9**(8): p. 808.
153. Kozlow, W. and T.A. Guise, *Breast cancer metastasis to bone: mechanisms of osteolysis and implications for therapy.* J Mammary Gland Biol Neoplasia, 2005. **10**(2): p. 169-80.
154. Lipton, A., *Bone metastases in breast cancer.* Curr Treat Options Oncol, 2003. **4**(2): p. 151-8.
155. Roudier, M.P., et al., *Phenotypic heterogeneity of end-stage prostate carcinoma metastatic to bone.* Hum Pathol, 2003. **34**(7): p. 646-53.
156. Ooi, L.L., et al., *The bone remodeling environment is a factor in breast cancer bone metastasis.* Bone, 2010.
157. De Bock, K., M. Mazzone, and P. Carmeliet, *Antiangiogenic therapy, hypoxia, and metastasis: risky liaisons, or not?* Nat Rev Clin Oncol, 2011. **8**(7): p. 393-404.
158. Minn, A.J., et al., *Distinct organ-specific metastatic potential of individual breast cancer cells and primary tumors.* J Clin Invest, 2005. **115**(1): p. 44-55.
159. Kang, Y., et al., *A multigenic program mediating breast cancer metastasis to bone.* Cancer Cell, 2003. **3**(6): p. 537-49.
160. Sotiriou, C., et al., *Interleukins-6 and -11 expression in primary breast cancer and subsequent development of bone metastases.* Cancer Lett, 2001. **169**(1): p. 87-95.
161. Mancino, A.T., et al., *Breast cancer increases osteoclastogenesis by secreting M-CSF and upregulating RANKL in stromal cells.* J Surg Res, 2001. **100**(1): p. 18-24.
162. Southby, J., et al., *Immunohistochemical localization of parathyroid hormone-related protein in human breast cancer.* Cancer Res, 1990. **50**(23): p. 7710-6.
163. Powell, G.J., et al., *Localization of parathyroid hormone-related protein in breast cancer metastases: increased incidence in bone compared with other sites.* Cancer Res, 1991. **51**(11): p. 3059-61.
164. Henderson, M., et al., *Parathyroid hormone-related protein production by breast cancers, improved survival, and reduced bone metastases.* J Natl Cancer Inst, 2001. **93**(3): p. 234-7.
165. Guise, T.A., et al., *Evidence for a causal role of parathyroid hormone-related protein in the pathogenesis of human breast cancer-mediated osteolysis.* J Clin Invest, 1996. **98**(7): p. 1544-9.
166. Zheng, Y., et al., *Bone resorption increases tumour growth in a mouse model of osteosclerotic breast cancer metastasis.* Clin Exp Metastasis, 2008. **25**(5): p. 559-67.
167. Morony, S., et al., *Osteoprotegerin inhibits osteolysis and decreases skeletal tumor burden in syngeneic and nude mouse models of experimental bone metastasis.* Cancer Res, 2001. **61**(11): p. 4432-6.
168. Neudert, M., et al., *Site-specific human breast cancer (MDA-MB-231) metastases in nude rats: model characterisation and in vivo effects of ibandronate on tumour growth.* Int J Cancer, 2003. **107**(3): p. 468-77.
169. Dai, J., et al., *Reversal of chemotherapy-induced leukopenia using granulocyte macrophage colony-stimulating factor promotes bone metastasis that can be blocked with osteoclast inhibitors.* Cancer Res, 2010. **70**(12): p. 5014-23.
170. Zheng, Y., et al., *Accelerated bone resorption, due to dietary calcium deficiency, promotes breast cancer tumor growth in bone.* Cancer Res, 2007. **67**(19): p. 9542-8.

171. Ooi, L.L., et al., *Vitamin D deficiency promotes human breast cancer growth in a murine model of bone metastasis.* Cancer Res, 2010. **70**(5): p. 1835-44.
172. Ooi, L.L., et al., *Vitamin D deficiency promotes growth of MCF-7 human breast cancer in a rodent model of osteosclerotic bone metastasis.* Bone, 2010.
173. Senaratne, S.G., et al., *Bisphosphonates induce apoptosis in human breast cancer cell lines.* Br J Cancer, 2000. **82**(8): p. 1459-68.
174. Knupfer, H. and R. Preiss, *Significance of interleukin-6 (IL-6) in breast cancer (review).* Breast Cancer Res Treat, 2007. **102**(2): p. 129-35.
175. Salgado, R., et al., *Circulating interleukin-6 predicts survival in patients with metastatic breast cancer.* Int J Cancer, 2003. **103**(5): p. 642-6.
176. Sansone, P., et al., *IL-6 triggers malignant features in mammospheres from human ductal breast carcinoma and normal mammary gland.* J Clin Invest, 2007. **117**(12): p. 3988-4002.
177. Utsumi, K., et al., *Enhanced production of IL-6 in tumor-bearing mice and determination of cells responsible for its augmented production.* J Immunol, 1990. **145**(1): p. 397-403.
178. Underhill-Day, N. and J.K. Heath, *Oncostatin M (OSM) cytostasis of breast tumor cells: characterization of an OSM receptor beta-specific kernel.* Cancer Res, 2006. **66**(22): p. 10891-901.
179. Hirano, T., K. Ishihara, and M. Hibi, *Roles of STAT3 in mediating the cell growth, differentiation and survival signals relayed through the IL-6 family of cytokine receptors.* Oncogene, 2000. **19**(21): p. 2548-56.
180. Berishaj, M., et al., *Stat3 is tyrosine-phosphorylated through the interleukin-6/glycoprotein 130/Janus kinase pathway in breast cancer.* Breast Cancer Res, 2007. **9**(3): p. R32.
181. Basolo, F., et al., *Expression of and response to interleukin 6 (IL6) in human mammary tumors.* Cancer Res, 1996. **56**(13): p. 3118-22.
182. Sehgal, P.B., *Interleukin-6 induces increased motility, cell-cell and cell-substrate dyshesion and epithelial-to-mesenchymal transformation in breast cancer cells.* Oncogene, 2010. **29**(17): p. 2599-600; author reply 2601-3.
183. Grivennikov, S. and M. Karin, *Autocrine IL-6 signaling: a key event in tumorigenesis?* Cancer Cell, 2008. **13**(1): p. 7-9.
184. Sasser, A.K., et al., *Interleukin-6 is a potent growth factor for ER-{alpha}-positive human breast cancer.* FASEB J., 2007. **21**(13): p. 3763-3770.
185. Leu, C.M., et al., *Interleukin-6 acts as an antiapoptotic factor in human esophageal carcinoma cells through the activation of both STAT3 and mitogen-activated protein kinase pathways.* Oncogene, 2003. **22**(49): p. 7809-18.
186. Leslie, K., et al., *Cyclin D1 is transcriptionally regulated by and required for transformation by activated signal transducer and activator of transcription 3.* Cancer Res, 2006. **66**(5): p. 2544-52.
187. Brocke-Heidrich, K., et al., *Interleukin-6-dependent gene expression profiles in multiple myeloma INA-6 cells reveal a Bcl-2 family-independent survival pathway closely associated with Stat3 activation.* Blood, 2004. **103**(1): p. 242-51.
188. Clevenger, C.V., *Roles and regulation of stat family transcription factors in human breast cancer.* Am J Pathol, 2004. **165**(5): p. 1449-60.
189. Hess, S., et al., *Loss of IL-6 receptor expression in cervical carcinoma cells inhibits autocrine IL-6 stimulation: abrogation of constitutive monocyte chemoattractant protein-1 production.* J Immunol, 2000. **165**(4): p. 1939-48.
190. Walter, M., et al., *Interleukin 6 secreted from adipose stromal cells promotes migration and invasion of breast cancer cells.* Oncogene, 2009. **28**(30): p. 2745-55.

191. Selander, K.S., et al., *Inhibition of gp130 signaling in breast cancer blocks constitutive activation of Stat3 and inhibits in vivo malignancy.* Cancer Res, 2004. **64**(19): p. 6924-33.
192. Choy, E., *Clinical experience with inhibition of interleukin-6.* Rheum Dis Clin North Am, 2004. **30**(2): p. 405-15, viii.
193. Mihara, M., et al., *Tocilizumab inhibits signal transduction mediated by both mIL-6R and sIL-6R, but not by the receptors of other members of IL-6 cytokine family.* Int Immunopharmacol, 2005. **5**(12): p. 1731-40.
194. Uchiyama, Y., et al., *Anti-IL-6 receptor antibody increases blood IL-6 level via the blockade of IL-6 clearance, but not via the induction of IL-6 production.* Int Immunopharmacol, 2008. **8**(11): p. 1595-601.
195. Axmann, R., et al., *Inhibition of interleukin-6 receptor directly blocks osteoclast formation in vitro and in vivo.* Arthritis Rheum, 2009. **60**(9): p. 2747-56.
196. Mori, K., et al., *Effects of interleukin-6 blockade on the development of autoimmune thyroiditis in nonobese diabetic mice.* Autoimmunity, 2009. **42**(3): p. 228-34.
197. Okazaki, M., et al., *Characterization of anti-mouse interleukin-6 receptor antibody.* Immunol Lett, 2002. **84**(3): p. 231-40.
198. Mihara, M., et al., *Anti-interleukin 6 receptor antibody inhibits murine AA-amyloidosis.* J Rheumatol, 2004. **31**(6): p. 1132-8.
199. Okiyama, N., et al., *Therapeutic effects of interleukin-6 blockade in a murine model of polymyositis that does not require interleukin-17A.* Arthritis Rheum, 2009. **60**(8): p. 2505-12.
200. Katsume, A., et al., *Anti-interleukin 6 (IL-6) receptor antibody suppresses Castleman's disease like symptoms emerged in IL-6 transgenic mice.* Cytokine, 2002. **20**(6): p. 304-11.
201. Mori, K., et al., *Novel models of cancer-related anemia in mice inoculated with IL-6-producing tumor cells.* Biomed Res, 2009. **30**(1): p. 47-51.
202. Mihara, M., et al., *Influences of anti-mouse interleukin-6 receptor antibody on immune responses in mice.* Immunol Lett, 2002. **84**(3): p. 223-9.
203. Grano, M., et al., *Breast cancer cell line MDA-231 stimulates osteoclastogenesis and bone resorption in human osteoclasts.* Biochem Biophys Res Commun, 2000. **270**(3): p. 1097-100.
204. Yoneda, T., et al., *A bone-seeking clone exhibits different biological properties from the MDA-MB-231 parental human breast cancer cells and a brain-seeking clone in vivo and in vitro.* J Bone Miner Res, 2001. **16**(8): p. 1486-95.
205. Saito, T., et al., *Preparation of soluble murine IL-6 receptor and anti-murine IL-6 receptor antibodies.* J Immunol, 1991. **147**(1): p. 168-73.
206. Cailleau, R., et al., *Breast tumor cell lines from pleural effusions.* J Natl Cancer Inst, 1974. **53**(3): p. 661-74.
207. Collan, Y.U., et al., *Standardized mitotic counts in breast cancer. Evaluation of the method.* Pathol Res Pract, 1996. **192**(9): p. 931-41.
208. Lindunger, A., et al., *Histochemistry and biochemistry of tartrate-resistant acid phosphatase (TRAP) and tartrate-resistant acid adenosine triphosphatase (TrATPase) in bone, bone marrow and spleen: implications for osteoclast ontogeny.* Bone Miner, 1990. **10**(2): p. 109-19.
209. Fisher, J.L., et al., *An in vivo model of prostate carcinoma growth and invasion in bone.* Cell Tissue Res, 2002. **307**(3): p. 337-45.
210. Jalava, P., et al., *Ki67 immunohistochemistry: a valuable marker in prognostication but with a risk of misclassification: proliferation subgroups formed based on Ki67*

immunoreactivity and standardized mitotic index. Histopathology, 2006. **48**(6): p. 674-82.
211. Negoescu, A., et al., *In situ apoptotic cell labeling by the TUNEL method: improvement and evaluation on cell preparations.* J Histochem Cytochem, 1996. **44**(9): p. 959-68.
212. Labat-Moleur, F., et al., *TUNEL apoptotic cell detection in tissue sections: critical evaluation and improvement.* J Histochem Cytochem, 1998. **46**(3): p. 327-34.
213. Halleen, J.M., et al., *Tartrate-resistant acid phosphatase 5b: a novel serum marker of bone resorption.* J Bone Miner Res, 2000. **15**(7): p. 1337-45.
214. Chu, P., et al., *Correlation between histomorphometric parameters of bone resorption and serum type 5b tartrate-resistant acid phosphatase in uremic patients on maintenance hemodialysis.* Am J Kidney Dis, 2003. **41**(5): p. 1052-9.
215. Ehlers, M., et al., *Identification of two novel regions of human IL-6 responsible for receptor binding and signal transduction.* J Immunol, 1994. **153**(4): p. 1744-53.
216. Igawa, T., et al., *Antibody recycling by engineered pH-dependent antigen binding improves the duration of antigen neutralization.* Nat Biotechnol, 2010. **28**(11): p. 1203-7.
217. Igawa, T., et al., *Antibody recycling by engineered pH-dependent antigen binding improves the duration of antigen neutralization.* Nat Biotechnol, 2011. **28**(11): p. 1203-7.
218. Axmann, R., et al., *Inhibition of interleukin-6 receptor directly blocks osteoclast formation in vitro and in vivo.* Arthritis & Rheumatism, 2009. **60**(9): p. 2747-2756.
219. Franchimont, N., S. Rydziel, and E. Canalis, *Interleukin 6 is autoregulated by transcriptional mechanisms in cultures of rat osteoblastic cells.* J Clin Invest, 1997. **100**(7): p. 1797-803.
220. Yoshimatsu, M., et al., *IL-12 inhibits TNF-alpha induced osteoclastogenesis via a T cell-independent mechanism in vivo.* Bone, 2009. **45**(5): p. 1010-6.
221. Bachelot, T., et al., *Prognostic value of serum levels of interleukin 6 and of serum and plasma levels of vascular endothelial growth factor in hormone-refractory metastatic breast cancer patients.* Br J Cancer, 2003. **88**(11): p. 1721-6.
222. Tawara, K., J.T. Oxford, and C.L. Jorcyk, *Clinical significance of interleukin (IL)-6 in cancer metastasis to bone: potential of anti-IL-6 therapies.* Cancer Manag Res, 2011. **3**: p. 177-89.
223. Nishimoto, N., *[Humanized anti-human IL-6 receptor antibody, tocilizumab].* Nihon Rinsho, 2007. **65**(7): p. 1218-25.
224. Shinriki, S., et al., *Humanized anti-interleukin-6 receptor antibody suppresses tumor angiogenesis and in vivo growth of human oral squamous cell carcinoma.* Clin Cancer Res, 2009. **15**(17): p. 5426-34.
225. Matsuyama, Y., et al., *Successful treatment of a patient with rheumatoid arthritis and IgA-kappa multiple myeloma with tocilizumab.* Intern Med, 2011. **50**(6): p. 639-42.
226. Juul, P., et al., *Athymic experimental animals in pharmaco-immunological research.* Toxicol Lett, 1992. **64-65 Spec No**: p. 85-92.
227. Pesce, B., et al., *Effect of interleukin-6 receptor blockade on the balance between regulatory T cells and T helper type 17 cells in rheumatoid arthritis patients.* Clin Exp Immunol, 2013. **171**(3): p. 237-42.
228. Kishimoto, T., *The biology of interleukin-6.* Blood, 1989. **74**(1): p. 1-10.
229. Bottcher, J.P., et al., *IL-6 trans-Signaling-Dependent Rapid Development of Cytotoxic CD8(+) T Cell Function.* Cell Rep, 2014. **8**(5): p. 1318-27.
230. Rosol, T.J., et al., *Animal models of bone metastasis.* Cancer, 2003. **97**(3 Suppl): p. 748-57.
231. Campbell, J.P., et al., *Models of bone metastasis.* J Vis Exp, 2012(67): p. e4260.

232. Koike, R., et al., *Japan College of Rheumatology 2009 guidelines for the use of tocilizumab, a humanized anti-interleukin-6 receptor monoclonal antibody, in rheumatoid arthritis.* Mod Rheumatol, 2009. **19**(4): p. 351-7.
233. Wang, D., et al., *The use of biologic therapies in the treatment of rheumatoid arthritis.* Curr Pharm Biotechnol, 2014. **15**(6): p. 542-8.
234. Navarro-Millan, I., J.A. Singh, and J.R. Curtis, *Systematic review of tocilizumab for rheumatoid arthritis: a new biologic agent targeting the interleukin-6 receptor.* Clin Ther, 2012. **34**(4): p. 788-802 e3.
235. Davies, B. and T. Morris, *Physiological parameters in laboratory animals and humans.* Pharm Res, 1993. **10**(7): p. 1093-5.
236. Yoshida, H., et al., *Induction of high-dose tolerance to the rat anti-mouse IL-6 receptor antibody in NZB/NZW F1 mice.* Rheumatol Int, 2011. **31**(11): p. 1445-9.
237. Hussein, O. and S.V. Komarova, *Breast cancer at bone metastatic sites: recent discoveries and treatment targets.* J Cell Commun Signal, 2011. **5**(2): p. 85-99.
238. Wu, H., et al., *Caspases: a molecular switch node in the crosstalk between autophagy and apoptosis.* Int J Biol Sci, 2014. **10**(9): p. 1072-83.
239. Aad, G., et al., *Evidence for Electroweak Production of W^{+/-}W^{+/-}jj in pp Collisions at sqrt[s]=8 TeV with the ATLAS Detector.* Phys Rev Lett, 2014. **113**(14): p. 141803.
240. Heinrich, P.C., et al., *Membrane-bound and soluble interleukin-6 receptor: studies on structure, regulation of expression, and signal transduction.* Ann N Y Acad Sci, 1995. **762**: p. 222-36; discussion 236-7.
241. Chang, Q., et al., *The IL-6/JAK/Stat3 feed-forward loop drives tumorigenesis and metastasis.* Neoplasia, 2013. **15**(7): p. 848-62.
242. Aad, G., et al., *Measurements of four-lepton production at the Z resonance in pp collisions at sqrt[s] = 7 and 8 TeV with ATLAS.* Phys Rev Lett, 2014. **112**(23): p. 231806.
243. Zheng, L., et al., *PTHrP expression in human MDA-MB-231 breast cancer cells is critical for tumor growth and survival and osteoblast inhibition.* Int J Biol Sci, 2013. **9**(8): p. 830-41.
244. Zheng, Y., et al., *Direct crosstalk between cancer and osteoblast lineage cells fuels metastatic growth in bone via auto-amplification of IL-6 and RANKL signaling pathways.* J Bone Miner Res, 2014. **29**(9): p. 1938-49.
245. Sosnoski, D.M., et al., *Changes in Cytokines of the Bone Microenvironment during Breast Cancer Metastasis.* Int J Breast Cancer, 2012. **2012**: p. 160265.
246. Li, L. and P.E. Shaw, *Autocrine-mediated activation of STAT3 correlates with cell proliferation in breast carcinoma lines.* J Biol Chem, 2002. **277**(20): p. 17397-405.
247. Zinonos, I., et al., *Pharmacologic inhibition of bone resorption prevents cancer-induced osteolysis but enhances soft tissue metastasis in a mouse model of osteolytic breast cancer.* Int J Oncol, 2014. **45**(2): p. 532-40.
248. He, F., et al., *Interleukin-6 receptor rs7529229 T/C polymorphism is associated with left main coronary artery disease phenotype in a Chinese population.* Int J Mol Sci, 2014. **15**(4): p. 5623-33.
249. Yoneda, T. and T. Hiraga, *Crosstalk between cancer cells and bone microenvironment in bone metastasis.* Biochem Biophys Res Commun, 2005. **328**(3): p. 679-87.
250. Romano, M., et al., *Role of IL-6 and its soluble receptor in induction of chemokines and leukocyte recruitment.* Immunity, 1997. **6**(3): p. 315-25.
251. Gritsko, T., et al., *Persistent activation of stat3 signaling induces survivin gene expression and confers resistance to apoptosis in human breast cancer cells.* Clin Cancer Res, 2006. **12**(1): p. 11-9.

Appendix

Statement / Eidesstattliche Versicherung

„Ich, Katja Börnert, versichere an Eides statt durch meine eigenhändige Unterschrift, dass ich die vorgelegte Dissertation mit dem Thema: „The Influence of Interleukin-6 Receptor Antibodies on Breast Cancer Metastases in Bone“ selbstständig und ohne nicht offengelegte Hilfe Dritter verfasst und keine anderen als die angegebenen Quellen und Hilfsmittel genutzt habe.
Alle Stellen, die wörtlich oder dem Sinne nach auf Publikationen oder Vorträgen anderer Autoren beruhen, sind als solche in korrekter Zitierung (siehe „Uniform Requirements for Manuscripts (URM)“ des ICMJE -*www.**icmje**.org*) kenntlich gemacht. Die Abschnitte zu Methodik (insbesondere praktische Arbeiten, Laborbestimmungen, statistische Aufarbeitung) und Resultaten (insbesondere Abbildungen, Graphiken und Tabellen) entsprechen den URM (s.o) und werden von mir verantwortet.
Meine Anteile an etwaigen Publikationen zu dieser Dissertation entsprechen denen, die in der untenstehenden gemeinsamen Erklärung mit dem/der Betreuer/in, angegeben sind. Sämtliche Publikationen, die aus dieser Dissertation hervorgegangen sind und bei denen ich Autor bin, entsprechen den URM (s.o) und werden von mir verantwortet.

Die Bedeutung dieser eidesstattlichen Versicherung und die strafrechtlichen Folgen einer unwahren eidesstattlichen Versicherung (§156,161 des Strafgesetzbuches) sind mir bekannt und bewusst.“

Datum Unterschrift

Anteilserklärung an etwaigen erfolgten Publikationen

Katja Börnert hatte folgenden Anteil an den folgenden Publikationen:

Publikation 1: Zheng Y, Chow S, **Boernert K**, Basel D, Mikuscheva A, Kim S, Fong-Yee C, Trivedi T, Buttgereit F, Sutherland SL, Dunstan CR, Zhou H, Seibel MJ*. Direct cross-talk between cancer and osteoblast lineage cells fuels metastatic growth in bone via auto-amplification of IL-6 and RANKL signalling pathways. **J Bone Miner Res.** 2014 Sep;29(9):1938-49.

Beitrag im Einzelnen: Planung der Durchführung der Experimente mit Tocilizumab und MR16-1, welche den Einfluss dieser Antikörper auf Mammakarzinommetastasen im Knochen untersuchen und Aufbereitung der Ergebnisse

Unterschrift der Doktorandin: ……..

Curriculum vitae

Mein Lebenslauf wird aus datenschutzrechtlichen Gründen in der elektronischen Version meiner Arbeit nicht veröffentlicht

Publikationsliste

Zheng Y, Chow S, **Boernert K**, Basel D, Mikuscheva A, Kim S, Fong-Yee C, Trivedi T, Buttgereit F, Sutherland SL, Dunstan CR, Zhou H, Seibel MJ*. Direct cross-talk between cancer and osteoblast lineage cells fuels metastatic growth in bone via auto-amplification of IL-6 and RANKL signalling pathways. **J Bone Miner Res.** 2014 Sep;29(9):1938-49.

Abstracts

Boernert K, Zheng Y, Zhou H, Mikuscheva A, Buttgereit F, Dunstan CR and Seibel MJ Treatment with Interleukin 6 Receptor Antibodies Inhibits Breast Cancer Growth in a Murine Model of Bone Metastasis. 2010. Poster (plenary) presented at the 32nd Annual Meeting of the American Society for Bone and Mineral Research, Toronto, ON, Canada. J Bone Miner Res 25 (Suppl 1).

Boernert K, Zheng Y, Zhou H, Mikuscheva A, Buttgereit F, Dunstan CR and Seibel MJ Treatment with Interleukin 6 Receptor Antibodies Inhibits Breast Cancer Growth in a Murine Model of Bone Metastasis. 2010. Oral presentation at the ANZBMS 20th Annual Scientific Meeting, Adelaide, SA, Australia.

Acknowledgements

This work was conducted at the Charité University Hospital, Berlin, Germany, in cooperation with the ANZAC Research Institute, The University of Sydney, Sydney, Australia.

I am very indebted to my supervisors, Prof. Dr. Frank Buttgereit and Prof. Dr. Markus Seibel, for giving me the opportunity to participate in this international research cooperation as a medical student and be an active member of a high-quality international reseach team.

I dearly thank Prof. Dr. med Buttgereit for giving me the unique opportunity to take part in this programme and his great advice for finishing this work.

My special thanks to Prof. Dr. med M. Seibel. He not only mentored me greatly throughout my reseach, but also helped to make me feel at home in Australia.

My enormous gratitude goes to my supervisor Yu Zheng for his excellent academic guidance, constant advice und endless patience throughout my reseach and the writing process of this thesis. I am most thankful for him sharing his great knowledge with me, advising me whenever I was in doubt and investing so much time in supporting me in writing this thesis. Without his constant help, this work would have not been possible.

I dearly thank Dr Hong Zhou for her constant guidance, technical advice and patience. Her great wisdom has taught me to always consider obvious facts from another point of view.

I am very appreciative to the Bone Biology group, especially to Trupti Trivedi and Li Laine Ooi, who always helped me whenever they could and who were also there for me as friends, and to Julian Kelly for acquiring the micro-CT images for me.

I wish to dearly thank Mr Mamdouh Khalil and his excellent animal house staff for maintaining the animal reseach facilities ath the ANZAC research and making all the *in vivo* research possible.

I am also indebted to the Bone Research Program at ANZAC Research Institute, the Department of Endocrinology at Concord Hospital, and the Charité Berlin for providing financial support through a scholarship.

Finally, I am dearly grateful for my family and friends for constantly supporting me and never failing to encourage me.